

Collapsing D-Branes in Calabi-Yau Moduli Space: I

B. R. Greene^a,
C. I. Lazaroiu^b

Departments of Physics and Mathematics
Columbia University
New York, N.Y. 10027

ABSTRACT

We study the quantum volume of D-branes wrapped around various cycles in Calabi-Yau manifolds, as the manifold's moduli are varied. In particular, we focus on the behaviour of these D-branes near phase transitions between distinct low energy physical descriptions of the resulting string theory. Whereas previous studies have solely considered quantum volumes in the context of two-cycles in perturbative string theory or D-branes in the specific example of the quintic hypersurface, we work more generally and find qualitatively new features. On the mathematical side, as we briefly note, our work has some interesting implications for certain issues in arithmetics.

^a greene@phys.columbia.edu

^b lazaroIU@phys.columbia.edu

Introduction

Over the years, studies in quantum geometry have revealed both quantitative and qualitative deviations from expectations based on classical geometry. Such distinctions, in turn, have helped us understand physical properties that are intrinsically “stringy”. From the earliest studies, based solely on perturbative string theory, we learned that a “quantum” Calabi-Yau is in some sense a classical Calabi-Yau manifold together with all of its rational curves [42]. More recently, with the advent of D-branes as non-perturbative probes, we realized that a “quantum” Calabi-Yau manifold is sensitive to all of its supersymmetric cycles since, regardless of the cycle’s dimension, there is some D-brane that can wrap around it (thinking collectively in type IIA and type IIB string theory).

In this paper, we focus on the notion of *volume* from a string theoretic perspective¹. There are two papers that provide the groundwork for this undertaking. The first is [33] which made use of mirror symmetry to calculate the instanton action associated with strings whose worldsheet is wrapped around a holomorphic two-cycle. The second is [35], in which another approach to measuring quantum volumes — based on the masses of wrapped D-branes — was proposed.

Our goal in this paper is to begin a systematic union of the analyses of those papers in the following sense: In [33] phase boundaries in the $N = 2$ moduli space were studied with only the crudest of tools — perturbative string dynamics. This implies that [33] only had access to the quantum volume of two-cycles. A natural question that immediately follows is: what can be learned from extending this analysis by probing phase boundaries with higher dimensional D-branes? In [35] we learned, in one example (the quintic hypersurface of [42]), of the kind of surprises that such a study may reveal: it was shown there that the six-cycle acquires zero quantum volume at the mirror of the conifold point, though the quantum volumes of two and four cycles remain nonzero². This is a significant deviation from classical expectations since on a manifold with only one Kähler modulus — a single “breathing mode” — classical geometry requires that vanishing of a six-cycle’s volume entails the vanishing of all sub-cycle volumes.

We anticipate that some D-brane mass becomes zero at real codimension one along any phase boundary (since such boundaries intersect the discriminant locus of the mirror Calabi-Yau space), and the lesson of [35] is that classical geometric expectations regarding such degenerations can be completely misleading. We will see that this lesson is quite general by finding disagreement between the classical and quantum pictures in a variety of one and two-parameter models. As an interesting aside we point out that the vanishing of certain D-brane masses at special boundary points in $N = 2$ moduli space can be used as a tool for generating arithmetic identities which appear to be independent of known relations. While we have little insight beyond that afforded by

¹ Other approaches to quantum gravity — most notably, loop quantum gravity — have found interesting quantum mechanical features of volume [6] so perhaps this area may be a fruitful point of intersection.

²This was also found independently by [14].

the physics of D-branes, this mathematical question seems to be ripe for further study.

The present work can be thought of as complimentary to the approach of [45]. The authors of that paper use conformal field theory methods [49, 50] to construct D-brane boundary states at the Landau-Ginsburg point in the quintic moduli space, and then study the behaviour of those states as one perturbs away from this limit. Their goal, which they largely accomplish, is to find the geometric interpretation of such states in terms of wrapped D-branes and extract quantum geometrical implications from a conformal field theory analysis. In our work, we start at the “other end” of the moduli-space (the large radius limit), in which the classical geometry is manifest. We then move toward other phases (including but not limited to the Landau-Ginsburg phase) and study what happens to wrapped D-branes. In time, these two approaches should shed substantial light on the non-perturbative structure of the string theory moduli space.

In Section 1 we briefly review the results of [33] and [35] in the light of modern understanding of D-branes. We also give a short discussion of what has (and has not) been achieved in the literature. Section 2 introduces some old but largely overlooked³ mathematical methods that will greatly assist the calculations we perform. In section 3 we discuss some relevant issues regarding mirror symmetry and integral structures. In Sections 4 through 7 we apply these methods to a number of compact and non-compact examples, investigating the quantum volumes of two, four, and six-cycles at various interesting points in their moduli space. Finally, Section 8 discusses some open problems and presents our conclusions. The two appendices give a brief primer on the notion of monodromy weight filtration, as well as a list of useful identities.

1 Quantum Volumes

In this section we review some ideas relevant for the analysis of quantum volumes in string theory, and then outline our strategy for implementing them.

1.1 Perturbative Quantum Volumes

String theory on Calabi-Yau manifolds provides a rich arena for investigating quantum geometry. When a Calabi-Yau space X is “large”, observables in the corresponding string model can be expressed in terms of geometrical properties of the compactification manifold. As this space decreases in size, the values of many observables continuously shift from their large radius limits, thereby requiring shifted or deformed geometrical constructs for their interpretation. Collectively, these constructs — which reduce to classical geometric counterparts in the limit of large scales — yield what we mean by

³An example where Meijer functions were used to perform the analytic continuation of periods can be found in [1]. We thank E. Zaslow for bringing this reference to our attention. Issues of analytic continuation were also recently discussed in [2], in connection with the Kontsevitch conjecture [17].

“quantum” geometry ⁴.

A well known example of this idea arises in perturbative string theory, and provides the first approach to discussing quantum volumes. If we consider the three-point correlation function of chiral primary operators \mathcal{O}_i associated with classes A_i in $H^{1,1}(X, \mathbb{C})$, we find:

$$\langle \mathcal{O}_i \mathcal{O}_j \mathcal{O}_k \rangle = \int_X A_i \wedge A_j \wedge A_k + \sum_{\Gamma} \frac{\mathbf{q}^{\Gamma}}{1 - \mathbf{q}^{\Gamma}} N_{\Gamma}(A_i, A_j, A_k) \quad , \quad (1)$$

where Γ runs over the homology classes of rational curves in X , \mathbf{q}^{Γ} is a monomial in the variables $q_l = e^{2\pi i t_l}$, with t_l the coordinates of the complexified Kähler class $B + iJ = \sum_l t_l E_l$ in a basis E_l of $H^2(X, \mathbb{Z})$ and $N_{\Gamma}(A_i, A_j, A_k)$ are the Gromov-Witten invariants [3, 4] of X (see [26] for a review). The sum over Gromov-Witten invariants in the right hand side appears through an instanton expansion in the nonlinear sigma model, with the powers of q_l characterizing the contributions from instantons wrapping various holomorphic 2-cycles. In the limit that the volume of X and all of its rational curves goes to infinity, the instanton corrections are suppressed and the correlator can be interpreted in terms of the triple intersection form of X :

$$\langle \mathcal{O}_i \mathcal{O}_j \mathcal{O}_k \rangle \approx \int_X A_i \wedge A_j \wedge A_k \quad . \quad (2)$$

But as we move away from this limit, the instanton corrections are generally nonzero, yielding the *quantum* triple intersection — the quantum cohomology ring — on $H^{1,1}(X, \mathbb{C})$.

The right hand side of (1) is computationally unwieldy, but as first shown in [57] and subsequently evaluated to successful conclusion in [42], if X has a mirror Y then (1) can be evaluated *exactly* by a variation of Hodge structure calculation on Y . This procedure has been employed in a variety of circumstances, one of the most well-known being the enumeration of rational curves on the quintic hypersurface carried out in [42]. Our interest here, though, is not in enumerating rational curves. Rather, as implicitly used in [42] and developed in [33], we note that at a given point in the conformal field theory moduli space we can use the instanton expansion on the right hand side to *define* the ‘quantum volume’ of the rational curves in X . Namely, the curves are assigned whatever volume is necessary to make the expansion correct. More precisely, the variables t_l appearing in the instanton expansion are tuned to those values which ensure that equality (1) holds. Since $t_l = \int_{e_l} (B + iJ)$ (with (e_l) the basis of $H_2(X, \mathbb{Z})$ dual to (E_l)), we interpret the absolute value of t_l as the quantum volume of the holomorphic two-cycles in the class e_l .

⁴We adhere to common terminology which does not distinguish between “stringy” geometry and “quantum” geometry. More precisely, stringy geometry is concerned with the behaviour of compactified string theory for small string coupling constant, i.e. with the moduli space of closed conformal field theory defined on the Riemann sphere. In this paper, we go beyond this framework by including D-branes, so strictly speaking we study the moduli space of *open* conformal field theory at genus zero, i.e. the moduli space of boundary conformal field theory on a sphere.

As strongly motivated in [42] and subsequently proved in [23], this constraint is met if t_l are related to the complex structure of the mirror Y through the mirror map:

$$t_l = B_l + iJ_l = \frac{\int_{\gamma_l} \Omega(z)}{\int_{\gamma_0} \Omega(z)} \quad (3)$$

where z are coordinates on the complex structure moduli space of Y , $\gamma_l \in H_3(Y, \mathbb{Z})$ are suitably chosen three-cycles in Y (to be discussed in more detail shortly), and $\Omega(z)$ is the holomorphic three-form of Y at the point z .

Given a mirror pair (X, Y) , it follows that we can map out the quantum volumes of rational curves in X as its Kähler structure is varied by calculating appropriate ratios of periods of Ω , as functions of the complex structure of Y . Classically, $B_l + iJ_l$ can take on any value such that $J_l \geq 0$, but the approach just described generally yields a different conclusion. For instance, in some examples, $J_l \geq r_l > 0$, implying a minimum size for certain rational curves. This departure from the classically allowed two-cycle volumes motivates the use of the term “quantum volume” even though in this case $B_l + iJ_l = \int_{e_l} (B + iJ)$ is a classical formula. The quantum aspect arises when this formula is examined over the space of physically realizable models.

This approach for studying the quantum volumes of two-cycles was developed and applied in a number of different contexts in [33] and [34]. For example, the quantum volume of two-cycles involved in the flop transitions of [32] were shown to attain zero value at the center of the flop (the conifold point of the transition), in keeping with classical expectations. But in another example in which one moves from a smooth Calabi-Yau phase to a phase in which the Calabi-Yau manifold acquires a \mathbb{Z}_3 orbifold singularity, two-cycle volumes were shown to be bounded from below, in conflict with geometric expectations (at an abelian quotient singularity of this type, an exceptional divisor has been blown down to a point, which entails vanishing of the geometric volume of all holomorphic two-cycles embedded in the divisor). Thus, there can be significant differences between the quantum and classical properties of two-cycle volumes.

While revealing these interesting features of quantum volumes, the approach of [33] is deficient for two main reasons: First, it is limited to the study of two-cycle volumes and second (relatedly) it only uses perturbative string probes. D-branes, as emphasized in [35] provide a natural tool for going further.

1.2 Nonperturbative Quantum Volumes

Since BPS saturated D-brane states wrapped around cycles in a Calabi-Yau space have a mass that depends on the “size” of the cycles they wrap, we can use these masses to define the quantum volume of cycles. Since Type IIA string theory has even dimensional branes while Type IIB string theory has odd dimensional branes, considering both theories compactified on the same Calabi-Yau manifold X allows us to define a notion of quantum volume for cycles of all possible dimensions.

More specifically, in Type IIB string theory on X , BPS saturated D3-branes wrap three-dimensional special Lagrangian cycles of X [44] (these are the type A branes of

[43]). While it is a difficult mathematical problem to identify the special Lagrangian 3-cycles of a Calabi-Yau space, if C is such a cycle then the mass of a D3-brane wrapped on C depends only on the homology class $\gamma = [C] \in H_3(X)$ of C , and identifying elements γ of $H_3(X, \mathbb{Z})$ is a much easier problem. If, for example, we choose an integral basis γ_i of $H_3(X, \mathbb{Z})$, then we can express $\gamma = q^i \gamma_i$ with $q^i \in \mathbb{Z}$ (note that $[C]$ is an integral class since C is a submanifold of X) and write the BPS mass as [18, 35]:

$$m(\gamma) = \frac{|\int_{\gamma} \Omega|}{(\int_X \Omega \wedge \overline{\Omega})^{1/2}} = \frac{|q^i \int_{\gamma_i} \Omega|}{(\int_X \Omega \wedge \overline{\Omega})^{1/2}} . \quad (4)$$

The integers q^i can be interpreted as gauge charges with respect to the $U(1)$ -gauge fields resulting from the Kaluza-Klein reduction of the Ramond-Ramond four-form along the cycles γ_i , while the periods $\int_{\gamma_i} \Omega$ are related to the vacuum expectation values of the scalar fields which parameterize the complex structure moduli space. Hence (4) takes the standard form of charges times vevs. Since C is special Lagrangian⁵, we have $m(\gamma) = \text{vol}(C)$ with the proper normalization of Ω . Hence the mass of an A-type D-brane is proportional to the volume of the cycle it wraps, a relation which is quantum-mechanically exact. Thus, modulo issues of marginal stability, no interesting quantum effects contribute to the masses of A-type D-branes.

In the type IIA theory on X , BPS saturated D-branes wrap holomorphic cycles (these are the type B-branes of [43]). If we choose an integral basis h_i of $H_{\text{even}}(X, \mathbb{Z}) = H_0(X, \mathbb{Z}) \oplus H_2(X, \mathbb{Z}) \oplus H_4(X, \mathbb{Z}) \oplus H_6(X, \mathbb{Z})$, then a D-brane wrapping a holomorphic cycle in the class $h = \tilde{q}^i h_i$ has mass of the form $|\tilde{q}^i \phi_i|$ where ϕ_i are the vevs of the scalar fields associated with the Kähler structure of X . In the large radius limit the mass of the D-brane is proportional to the classical volume of the cycle it wraps, but this simple relation is destroyed by quantum corrections as one moves away from this limit.

As observed in [35], one can turn this argument around and *define* the *quantum volume* of a holomorphic cycle of X to be proportional to the mass of the type B-brane wrapping it. This is a natural generalization of the geometric notion of volume inasmuch as it reduces to the former in the large radius limit, where the full content of the string theory compactified on X (at weak string coupling) can be described in terms of standard geometric concepts.

Unfortunately, whereas the integrals $\int_{\gamma_i} \Omega$ give a simple, closed form for the relevant vevs for the odd-dimensional branes on X (associated with the complex structure of X) there is no simple, closed form expression for the ϕ_i . Indeed, the semiclassical formula relating the mass of such a brane to the volume of the associated holomorphic cycle (and the values of the B -field and worldvolume gauge field) is known to receive important quantum corrections, which are difficult to analyze directly on X . The situation is in many ways similar to that encountered for the action of string instantons wrapped over

⁵We assume that C is special Lagrangian with respect to $\Omega(z)$. This condition depends on the point z on the moduli space, as discussed in some detail in [9]—such dependence is related to issues of marginal stability, which we ignore in this paper.

rational curves and encoded by relations (1) and (3). However, we can follow [35] and circumvent this obstacle by using mirror symmetry.

For this, consider the Type IIB theory compactified on the mirror Y of X . Conformal and effective field theory arguments [43] show that under mirror symmetry D_{2k} -branes in the IIA theory on X are mapped to $D3$ -branes in the IIB-theory on Y ⁶. This identifies the mass of a type B D-brane with the mass of its mirror type A brane, which is amenable to direct computation via equation (4). Hence invoking both X and its mirror allows us reduce the problem of computing masses of BPS saturated D-branes to computing periods of holomorphic three-forms⁷.

1.3 Strategy of Calculation

In view of (4), our strategy for “measuring” quantum volumes of holomorphic submanifolds of X is in principle as follows:

- (1) Choose an integral basis of three-cycles γ_i in $H_3(Y, \mathbb{Z})$.
- (2) Calculate the periods $\int_{\gamma_i} \Omega$ with respect to this basis for all points in the complex structure moduli space of Y .
- (3) Find the explicit mirror map between $\oplus_j H_{2j}(X, \mathbb{Z})$ and $H_3(Y, \mathbb{Z})$.
- (4) Determine the quantum volume of any even-dimensional cycle in $\oplus_j H_{2j}(X, \mathbb{Z})$ by equating it (up to an overall normalization) with the mass of a D-3-brane wrapped on the mirror three-cycle in Y .

In practice, one encounters two⁸ difficulties in carrying out this strategy. First, it is generally a significant challenge to find explicitly a basis of integer three-cycles, i.e.

⁶More precisely, they are mapped to $D3$ -branes wrapping special Lagrangian cycles whose homology classes belong to the component \mathcal{W}_k of the reduced monodromy weight filtration associated with the large complex structure point of Y (see appendix A).

⁷It is believed [19] that the moduli space of type B branes admits a physically correct compactification related to certain moduli spaces of semi-stable simple sheaves on X , which should form the natural framework for finding an expression of the associated BPS charge directly in terms of type B D-brane data. Such an analysis will necessarily encode important information about moduli spaces of stable sheaves on X . By using mirror symmetry, we are somehow ‘summing up’ this information and re-expressing it in terms of the data of Y — its complex structure and the collection of its special Lagrangian 3-cycles. It should be possible to follow this approach in the other direction, in order to extract information about moduli spaces of sheaves on X .

⁸In fact, there is a third – and much more serious – problem involved in the whole subject, which belies many difficulties of interpretation and various issues of marginal stability touched upon in [45]. This rests on the following question: given an integral class $\gamma \in H_3(Y, \mathbb{Z})$, does this class support a special Lagrangian 3-cycle? If so, what is the moduli space of cycles in this class? We will mostly ignore this issue in the present paper, though we plan to discuss some aspects of this problem elsewhere. For recent work on this subject we refer the reader to [9] (see also [10] for a partial physical translation of some of those results). A complete understanding of this issue will most probably require a systematic development of the theory of moduli spaces of special Lagrangian submanifolds along the lines of [7], [8].

it is difficult to carry out step (1). Second, while the mirror map between $H_2(X, \mathbb{C})$ and (a part ⁹ of) $H_3(Y, \mathbb{C})$ is well understood, and while we certainly know that this map extends to an isomorphism between $\oplus_j H_{2j}(X, \mathbb{Z})$ and $H_3(Y, \mathbb{Z})$, realizing this map explicitly is generally beyond what as yet has been worked out, i.e. step (3) nontrivial. How, then, do we proceed?

Let us deal with the second problem first. In [42] the authors showed that integral two-cycles on X are mirror to integral three-cycles on Y with prescribed monodromy properties around a large complex structure point in the moduli space. Concretely, in a one-parameter example, the three-cycle γ_l in the numerator of (3) must satisfy $\gamma_l \rightarrow \gamma_l + \gamma_0$ upon parallel transport about a large complex structure point. When translated into the language of periods, this implies that $\int_{\gamma_l} \Omega$ has a logarithmic dependence on the coordinate z (chosen such that $z = 0$ is the large complex structure point). In [42, 61, 21, 12, 15], this notion was formalized and generalized to the statement that holomorphic cycles of real dimension $2j$ on X are mirror to three-cycles on Y whose periods have leading $\log^j z$ behavior near $z = 0$. Thus, finding a complete set of periods of Ω and classifying their leading logarithmic behavior gives us a means of identifying the dimension of their even-cycle counterpart on X .

Although this is part of the approach we will follow, it is certainly deficient since it says nothing about the subleading logarithmic dependence of the periods. For instance, is the six-cycle on X mirror to a three-cycle on Y whose period is purely proportional to $\log^3(z)$ or is there some nontrivial dependence on $\log^2(z)$ and $\log(z)$? This is a question that, at present, we do not know how to answer completely—it awaits a more thorough understanding of the action of mirror symmetry on the integral structure of a mirror pair. Thus, in this paper when we speak about a cycle on X of real dimension $2j$, that will often refer to a cycle on X with $2j$ being the maximal dimensional component, but with the identity of the admixture of lower cycles left unspecified. In Section 3 we will quantify how close we can currently get toward erasing this ambiguity. Gaining greater precision in this regard is an important problem for future work.

As for the first problem mentioned above—that of ensuring that the three cycles with which we work are integral—we propose the following. First, our main focus in this paper is to examine D-branes wrapping cycles whose mass vanishes at special points in the moduli space. For this purpose we can weaken the requirement that the γ_i are integral classes, and demand only that they are *proportional* to such classes. That is, if $\Lambda = H_3(Y, \mathbb{Z})$ is the integral lattice of 3-cycles in $H_3(Y, \mathbb{C})$, then all we require is that each of the γ_i we study is proportional to an element in Λ , with a *common* proportionality factor. In this case, given a cycle γ which is an integral linear combination of γ_i , the vanishing of $\int_{\gamma} \Omega$ at some point in the moduli space implies the existence of an integral cycle (of class proportional to γ) having the same property. We call cycles that are proportional to integral cycles *weakly integral*. Second, given a three-cycle γ which is weakly integral, we can generate other weakly integral cycles $\gamma^{(j)}$

⁹This is the component $\mathcal{W}_1 \subset H_3(Y)$ of the large complex structure reduced monodromy weight filtration. The behaviour of the elements of \mathcal{W}_1 under mirror symmetry is clearly discussed in [29, 62].

in $H_3(Y, \mathbb{C})$ by acting on it with monodromy transformations. A cycle $\gamma \in H_3(Y, \mathbb{C})$ with the property that the set of weakly integral cycles thus produced is a system of generators for the complex vector space $H_3(Y, \mathbb{C})$ will be called *cyclic*; indeed, it is a cyclic vector for the monodromy representation of the fundamental group of the moduli space by automorphisms of $H_3(Y, \mathbb{C})$. If γ is both cyclic and weakly integral, then there exists some complex constant λ such that $\lambda^{-1}\gamma$ is integral. Since the monodromy operators preserve the lattice Λ , it follows that the cycles $\lambda^{-1}\gamma^{(j)}$ are integral as well. Then one can easily construct the maximal lattice $\Lambda_0 \subset H^3(Y, \mathbb{C})$ having the property that it contains all $\gamma^{(j)}$, and it is an easy exercise to show that $\Lambda' := \lambda^{-1}\Lambda_0$ is a full sublattice¹⁰ of Λ , though it may fail to coincide with Λ itself.

For example, in compact one parameter models, three-cycles undergo monodromy transformations not only about the large complex structure point $z = 0$ but also about the points $z = 1$ and $z = \infty$ (with our choice of coordinate on the moduli space). There always exists a *fundamental cycle* $\gamma_0 \in H_3(Y, \mathbb{C})$ with the property that it is left invariant by all monodromy transformations about the large complex structure point (in the framework of [15], this is the cycle mirror to a 0-cycle, namely the homology class of the fiber of the special Lagrangian T^3 -fibration of Y). However, γ_0 will not generally be invariant under $T[\infty]$ and $T[1]$, and it is often the case that it is a cyclic vector for the action of these monodromy operators. In fact, a particular version of this procedure (involving only the monodromy operator $T[\infty]$ and applicable for the case when $z = \infty$ is a Landau-Ginzburg point) underlies the method used in [42] for producing a basis of periods.

We can now recast our strategy for measuring quantum volumes into the following form:

- (1) Calculate the period $\int_{\gamma_0} \Omega$ for a weakly integral three-cycle γ_0 .
- (2) Calculate the monodromy matrices $T[0]$, $T[1]$, and $T[\infty]$, and use them to produce a weakly integral basis of three-cycles, and their corresponding periods
- (3) Search for places in moduli space where a period associated to a weakly integral three-cycle vanishes.
- (4) Interpret the vanishing period of a weakly integral three-cycle on Y with leading $\log^j(z)$ behavior around $z = 0$ as the vanishing quantum volume of a holomorphic cycle on X of real dimension $2j$.

As mentioned before, a more precise version of step (4) would involve identifying the admixture of lower dimensional cycles on X mirror to the vanishing cycle on Y . This requires understanding mirror symmetry at the level of integral structures and in Section 3 we discuss aspects of this issue. In the next section we consider the problem of efficiently calculating a complete set of periods over a basis of three-cycles, together with procedures for identifying the monodromy matrices — that is, techniques for

¹⁰That is, a maximal rank sublattice of Λ , i.e. a sublattice such that the Λ/Λ_0 is a finite group.

carrying out steps (1) through (3). We will then use these results to carry out the four steps above in various examples.

Before proceeding with this analysis, let us make a few brief remarks on the status of results which can be found in the literature. Most previous work which involved the calculation of periods was concerned with deepening and generalizing the computation of Gromov-Witten invariants first performed in [42]. Since these invariants can be extracted from the mirror map (3), the literature is mainly focused on the computation of the fundamental and \log^1 periods. Ironically, though, some of the earliest works on applying mirror symmetry to enumerative geometry did consider the higher periods (e.g. [42, 36, 37, 21]), but their physical relevance in those pre-D-brane studies was, of course, not considered. In this work we present a method for analyzing all of the periods, throughout the moduli space, in a scheme that is computationally easier than previous methods and which allows their physical content to be directly extracted.

2 Techniques

Although we shall consider an example with $h^{1,1} > 1$, we will follow [33] and focus on judiciously chosen one-dimensional subspaces in the relevant moduli space. Hence, in this section we start by discussing a computationally efficient technique for analyzing one-parameter systems. The approach we describe is based on classical mathematical results due to C. S. Meijer and uses the so-called G-functions (or Meijer functions). As we show below, these functions are especially well-suited for a systematic computation of a basis of periods and its monodromies. Our use of G-functions grew out of our effort to find a more effective approach to such computations, and hopefully represents an improvement over the methods used in [42]. From an abstract point of view, the approach taken there consists of the following four steps. First, one computes the fundamental period ω_0 near a large complex structure point by explicitly integrating the holomorphic 3-form Ω along a carefully chosen 3-cycle. Second, one analytically continues this period to a point of finite-order monodromy (assuming that such a point exists, which is not always the case). Third, assuming that the order of the monodromy action at that point is sufficiently high and that the fundamental period is a cyclic vector for the corresponding monodromy operator, one can produce a basis of periods ω_j by repeatedly acting with this operator on ω_0 . In practice, this is carried out by using an explicit realization of the finite-order monodromy as a local orbifold action on a branched multiple cover of the moduli space; this procedure then amounts to ‘rotating the branch cut’ used in the expansion of ω_0 near the small radius point in order to obtain the ‘higher’ periods ω_j . Finally, one can in principle analytically continue back from the finite-monodromy point to the large complex structure point by using carefully chosen integral representations compatible with the branch-cuts introduced in defining ω_j . In practice, finding convenient integral representations of ω_j for this purpose is not always straightforward.

This approach depends on various assumptions and can be difficult to carry out in

practice, due to the computational complexity involved and the less than algorithmic nature of some of the steps. The alternative we propose is computationally simpler and more algorithmic. It consists of the following steps.

First, we use the theory of Meijer functions to systematically (and rather easily) produce a special basis of periods adapted to the large complex structure monodromy-weight filtration. (The reader unfamiliar with this concept can find a brief description in Appendix A). These periods (which we will call ‘Meijer periods’) are expressed in terms of Meijer functions, which are *defined* by certain integral representations of Mellin type. Analytic continuation of the Meijer periods is thus straightforward to perform, with the choice of branch-cuts automatically fixed by the condition of convergence of the associated contour integral. This systematically produces the expansions of the periods in all regions of the moduli space, without requiring the computation of monodromies. If knowledge of the monodromy matrices is required, then they can be computed systematically from the expansions of the Meijer periods. Once this has been achieved, a ‘cyclic basis’ of the type considered in [42] can be easily produced, and can be used to provide some (but generally not complete) information about the integral lattice $H^3(X, \mathbb{Z}) \subset H^3(X)$.

We begin with a short review of Meijer functions, with the main purpose of fixing our notation and conventions. Then we illustrate the technique outlined above in a class of one-parameter examples which includes the mirror quintic as well as other models considered in the literature. Finally, we consider a certain ‘degeneration’ of this class of models, which in particular contains a model we will encounter again when studying a two-parameter example in Section 6.

2.1 Meijer functions

We start by reviewing a few basic facts about a class of higher transcendental functions introduced by C. S. Meijer. These functions can be used to generate a fundamental system of solutions of a generalized hypergeometric equation, and therein lies their utility. In a sense, they form the ‘natural’ class of functions associated with hypergeometric systems. As the periods of the holomorphic three-form satisfy a generalized hypergeometric equation, we will be able to use these methods to calculate quantum volumes. (We refer the interested reader to [52] for details about the general theory of such functions and to the excellent paper [55] for a review of their applications to hypergeometric equations.)

The modern definition of Meijer functions proceeds via Mellin-Barnes integrals. To simplify subsequent formulae, we introduce the notation:

$$\Gamma \left(\begin{matrix} x_1 & \dots & x_n \\ y_1 & \dots & y_m \end{matrix} \right) := \frac{\Gamma(x_1) \dots \Gamma(x_n)}{\Gamma(y_1) \dots \Gamma(y_m)} \quad (5)$$

for any complex numbers x_i, y_j . Consider the Mellin-Barnes integral in the complex

plane:

$$\mathbf{I} \left(\begin{array}{cc} a_1 \dots a_A & b_1 \dots b_B \\ c_1 \dots c_C & d_1 \dots d_D \end{array} \right) (z) = \frac{1}{2\pi i} \int_{\gamma} ds \, \Gamma \left(\begin{array}{c} a_1 - s \dots a_A - s, \, b_1 + s \dots b_B + s \\ c_1 - s \dots c_C - s, \, d_1 + s \dots d_D + s \end{array} \right) z^s, \quad (6)$$

with complex a_i, b_j, c_k, d_l and z . For generic a, b, c, d , the integrand has two series of poles:

$$(A) \, a_i - s = -n$$

$$(B) \, b_j + s = -n$$

with n a nonnegative integer. The contour γ is taken to extend from $-i\infty$ to $+i\infty$ (in this order) in such a way as to separate the A-type poles from the B-type poles (see Figure 1). The conditions for convergence of (6) are discussed [52], to which we refer the reader for details. Here we only mention that an essential requirement is that $|\arg(z)| < \pi$, which is necessary in order to assure rapid decrease of the integrand at imaginary infinity. This is an important point implicit in the following sections: when considering the analytic continuation of periods from large to small radius for one-parameter models, the choice of branch-cuts is *automatically* enforced by the use of Mellin-Barnes representations.

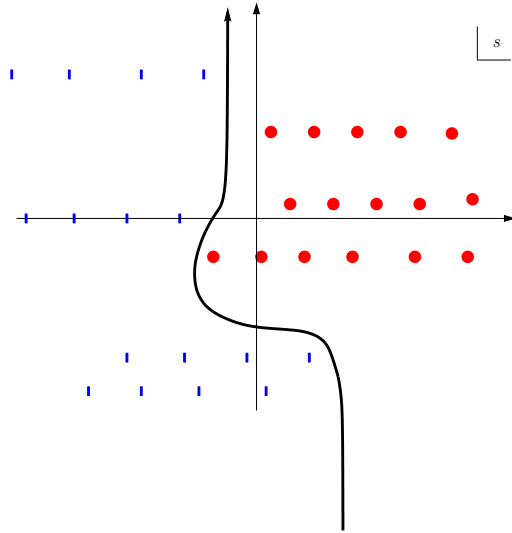


Figure 1. The defining contour for a Mellin-Barnes integral. A-type poles are represented by circles and B-type poles by short vertical lines.

The *Meijer functions* are defined by:

$$\mathbf{G} \left(\begin{array}{cc} \rho_1 \dots \rho_r & \rho'_1 \dots \rho'_{r'} \\ \sigma_1 \dots \sigma_s & \sigma'_1 \dots \sigma'_{s'} \end{array} \right) (z) = \mathbf{I} \left(\begin{array}{cc} \sigma_1 \dots \sigma_s & 1 - \rho_1 \dots 1 - \rho_r \\ \rho'_1 \dots \rho'_{r'} & 1 - \sigma'_1 \dots 1 - \sigma'_{s'} \end{array} \right) (z) \quad (7)$$

whenever the Mellin integral appearing on the right hand side converges. We will frequently use \mathbf{I} rather than \mathbf{G} since the former displays the structure of the Mellin-Barnes integrand more clearly. The functions \mathbf{I} and \mathbf{G} satisfy certain differential equations which can be obtained by considering the finite difference identities obeyed by the associated integrands. This is easiest to write down for \mathbf{G} . Indeed, it is not hard

to see that the function $u(z) = \mathbf{G} \left(\begin{array}{cc} \rho_1 \dots \rho_r & \rho_{r+1} \dots \rho_R \\ \sigma_1 \dots \sigma_s & \sigma_{s+1} \dots \sigma_S \end{array} \right) (z)$ satisfies:

$$D_z^\mu \left(\begin{array}{cc} \rho_1 \dots \rho_R \\ \sigma_1 \dots \sigma_S \end{array} \right) u = 0 \quad , \quad (8)$$

with the operator:

$$D_z^\mu \left(\begin{array}{cc} \rho_1 \dots \rho_R \\ \sigma_1 \dots \sigma_S \end{array} \right) = \prod_{i=1 \dots s} (\delta - \sigma_i) - (-1)^\mu z \prod_{j=1 \dots R} (\delta - \rho_j + 1) \quad , \quad (9)$$

where $\delta = z \frac{d}{dz}$ and $\mu = R - r - s \pmod{2} = r' - s \pmod{2}$. While u depends strongly on the partitions $(\rho_1 \dots \rho_R) = (\rho_1 \dots \rho_r ; \rho'_1 \dots \rho'_{r'})$ and $(\sigma_1 \dots \sigma_S) = (\sigma_1 \dots \sigma_s ; \sigma'_1 \dots \sigma'_{s'})$ used for its definition, the differential operator (9) depends on these partitions only through the number $\mu \in \mathbb{Z}_2$. Thus, by considering different partitions of $(\rho_1 \dots \rho_R)$ and $(\sigma_1 \dots \sigma_S)$ as arguments in G , together with the observation that $D_{-z}^\mu \left(\begin{array}{cc} \rho_1 \dots \rho_R \\ \sigma_1 \dots \sigma_S \end{array} \right) = D_z^{\mu+1} \left(\begin{array}{cc} \rho_1 \dots \rho_R \\ \sigma_1 \dots \sigma_S \end{array} \right)$, we learn that the functions

$$\mathbf{I} \left(\begin{array}{cc} a_1 \dots a_A & b_1 \dots b_B \\ c_1 \dots c_C & d_1 \dots d_D \end{array} \right) (z) \quad ,$$

$$\mathbf{I} \left(\begin{array}{cc} a_1 \dots 1 - d_l \dots a_A & b_1 \dots b_B \\ c_1 \dots c_C & d_1 \dots \hat{d}_l \dots d_D \end{array} \right) (-z) \text{ and } \mathbf{I} \left(\begin{array}{cc} a_1 \dots a_A & b_1 \dots \hat{b}_j \dots b_B \\ c_1 \dots 1 - b_j \dots c_C & d_1 \dots d_D \end{array} \right) (-z)$$

(where a hat indicates removal of the corresponding element from the list) satisfy the *same* differential equation. Therefore, given a Meijer function \mathbf{I} , one can produce other solutions of the same equation by the simple procedure of lifting/lowering the parameters ‘diagonally’ in the symbol of \mathbf{I} , together with replacing each parameter α thus moved by $1 - \alpha$ and performing a change of sign of the argument z for each such operation. This simple observation is the basis of our procedure for obtaining all

\log^j -monodromy periods starting from the fundamental period, as we explain in more detail below.

The Meijer functions are relevant to our problem for the following reason. The periods of the holomorphic three-form on a Calabi-Yau manifold are closely related to generalized hypergeometric functions ¹¹,

$${}_pF_q \left(\begin{matrix} \alpha_1 & \dots & \alpha_p \\ \beta_1 & \dots & \beta_q \end{matrix} \right) (z) = \Gamma \left(\begin{matrix} \beta_1 & \dots & \beta_q \\ \alpha_1 & \dots & \alpha_p \end{matrix} \right) \sum_{n=0}^{\infty} \Gamma \left(\begin{matrix} \alpha_1 + n & \dots & \alpha_p + n \\ \beta_1 + n & \dots & \beta_q + n \end{matrix} \right) \frac{z^n}{n!} = \sum_{n=0}^{\infty} \frac{(\alpha_1)_n \dots (\alpha_p)_n}{(\beta_1)_n \dots (\beta_q)_n} \frac{z^n}{n!} ,$$

(with $p = q + 1$), which are solutions to the generalized hypergeometric equation:

$$\left[\delta \prod_{i=1..q} (\delta + \beta_i - 1) - z \prod_{j=1..p} (\delta + \alpha_j) \right] u = 0 . \quad (10)$$

The generalized hypergeometric functions, in turn, are particular cases of Meijer functions ¹²:

$${}_pF_q \left(\begin{matrix} \alpha_1 & \dots & \alpha_p \\ \beta_1 & \dots & \beta_q \end{matrix} \right) (z) = \Gamma \left(\begin{matrix} \beta_1 & \dots & \beta_q \\ \alpha_1 & \dots & \alpha_p \end{matrix} \right) \mathbf{G} \left(\begin{matrix} 1 - \alpha_1 & \dots & 1 - \alpha_p & . \\ 0 & & 1 - \beta_1 & \dots & 1 - \beta_q \end{matrix} \right) (-z) =$$

$$\Gamma \left(\begin{matrix} \beta_1 & \dots & \beta_q \\ \alpha_1 & \dots & \alpha_p \end{matrix} \right) \mathbf{I} \left(\begin{matrix} 0 & \alpha_1 & \dots & \alpha_p \\ . & \beta_1 & \dots & \beta_q \end{matrix} \right) (-z)$$

(where \cdot indicates that the corresponding group of parameters is missing). Indeed, the hypergeometric operator:

$$d_z \left(\begin{matrix} \alpha_1 & \dots & \alpha_p \\ \beta_1 & \dots & \beta_q \end{matrix} \right) = \delta \prod_{i=1..q} (\delta + \beta_i - 1) - z \prod_{j=1..p} (\delta + \alpha_j) \quad (11)$$

is related to the Meijer operator by:

$$d_z \left(\begin{matrix} \alpha_1 & \dots & \alpha_p \\ \beta_1 & \dots & \beta_q \end{matrix} \right) = D_{-z}^1 \left(\begin{matrix} 1 - \alpha_1 & \dots & 1 - \alpha_p \\ 0, 1 - \beta_1 & \dots & 1 - \beta_q \end{matrix} \right) . \quad (12)$$

In our Calabi-Yau applications, the hypergeometric equations arise as typical Picard-Fuchs equations obeyed by the periods of a one-parameter model. In such a model, we will always choose the coordinate z on the moduli space such that $z = 0$ corresponds to the large complex structure (or large radius) point, $z = \infty$ to the small radius limit and $z = 1$ to the other regular singular point (the analogue of the conifold point of [42]). This assures that the Picard-Fuchs equation will always have the standard hypergeometric form (10). We will sometimes call this coordinate on the moduli

¹¹Here $(x)_n := x(x+1) \dots (x+n-1)$, $(x)_0 := 1$ denotes the Pochhammer symbol.

¹²Note that convergence of the integral on the right hand side requires $|\arg(-z)| < \pi$.

space the ‘standard’ or ‘hypergeometric’ coordinate. Then the parameters α_i, β_j will always be such that $z = 0$ is a point of maximally unipotent monodromy, which implies that the only solutions of (10) which are regular at the origin are multiples of ${}_pF_q \left(\begin{smallmatrix} \alpha_1 & \dots & \alpha_p \\ \beta_1 & \dots & \beta_q \end{smallmatrix} \right) (z)$ (the hypergeometric function itself is characterized among such solutions by the fact that it has value 1 at $z = 0$). The hypergeometric solution thus corresponds to the fundamental period of [39], and is trivial to write down in practice. Writing this solution as a Meijer function and making simple operations on its symbol as above will allow us to produce a basis of solutions of (10), i.e. a basis of periods for the model. Moreover, the ‘Meijer periods’ thus produced are automatically adapted to the monodromy weight filtration (see Appendix A for an explanation of this concept) associated with the large complex structure point. In fact, these periods display a rather universal behaviour around $z = 0$, as we will see in detail below.

2.2 Monodromies

The strategy outlined in Section 1 requires that we understand the behavior of the Meijer periods under monodromy transformations. In this section we set up some general formalism that will allow us to accomplish this goal. Our remarks will clarify the connection with the general theory of Fuchsian systems as explained, for example in [53] (see also [54]).

2.2.1 General remarks

Let us start with a discussion of monodromies for the Meijer equation (8). For simplicity (and direct relevance to this paper) we consider only the case $S = R := p$, which includes the hypergeometric equation. The logarithmic form of the Meijer operator (9) is:

$$\frac{1}{1 + (-1)^{\mu+1}z} D_z^\mu \left(\begin{smallmatrix} \rho_1 & \dots & \rho_p \\ \sigma_1 & \dots & \sigma_p \end{smallmatrix} \right) = \delta^p + \sum_{k=0}^{p-1} B_k(z) \delta^k, \quad (13)$$

where we defined:

$$B_k(z) := \frac{Q_k + (-1)^{\mu+1}z R_k}{1 + (-1)^{\mu+1}z}, \quad (14)$$

with:

$$Q_k := (-1)^{p-k} \sum_{1 \leq i_1 < \dots < i_{p-k} \leq p} \sigma_{i_1} \dots \sigma_{i_{p-k}} \quad (15)$$

$$R_k := (-1)^{p-k} \sum_{1 \leq i_1 < \dots < i_{p-k} \leq p} (\rho_{i_1} - 1) \dots (\rho_{i_{p-k}} - 1). \quad (16)$$

$$(17)$$

The coefficient functions $B_k(z)$ interpolate between $B_k(0) = Q_k$ and $B_k(\infty) = R_k$.

The Meijer equation (8) can be rewritten as the first order system:

$$\delta w(z) = A(z) w(z) \quad , \quad (18)$$

where $w(z) := \begin{bmatrix} u(z) \\ \delta u(z) \\ \dots \\ \delta^{p-1}u(z) \end{bmatrix}$ and we set:

$$A(z) := \begin{bmatrix} 0 & 1 & 0 & \dots & 0 & 0 \\ 0 & 0 & 1 & \dots & 0 & 0 \\ \dots & \dots & \dots & \dots & \dots & \dots \\ 0 & 0 & 0 & \dots & 0 & 1 \\ -B_0(z) & -B_1(z) & \dots & \dots & -B_{p-2}(z) & -B_{p-1}(z) \end{bmatrix} \quad (19)$$

Given an arbitrary basis $\{U_j(z)\}_{j=0\dots p-1}$ of solutions of (8), we define its monodromy matrices $T[0]$ and $T[\infty]$ around $z = 0$ and $z = \infty$ by:

$$\begin{aligned} U(e^{2\pi i}z) &= T[0]U(z) \quad \text{for } |z| \ll 1 \quad , \\ U(e^{2\pi i}z) &= T[\infty]U(z) \quad \text{for } |z| \gg 1 \quad , \end{aligned}$$

where $U(z) := \begin{bmatrix} U_0(z) \\ U_1(z) \\ \dots \\ U_{p-1}(z) \end{bmatrix}$. If $\Phi(z)$ is the associated fundamental matrix of (18),

i.e. the matrix having $w_j = \begin{bmatrix} U_j(z) \\ \delta U_j(z) \\ \dots \\ \delta^{p-1}U_j(z) \end{bmatrix}$ ($j = 0 \dots p-1$) as its columns, then the

differential version of the nilpotent orbit theorem states that there exists a regular¹³ matrix-valued function S (which, following modern terminology, we call the nilpotent orbit of Φ) and a matrix R such that¹⁴:

$$\Phi(z) = S(z) z^R \quad . \quad (20)$$

This immediately gives $T = e^{2\pi i R^t}$ and implies that $S(z)$ satisfies the matrix differential equation:

$$\delta S(z) = A(z)S(z) - S(z)R \quad . \quad (21)$$

Expanding $S(z) = \sum_{n=0}^{\infty} S^{(n)} z^n$ shows that the matrix $S^{(0)} := S(0)$ (which plays the role of initial condition for (21), and thus must be invertible if $\Phi(z)$ is to be a fundamental matrix for (18)) must satisfy:

$$S(0)^{-1} A(0) S(0) = R \quad . \quad (22)$$

¹³Regular in the vicinity of $z = 0$.

¹⁴This decomposition has a standard geometric interpretation, which we recall in Appendix A.

Under a change of basis $U(z) \rightarrow MU(z)$, we have $\Phi(z) \rightarrow \Phi(z)M^t$ and:

$$R \rightarrow M^{-t}RM^t \quad (23)$$

$$S(z) \rightarrow S(z)M^t \quad (24)$$

(where $M^{-t} := (M^{-1})^t$). In particular, we have $S(0) \rightarrow S(0)M^t$. Choosing $M := S(0)^{-t}$ gives a distinguished fundamental system $\Phi_{can}(z)$ with the properties:

$$R_{can}[0] := A(0) = \begin{bmatrix} 0 & 1 & 0 & \dots & 0 & 0 \\ 0 & 0 & 1 & \dots & 0 & 0 \\ \dots & \dots & \dots & \dots & \dots & \dots \\ 0 & 0 & 0 & \dots & 0 & 1 \\ -Q_0 & -Q_1 & \dots & \dots & -Q_{p-2} & -Q_{p-1} \end{bmatrix} \quad (25)$$

$$S_{can}(0) := I, \quad (26)$$

whose associated basis U_{can} will be called the *canonical basis*.

To understand the behaviour at $z = \infty$, note that $\delta_{1/z} = -\delta_z$, which gives:

$$D_{1/z}^\mu \begin{pmatrix} \rho_1 & \dots & \rho_p \\ \sigma_1 & \dots & \sigma_p \end{pmatrix} = \frac{(-1)^{\mu+p+1}}{z} D_z^\mu \begin{pmatrix} 1 - \sigma_1 & \dots & 1 - \sigma_p \\ 1 - \rho_1 & \dots & 1 - \rho_p \end{pmatrix}. \quad (27)$$

This is again a Meijer operator, with symbols $\rho'_j := 1 - \sigma_j$ and $\sigma'_i := 1 - \rho_i$. The canonical monodromy is again of the form (25), but with Q_k replaced by $Q'_k := (-1)^{p-k} R_k$:

$$R_{can}[\infty] := - \begin{bmatrix} 0 & 1 & 0 & \dots & 0 & 0 \\ 0 & 0 & 1 & \dots & 0 & 0 \\ \dots & \dots & \dots & \dots & \dots & \dots \\ 0 & 0 & 0 & \dots & 0 & 1 \\ -Q'_0 & -Q'_1 & \dots & \dots & -Q'_{p-2} & -Q'_{p-1} \end{bmatrix}. \quad (28)$$

The minus sign in front of this expression keeps track of the fact that the transformation $z \rightarrow e^{2\pi i} z$ corresponds to $\frac{1}{z} \rightarrow e^{-2\pi i} \frac{1}{z}$; that is, inversion in the complex plane reverses the orientation of a contour which surrounds the origin. This amounts to inversion of the associated monodromy matrix, an observation which will be used again in Subsection 4.3.

2.2.2 The hypergeometric case

Let us now apply these results to the hypergeometric case, which is the case of interest for us. In view of (11), this is defined by $R = S = p = q + 1$ and:

$$\begin{aligned} \rho_i &:= 1 - \alpha_i \quad (i = 1 \dots p) \\ \sigma_1 &:= 0, \quad \sigma_{j+1} := 1 - \beta_j \quad (j = 1 \dots q). \end{aligned}$$

According to the discussion above, if $u(z)$ satisfies the generalized hypergeometric equation with (hypergeometric) symbol $\begin{pmatrix} \alpha_1 \dots \alpha_{q+1} \\ \beta_1 \dots \beta_q \end{pmatrix}$, then $\tilde{u}(t) := u(1/t)$ satisfies

the Meijer equation $D_t^\mu \begin{pmatrix} 1, \beta_1 \dots \beta_q \\ \alpha_1 \dots \alpha_{q+1} \end{pmatrix} \tilde{u} = 0$ (note that this equation is *not* generally of hypergeometric type). Applying the general results derived above shows that the canonical forms of the hypergeometric monodromies around $z = 0$ and $z = \infty$ are:

$$R_{can}[0] : = \begin{bmatrix} 0 & 1 & 0 & \dots & 0 & 0 \\ 0 & 0 & 1 & \dots & 0 & 0 \\ \dots & \dots & \dots & \dots & \dots & \dots \\ 0 & 0 & 0 & \dots & 0 & 1 \\ 0 & -Q_1 & \dots & \dots & -Q_{q-1} & -Q_q \end{bmatrix} \quad (29)$$

$$R_{can}[\infty] : = - \begin{bmatrix} 0 & & 1 & & 0 & \dots & 0 & 0 \\ 0 & & 0 & & 1 & \dots & 0 & 0 \\ \dots & & \dots & & \dots & \dots & \dots & \dots \\ 0 & & 0 & & 0 & \dots & 0 & 1 \\ (-1)^q R_0 & -(-1)^{q-1} R_1 & \dots & \dots & -R_{q-1} & R_q \end{bmatrix}, \quad (30)$$

with:

$$Q_k : = \sum_{1 \leq i_1 < \dots < i_{q-k+1} \leq q} (\beta_{i_1} - 1) \dots (\beta_{i_{q-k+1}} - 1) \quad (31)$$

$$R_k : = \sum_{1 \leq i_1 < \dots < i_{q-k+1} \leq q+1} \alpha_{i_1} \dots \alpha_{i_{q-k+1}}, \quad (32)$$

where $k = 0 \dots q$. In this paper we only consider models for which all β_i are equal to 1. Then all Q_k are zero and the matrix $R_{can}[0]$ is in Jordan form. On the other hand, the Jordan form of the matrix $R_{can}[\infty]$ depends on the relative values of the parameters α_k , as we will illustrate in detail below.

Before proceeding to apply the theory of Meijer functions to various examples, let us mention that the remaining regular singular point of (10) (namely the point $z = 1$) is somewhat special in the following sense. While one can change variables (for example, by the transformation $z \rightarrow \frac{1-z}{z}$) in such a way as to move the point $z = 1$ to the origin of the complex plane, the resulting equation is not of Meijer type. This is the root of the technical difficulties encountered when studying the behaviour of a system of solutions of (10) around $z = 1$, and the main reason why a completely uniform treatment of this problem is not yet available. We refer the interested reader to [55] for a thorough discussion of what is known about this subject.

On the other hand, the monodromies around $z = 1$ can be easily computed for a convenient basis of solutions around that point, by making use of the general theory of [53]. However, this will not be relevant for us, for the following reason. The canonical bases associated with the points 0 and ∞ (as well as the more general standard basis associated with the point $z = 1$) generally correspond to different fundamental systems of solutions of (10). What one is interested in when studying one-parameter models is to compute the monodromies of a *given* basis around these three points; in other words, one considers the analytic continuation of a fundamental system throughout the entire complex plane and one asks for the monodromies of the basis of solutions thus obtained. If $T[0]$ and $T[\infty]$ are the monodromies of such a system about 0 and

∞ , then the monodromy of *that* system about $z = 1$ is easily obtained as $T[1] = T[0]^{-1}T[\infty]$, an equation which follows from the structure of the fundamental group of the thrice-punctured Riemann sphere $\mathbb{P}^1 - \{0, 1, \infty\}$. This relation, as well as our convention for the monodromy matrix $T[1]$ are depicted in Figure 2. In practice, it will thus suffice to compute $T[0]$ and $T[\infty]$ for an analytically continued fundamental system. As we illustrate in detail below, the most convenient choice is to consider the analytic continuation of the Meijer basis, which is easily obtained from its Mellin-Barnes representation through a computation of residues. This basis has the added advantage that it allows for a very systematic computation of the monodromies about 0 and ∞ . The utility of the canonical monodromies computed above is that they will appear as intermediate steps in this procedure, which essentially consists in computing the transition matrices from the Meijer basis to the two canonical bases associated with the points 0 and ∞ .

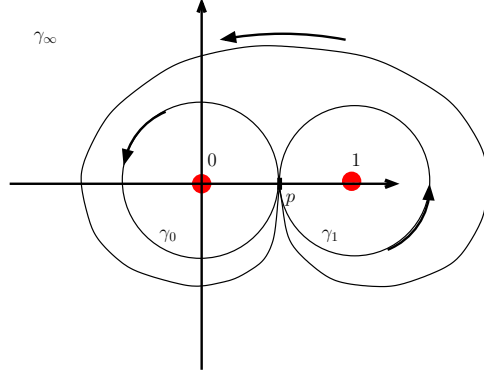


Figure 2. Generators of the fundamental group $\pi_1(\mathbb{P}^1 - \{0, 1, \infty\}, p)$ of the thrice punctured sphere (using the base point $p = \frac{1}{2}$). The monodromy operators $T[0], T[1], T[\infty]$ used in this paper correspond to the paths $\gamma_0, \gamma_1, \gamma_\infty$, all of which are oriented in counterclockwise manner. The relation $\gamma_0 \cdot \gamma_1 = \gamma_\infty$ induces the equality $T[1] = T[0]^{-1}T[\infty]$.

3 The Mirror Map and Integral Structure

Identifying the B-type D-brane state associated with a collapsing holomorphic cycle requires a deeper understanding of the map induced by mirror symmetry between $H_3(Y, \mathbb{Z})$ and $H_{\text{even}}(X, \mathbb{Z})$. In this section we discuss what is known about this issue and identify the obstacle that as yet needs to be surmounted. While we believe that the essential point we make below has not been widely appreciated, most of what follows involves manipulating and reinterpreting ideas of [5] and [42] to which we refer the reader for background and notation.

In deriving the mirror map $t_l = \frac{\int_{\gamma_l} \Omega}{\int_{\gamma_0} \Omega}$ for the quintic mirror-quintic pair (X, Y) , the authors of [42] proceeded in the following way. Choose an integral symplectic basis (A_a, B^b) of $H_3(Y, \mathbb{Z})$ with dual cohomology basis (α^a, β_b) , where $a, b = 1, 2$. Then write the holomorphic three-form Ω of Y as

$$\Omega = \left(\int_{A_a} \Omega \right) \alpha^a - \left(\int_{B^b} \Omega \right) \beta_b \quad , \quad (33)$$

and the prepotential \mathcal{G} as

$$\mathcal{G} = \frac{1}{2} \left(\int_{A_a} \Omega \right) \left(\int_{B^a} \Omega \right) \quad . \quad (34)$$

Defining coordinates z^a in terms of the periods through $z^a = \int_{A_a} \Omega$ allows us to write:

$$\Omega = \Pi^j g_j \quad , \quad (35)$$

with $\Pi^t = (\partial_{z_1} \mathcal{G}, \partial_{z_2} \mathcal{G}, z_1, z_2)$ and $g = (-\beta_1, -\beta_2, \alpha^1, \alpha^2)$.

One can follow a similar procedure for X . Choose an integral basis of cycles (E_1, E_2, F^1, F^2) for $H_0(X, \mathbb{Z})$, $H_2(X, \mathbb{Z})$, $H_4(X, \mathbb{Z})$, and $H_6(X, \mathbb{Z})$, respectively. Let $(\rho^1, \rho^2, \sigma_1, \sigma_2)$ be dual integral cohomology classes, and following [5], let λ and μ be anti-commuting constant Grassman parameters so that $(\theta^1, \theta^2, \theta_1, \theta_2) := (\lambda \rho^1, \lambda \rho^2, \mu \sigma_1, \mu \sigma_2)$ has a symplectic intersection form. Then, introduce $\Upsilon \in \oplus_k H^{k,k}(X, \mathbb{Z})$, the mirror to Ω , expressed as:

$$\Upsilon = \left(\int_{E_a} \Upsilon \right) \theta^a - \left(\int_{F^b} \Upsilon \right) \theta_b \quad , \quad (36)$$

and the mirror prepotential on X :

$$\mathcal{F} = \frac{1}{2} \left(\int_{E_a} \Upsilon \right) \left(\int_{F^a} \Upsilon \right) \quad . \quad (37)$$

The latter expression is purely formal as we know of no a priori means of calculating the periods of Υ , without recourse to mirror symmetry. However, following [5] and [42], we can write down an expression for \mathcal{F} which is valid up to worldsheet instanton corrections, by recalling that Yukawa couplings are given by third derivatives of the prepotential. Indeed, writing the complexified Kähler form on X as $B + iJ = \frac{w^1}{w^2} \rho^2$ for $w^1 \in \mathbb{C}$, we have:

$$\mathcal{F} = -\frac{1}{3!} \int_X (\rho^2)^3 \frac{(w^1)^3}{w^2} + \frac{1}{2} a (w^1)^2 + b w^1 w^2 + \frac{1}{2} c (w^2)^2 + \mathcal{O}(e^{-w^1/w^2}), \quad (38)$$

where w^2 is an auxiliary homogeneous coordinate on the moduli space and $t = w^1/w^2$. Now, if we could actually evaluate (38) directly (and exactly), then we could write

$$\Upsilon = \Pi^j f_j \quad , \quad (39)$$

with $\Pi^t = (\partial_{w_1} \mathcal{F}, \partial_{w_2} \mathcal{F}, w_1, w_2)$ and $f = (-\theta_1, -\theta_2, \theta^1, \theta^2)$. Then, the basis-independent equality $\Omega = \Upsilon$ (an equality that follows since in the underlying conformal field theory

Ω and Υ correspond to one and the same operator) can be expressed using (35) and (39) as:

$$\Pi^i = N_j^i \Pi_j \quad (40)$$

$$g_j = N_j^i f_i, \quad (41)$$

where N is a matrix relating the bases f and g .

In practice, we cannot carry out this program as written because we do not know how to evaluate (38) exactly. But as noticed and used in [42], if we call $\mathcal{F}^{\text{pert}}$ the approximation to \mathcal{F} with all instantons corrections dropped, equating Ω and Υ in the large complex structure/large radius limit via

$$\Pi^{\text{pert } i} = N_j^i \Pi_j \quad (42)$$

is enough to determine N . This statement relies on the conjecture of Aspinwall and Lutken [48] which asserts that N should be an integral symplectic matrix. As such, it can be determined exactly even if we only impose (42) in the large radius limit.

Once we have determined N , we can use it to relate the integral cohomologies of X and Y via (41), or the integral homologies via its dual relation:

$$(F^1, F^2, E_1, E_2)^t = N(B^1, B^2, A_1, A_2)^t. \quad (43)$$

In principle, this solves the problem of identifying the map between $H_3(Y, \mathbb{Z})$ and $\oplus_k H_{2k}(X, \mathbb{Z})$. Although we have recounted this discussion at the level of the quintic/mirror quintic example, it is of course more general. Nevertheless, there is an important outstanding issue: Even if we work in the large radius limit and thereby drop instanton corrections to \mathcal{F} , from (38) we see that there are three numbers, a, b, c which are as yet undetermined. As pointed out in [42], the real part of these numbers do not contribute to the Yukawa couplings or the metric on the moduli space, and the only imaginary parts they can contain (which do affect the metric) arise at four loops in the sigma model, thereby only contributing to c . In the case of the quintic, a, b, c enter into N in the following manner

$$N = \begin{bmatrix} -1 + 2a' & b' & -a' & 0 \\ 2b' & c' & -b' & -1 \\ 2 & 0 & -1 & 0 \\ 0 & 1 & 0 & 0 \end{bmatrix} \quad (44)$$

with $a' = a + \frac{11}{2}$, $b' = b - \frac{25}{12}$, $c' = c + \frac{25i}{\pi} \zeta(3)$. In [42], the authors arbitrarily chose $a' = b' = c' = 0$, noting that other choices differ by an integral symplectic change of basis that would not affect the calculations of their paper. In our case, though, such a change of basis affects the mirror map on integral homology and hence does affect our conclusions. For example, in the case of the quintic with the choice $a' = b' = c' = 0$, we have the map $A_2 \rightarrow F^2$. A_2 is the cycle whose period vanishes at the conifold point of the mirror quintic while F^2 is its mirror six-cycle on the quintic itself. Hence one is

tempted to conclude that the pure six-cycle collapses on the quintic when its Kähler form is tuned to be mirror to the conifold point [35]. But, for arbitrary $a' = b' = c'$, A_2 is mapped to a linear combination of the six, four, two, and zero cycles. The fact that the coefficient of the six-cycle is nonzero for any choice of $a' = b' = c'$ tells us that a six-brane is collapsing, but the lower order contributions dictate a particular binding of lower brane charges to the six-brane.

Can we calculate $a' = b' = c'$ from first principles? At the level of the sigma model its hard to see how, as their real parts seem to have no impact on sigma model observables. At the level of D-brane field theory, perhaps there is a way to calculate them, but as yet this is an unsolved problem. Hence, as discussed in the introduction, we are forced in this paper to discuss the masses of wrapped $2j$ -branes, leaving their lower brane content unspecified.

Let us add a few remarks about the connection with recent work on the relation between D-branes and K -theory. It is now well-known [11] that the charges of type B D-branes on X should generally be considered to take values in certain K -groups $K(X)$. While this was initially discovered [11] through anomaly-cancellation arguments, it is in fact not surprising given the relation between D-brane moduli spaces and moduli spaces of holomorphic vector bundles proposed in [19]. From this point of view, the lattice $H^{even}(X)$ appears as a coarser version of the space of charges, via the natural embedding $K(X) \rightarrow H(X)$. Above, we considered the problem of identifying the integral structure from a perturbative (conformal field-theoretic) point of view, but a probably more powerful approach to this question is to analyze the issue from the point of view of the Strominger-Yau-Zaslow conjecture [15, 16]. In that set-up, mirror symmetry is expected to map special Lagrangian submanifolds C of Y (together with a flat connection on C) to holomorphic vector bundles on X (or, rather, a certain type of gerbe generalization of this concept). The trace of such a map in some cohomology theory should then yield the mirror map between (a version of) $H(Y)$ and $K(X)$. Finally, the map $H^3(Y) \rightarrow H^{even}(X)$ would be induced from this through the embedding $K(X) \rightarrow H(X)$. Some expectations of these type are summarized by the homological mirror symmetry conjecture of Kontsevich (see [17]), but it is difficult to be more precise without first gaining of a proper understanding of the many physical and mathematical issues involved in such an approach.

4 Examples I: The ‘generic’ family of compact one-parameter models

We are now ready to apply the methods discussed above, and we begin with the hypergeometric equation satisfied by the periods of a class of one-parameter examples:

$$\left[\delta^4 - z(\delta + \alpha_1)(\delta + \alpha_2)(\delta + \alpha_3)(\delta + \alpha_4) \right] u = 0 \quad . \quad (45)$$

This is associated with the hypergeometric symbol $\left(\begin{smallmatrix} \alpha_1, \alpha_2, \alpha_3, \alpha_4 \\ 1, 1, 1 \end{smallmatrix} \right)$, where we take α_j to be *rational* numbers¹⁵. In particular, the mirror quintic of [42] is of this type. We first illustrate our method for computing a fundamental system of periods and the associated monodromies for this class of models.

To simplify subsequent discussion, we assume that:

- (1) None of the differences $\alpha_k - \alpha_l$ (with $k \neq l$) is an integer.
- (2) None of the number α_k is an integer.
- (3) $\alpha_k > 0$ for all $k = 1 \dots 4$.

These conditions will allow us to avoid certain exceptional cases in the discussion of analytic continuation below.

Before proceeding with a detailed analysis, let us make some brief comments on the role and range of applicability of the results we derive in this section. The models we consider are ‘generic’¹⁶ from the point of view of their hypergeometric equation, inasmuch as conditions (1) – (3) are satisfied for generic systems of *rational* parameters $\alpha_1 \dots \alpha_4$. This class of examples exhibits most of the qualitative features familiar from the study of the mirror quintic performed in [42]; in particular, such models admit a Landau-Ginsburg point, due to the fact that the expansion of the periods near the small radius limit does not contain logarithmic factors¹⁷. Of the three conditions above, only (1) is essential for assuring this behaviour; imposing the other conditions plays mostly the role of avoiding formulae which would be too complicated to treat in a general fashion.

On the other hand, there exist many one-parameter examples which do not satisfy condition (1) and hence do not entirely fit into this scheme. Even in such cases, however, the expansions and monodromies we derive near the large complex structure point can often be applied. Such models can be thought of as ‘degenerations’ of the ‘generic’ family considered here. Hence this class can be viewed as a ‘generating’ or ‘universal’ family which contains other models as various limits. This leads to a hierarchy of one-parameter models (discussed in more detail in Section 5), having the ‘generic’ family at its top.

¹⁵This seems to always be the case in practice, and thus is not a significant reduction in generality.

¹⁶This is not to say that such models are generic (meaning abundant) as a class of one-parameter examples. In fact, quite the contrary seems to be the case, at least based on a limited investigation of the models constructed in the literature.

¹⁷This is enforced by condition (1), which, as can be checked immediately by using the results of subsection 2.2, and will be confirmed by explicit computation below, assures that the monodromy around the point $z = \infty$ is of finite order

4.1 The Meijer periods

Starting with the fundamental period $U_0(z) = {}_4F_3 \left(\begin{smallmatrix} \alpha_1, \alpha_2, \alpha_3, \alpha_4 \\ 1, 1, 1 \end{smallmatrix} \right) (z)$ and applying the procedure discussed in the previous subsection gives the following fundamental system of solutions:

$$U_j(z) = \Gamma \left(\begin{smallmatrix} 1, 1, 1 \\ \alpha_1, \alpha_2, \alpha_3, \alpha_4 \end{smallmatrix} \right) \mathbf{I} \left(\begin{smallmatrix} 0^{(j+1)} & \alpha_1, \alpha_2, \alpha_3, \alpha_4 \\ & 1^{(3-j)} \end{smallmatrix} \right) ((-1)^{j+1} z) \quad , \quad (46)$$

where $j = 0 \dots 3$ and the notation $x^{(k)}$ indicates that the symbol x is repeated k times.

The expansions of (46) around the points $z = 0$ (large complex structure) and $z = \infty$ (Landau-Ginzburg) can be obtained easily by a computation of residues. Indeed, let us introduce the following notation for the integrand of the associated Mellin-Barnes representations:

$$\begin{aligned} \phi_j(s) &:= \Gamma \left(\begin{smallmatrix} 1, 1, 1 \\ \alpha_1, \alpha_2, \alpha_3, \alpha_4 \end{smallmatrix} \right) \Gamma \left(\begin{smallmatrix} (-s)^{(j+1)} & s + \alpha_1 \dots s + \alpha_4 \\ (s+1)^{(3-j)} \end{smallmatrix} \right) ((-1)^{j+1} z)^s = \\ &= \frac{1}{\prod_{i=1 \dots 4} \Gamma(\alpha_i)} \frac{\Gamma(-s)^{j+1} \prod_{i=1 \dots 4} \Gamma(s + \alpha_i)}{\Gamma(s+1)^{3-j}} ((-1)^{j+1} z)^s \quad . \end{aligned} \quad (47)$$

With this notation, we have:

$$U_j(z) = \frac{1}{2\pi i} \int_{\gamma} ds \phi_j(s) \quad . \quad (48)$$

The integrand $\phi_j(s)$ has poles at:

$$(A) \quad s = n$$

$$(B) \quad s = -\alpha_i - n,$$

for each nonnegative integer n .

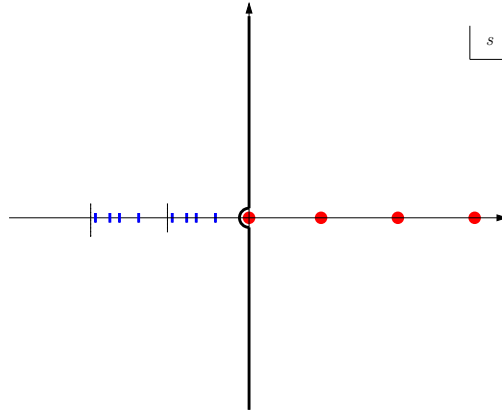


Figure 3. The defining contour for the Mellin-Barnes representation of the Meijer periods.

Consider first the expansions for $|z| < 1$. In this case, the asymptotic behaviour of the integrand in the complex plane allows us to close the contour to the right at $+\infty$ (see Figure 4).

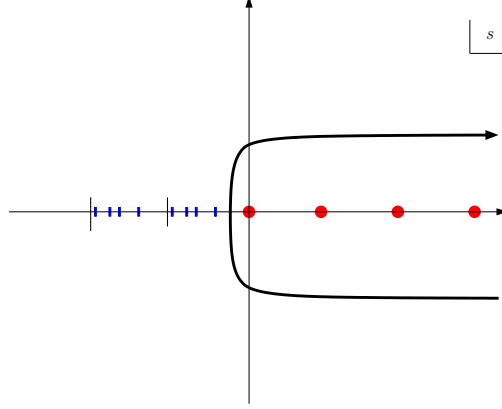


Figure 4. Contour for the expansion around the large complex structure point.

Only A-type poles contribute to the associated Cauchy expansion, and these poles are multiple of order $j + 1$. The computation of the associated residues proceeds in the following standard manner. In order to isolate the poles of the integrand, notice that the identity $\Gamma(-s) = \frac{(-1)^{n+1}}{s-n} \frac{\Gamma(-s+n+1)}{(s-n+1)_n}$ allows us to write:

$$\phi_j(s) := \frac{(-1)^{(j+1)(n+1)}}{\prod_{i=1} \dots 4 \Gamma(\alpha_i)} \frac{f_j(s)}{(s-n)^{j+1}}, \quad (49)$$

with:

$$f_j(s) = \frac{\Gamma(-s+n+1)^{j+1} \prod_{i=1} \dots 4 \Gamma(s+\alpha_i)}{\Gamma(s+1)^{3-j} [(s-n+1)_n]^{j+1}} ((-1)^{j+1} z)^s. \quad (50)$$

Computing the residues is thereby reduced to calculating the derivatives $f_j^{(j)}(n)$ for $j = 0 \dots 3$. One can achieve this efficiently by first computing the derivatives of $g_j(s) = \log(f_j(s))$, with the result that $f_j^{(j)}(n) = f_j(n)\nu_j(n)$, where:

$$\begin{aligned} \nu_0 &= 1 \\ \nu_1(n, z) = g'_1(n, z) &= \eta_1(n) + \log(z) \\ \nu_2(n, z) = g''_2(n, z) + [g'_2(n, z)]^2 &= \eta'_2(n) + (\eta_2(n) + \log(-z))^2 \\ \nu_3(n, z) = g'''_3(n, z) + 3g''_3(n, z)g'_3(n, z) + g'_3(n, z)^3 &= \eta''_3(n) + 3\eta'_3(n)(\eta_3(n) + \log z) + (\eta_3(n) + \log z)^3, \end{aligned} \quad (51)$$

with:

$$\eta_j^{(i)}(n) = \sum_{k=1}^4 \psi^{(i)}(n + \alpha_k) - (3-j)\psi^{(i)}(n+1) - (-1)^i(j+1) \left[\psi^{(i)}(1) + i! \sum_{l=1}^n \frac{1}{l^{i+1}} \right] . \quad (52)$$

This gives the expansion of the Meijer periods for $|z| < 1$:

$$U_j(z) = \frac{(-1)^j}{j!} \sum_{n=0}^{\infty} \frac{(\alpha_1)_n (\alpha_2)_n (\alpha_3)_n (\alpha_4)_n}{(n!)^4} \nu_j(n, z) z^n . \quad (53)$$

If $|z| > 1$ then one can close the contour to the left (Figure 5). In this case, we have contributions only from the (B)-type poles of the integrand, which are all simple:

$$\begin{aligned} \text{Res}_{-n-\alpha_k} \phi_j(s) &= \frac{(-1)^n}{n!} \frac{\Gamma(n + \alpha_k)^{j+1} \prod_{l=1 \dots 4}' \Gamma(\alpha_l - \alpha_k - n)}{\Gamma(1 - n - \alpha_k)^{3-j} \prod_{k=1 \dots 4} \Gamma(\alpha_k)} ((-1)^{j+1} z)^{-n-\alpha_k} = \\ &= \left(\frac{\sin(\pi \alpha_k)}{\pi} \right)^{3-j} \frac{\Gamma(\alpha_k)^4}{\prod_{i=1 \dots 4} \Gamma(\alpha_i)} \left[\prod_{l=1 \dots 4}' \Gamma(\alpha_l - \alpha_k) \right] ((-1)^{j+1} z)^{-\alpha_k} \frac{[(\alpha_k)_n]^4}{n! \prod_{l=1 \dots 4}' (1 + \alpha_k - \alpha_l)_n} z^{-n} , \end{aligned}$$

where $\prod_{l=1 \dots 4}' \{ \dots \} := \prod_{l=1 \dots 4, l \neq k} \{ \dots \}$ and the second equality follows upon using the completion formula:

$$\Gamma(x)\Gamma(1-x) = \frac{\pi}{\sin(\pi x)} . \quad (54)$$

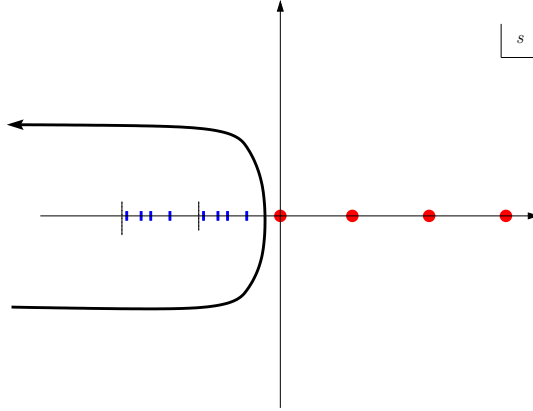


Figure 5. Contour for the expansion around the Landau-Ginzburg point.

Putting everything together, we obtain the expansion of the Meijer periods for $|z| > 1$:

$$\begin{aligned} U_j(z) &= \frac{1}{\prod_{i=1 \dots 4} \Gamma(\alpha_i)} \sum_{k=1}^4 \left(\frac{\sin(\pi \alpha_k)}{\pi} \right)^{3-j} \Gamma(\alpha_k)^4 \prod_{l=1 \dots 4}' \Gamma(\alpha_l - \alpha_k) ((-1)^{j+1} z)^{-\alpha_k} \times \\ &\quad \times {}_4F_3 \left(\begin{matrix} \alpha_k, \alpha_k, \alpha_k, \alpha_k \\ 1 + \alpha_k - \alpha_1, \dots, \hat{1}, \dots, 1 + \alpha_k - \alpha_4 \end{matrix} \right) (1/z) , \quad (55) \end{aligned}$$

where $\hat{1}$ indicates absence of $1 = 1 + \alpha_k - \alpha_k$ in the hypergeometric symbol.

4.2 Monodromies of the Meijer periods

The canonical form of the monodromies around the points $z = 0$ and $z = \infty$ is easily determined by making use of the general relations (29). In our case, one has $S_k = 0$ ($k = 1 \dots 3$) and $R_k := \sum_{1 \leq i_1 < \dots < i_{4-k} \leq 4} \alpha_{i_1} \dots \alpha_{i_{4-k}}$. In particular, it follows that the matrix $R_{can}[0]$ is in Jordan form:

$$R_{can}[0] = \begin{bmatrix} 0 & 1 & 0 & 0 \\ 0 & 0 & 1 & 0 \\ 0 & 0 & 0 & 1 \\ 0 & 0 & 0 & 0 \end{bmatrix}, \quad (56)$$

while the Jordan form of $R_{can}[\infty]$ is given by:

$$R_J[\infty] = \begin{bmatrix} -\alpha_1 & 0 & 0 & 0 \\ 0 & -\alpha_2 & 0 & 0 \\ 0 & 0 & -\alpha_3 & 0 \\ 0 & 0 & 0 & -\alpha_4 \end{bmatrix}. \quad (57)$$

Since α_i are all rational, it immediately follows that $T_J[\infty]$ (and thus $T_{can}[\infty]$) has finite order, so that $z = \infty$ can be interpreted as a Landau-Ginzburg point. Following the program outlined above, we proceed to compute the monodromies of the Meijer basis around the points $z = 0, 1, \infty$.

4.2.1 Meijer monodromies around $z = 0$

The Meijer monodromy $T[0] = e^{2\pi i R[0]^t}$ around $z = 0$ can be determined as follows. Let $U(z)$ be the column vector with entries $U_0(z) \dots U_3(z)$, $\Phi(z)$ be the associated fundamental matrix of the first order system (18), which has entries $\Phi_{ij}(z) := \delta^i U_j(z)$, and $S(z)$ the associated nilpotent orbit, which satisfies (20) and (21). We can separate the logarithmic factors in $U(z)$ by writing:

$$U(z)^t = Z(z)q(z), \quad (58)$$

i.e.

$$U_j(z) = \sum_{s=0}^3 q_{sj}(z)(\log z)^s, \quad (59)$$

where $Z(z)$ is the row vector:

$$Z(z) := \begin{bmatrix} 1 & \log z & (\log z)^2 & (\log z)^3 \end{bmatrix} \quad (60)$$

and $q(z)$ plays the role of the nilpotent orbit of $U(z)$ as discussed in subsection 2.2.

Under a change of basis $U(z) \rightarrow U'(z) = M^{-1}U(z)$ (with M an invertible matrix), we have $U'(z)^t = Z(z)q'(z)$ with $q'(z) = q(z)M^{-t}$ and $\Phi'(z) = \Phi(z)M^{-t}$, $S'(z) = S(z)M^{-t}$, $R' = M^t R M^{-t}$. As discussed earlier, choosing M such that $S'(0) = I$, we

have $R'(0) = A(0) = R_{can}[0]$. In this case, $\Phi'(z) = S'(z)z^{R_{can}[0]}$, and since $R_{can}[0]$ is in Jordan form, we immediately obtain:

$$z^{R_{can}[0]} = \begin{bmatrix} 1 & \log z & \frac{1}{2}(\log z)^2 & \frac{1}{6}(\log z)^3 \\ 0 & 1 & \log z & \frac{1}{2}(\log z)^2 \\ \cdots & \cdots & \cdots & \cdots \\ 0 & 0 & 0 & 1 \end{bmatrix}, \quad (61)$$

i.e. $(z^{R_{can}[0]})_{ij} = \frac{(\log z)^{j-i}}{(j-i)!}$. This allows us to write $U'(z)^t = Z(z)q'(z)$ with $q'(z)_{sj} := \frac{S'_{0,j-s}(z)}{s!}$. In particular, we obtain:

$$q'(0) = \text{diag}(1, 1, 1/2, 1/6) \quad , \quad (62)$$

which allows us to determine $M = q(0)^t q'(0)^{-1}$. Once M^t is known, the monodromy of the Meijer basis follows from the relation $T[0] = MT_{can}[0]M^{-1}$, where $T_{can}[0]^t = e^{2\pi i R_{can}[0]}$ is given by:

$$T_{can}[0]^t = \begin{bmatrix} 1 & 2\pi i & \frac{1}{2}(2\pi i)^2 & \frac{1}{6}(2\pi i)^3 \\ 0 & 1 & 2\pi i & \frac{1}{2}(2\pi i)^2 \\ \cdots & \cdots & \cdots & \cdots \\ 0 & 0 & 0 & 1 \end{bmatrix}. \quad (63)$$

In our class of examples, $q(0)$ can be easily determined from the expansions given above. Indeed, we can write:

$$\nu_j(n) = \sum_{s=0}^j v_{sj}(n)(\log z)^s \quad , \quad (64)$$

with:

$$\begin{array}{llll} v_{00} & := & 1 & v_{01}(n) := \eta_1(n) \\ v_{11} & := & 1 & v_{02}(n) := \eta_2'(n) + (\eta_2(n) + i\pi)^2 \\ v_{12}(n) & := & 2(\eta_2(n) + i\pi) & v_{22} := 1 \\ v_{03}(n) & := & \eta_3''(n) + 3\eta_3'(n)\eta_3(n) + \eta_3(n)^3 & v_{13}(n) := 3[\eta_3'(n) + \eta_3(n)^2] \\ v_{23}(n) & := & 3\eta_3(n) & v_{33} := 1 \end{array} \quad . \quad (65)$$

This gives $U_j(z) = \sum_{s=0}^j q_{sj}(z)(\log z)^s$, with:

$$q_{sj}(z) := \frac{(-1)^j}{j!} \sum_{n=0}^{\infty} \frac{(\alpha_1)_n (\alpha_2)_n (\alpha_3)_n (\alpha_4)_n}{(n!)^4} v_{sj}(n) z^n \quad . \quad (66)$$

In particular, we have $q_{sj}(0) = \frac{(-1)^j}{j!} v_{sj}(0)$. Substituting the formulae for $\eta_j^{(i)}$ given above, we obtain a complicated expression for $q(0)$ in terms of polygamma functions which we will not reproduce here. This expression can be simplified by the following indirect procedure. Let us introduce the variable $w = \kappa z$, where $\kappa = \exp(\sum_{k=1}^4 \psi(\alpha_k) - 4\psi(1))$ (in practice, this plays the role of the natural coordinate on the moduli space

dictated by the monomial-divisor mirror map of [28]). One can then consider isolating the factors $(\log w)^s$ instead of $(\log z)^s$ in the expansion of $U_j(z)$ around $z = 0$. Doing so amounts to writing:

$$U_j(w) = \sum_{s=0}^j \tilde{q}_{sj}(w) (\log w)^s . \quad (67)$$

where the functions $\tilde{q}_{sj}(w)$ are now given by:

$$\tilde{q}_{sj}(w) := \frac{(-1)^j}{j!} \sum_{n=0}^{\infty} \frac{(\alpha_1)_n (\alpha_2)_n (\alpha_3)_n (\alpha_4)_n}{(n!)^4} \tilde{v}_{sj}(n) \left(\frac{w}{\kappa} \right)^n , \quad (68)$$

as can be seen upon expanding:

$$\nu_s(n, w) = \sum_{s=0}^j \tilde{v}_{sj}(n) (\log w)^s , \quad (69)$$

with:

$$\begin{array}{llll} \tilde{v}_{00} & := & 1 & \tilde{v}_{01}(n) := \eta_1(n) \\ \tilde{v}_{11} & := & 1 & \tilde{v}_{02}(n) := \eta'_2(n) + (\theta_2(n) + i\pi)^2 \\ \tilde{v}_{12} & := & 2(\theta_2(n) + i\pi) & \tilde{v}_{22} := 1 \\ \tilde{v}_{03}(n) & := & \eta''_3(n) + 3\eta'_3(n)\theta_3(n) + \theta_3(n)^3 & \tilde{v}_{13}(n) := 3[\eta'_3(n) + \theta_3(n)^2] \\ \tilde{v}_{23}(n) & := & 3\theta_3(n) & \tilde{v}_{33} := 1 . \end{array} \quad (70)$$

Here $\theta(n)$ are defined through:

$$\eta_j(n) + \log((-1)^{j+1}z) = \theta_j(n) + \log((-1)^{j+1}w) . \quad (71)$$

Since $\log(w) = \log(z) + \log(\kappa) = \log(z) + \sum_{k=1}^4 \psi(\alpha_k) - 4\psi(1)$, we have:

$$\theta_j(n) := \sum_{k=1}^4 [\psi(n + \alpha_k) - \psi(\alpha_k)] + (3-j) [\psi(1) - \psi(n+1)] - (j+1) \sum_{l=1}^n \frac{1}{l} . \quad (72)$$

The new sequences $\theta_j(n)$ have the convenient property $\theta_j(0) = 0$, which allows us to obtain a simple expression for the matrix $\tilde{q}(0)$:

$$\tilde{q}(0) := \begin{bmatrix} 1 & 0 & \frac{1}{2}(\eta'_2(0) - \pi^2) & -\frac{1}{6}\eta''_3(0) \\ 0 & -1 & i\pi & -\frac{1}{2}\eta'_3(0) \\ 0 & 0 & \frac{1}{2} & 0 \\ 0 & 0 & 0 & -\frac{1}{6} \end{bmatrix} . \quad (73)$$

In this expression:

$$\begin{aligned} \eta'_2(0) &= \psi'(\alpha_1) + \psi'(\alpha_2) + \psi'(\alpha_3) + \psi'(\alpha_4) + 1/3\pi^2 \\ \eta'_3(0) &= \psi'(\alpha_1) + \psi'(\alpha_2) + \psi'(\alpha_3) + \psi'(\alpha_4) + 2/3\pi^2 \\ \eta''_3(0) &= \psi''(\alpha_1) + \psi''(\alpha_2) + \psi''(\alpha_3) + \psi''(\alpha_4) + 8\zeta(3) . \end{aligned} \quad (74)$$

Using $\log(w) = \log(\kappa) + \log(z)$, it is easy to see that:

$$q(0) = c\tilde{q}(0) \quad , \quad (75)$$

with c an upper triangular matrix whose nonzero entries are given by $c_{sp} := \binom{p}{s} (\log \kappa)^{p-s}$ for all $s \leq p$. Moreover, it is not hard to see that the matrix $q'(0)c^t q'(0)^{-1}$ commutes with R_{can}^t , so that we can use $\tilde{M} := \tilde{q}(0)^t q'(0)^{-1}$ instead of M . In other words, we have:

$$T[0] = \tilde{M} T_{can}[0] \tilde{M}^{-1} \quad , \quad (76)$$

which allows for the computation of $T[0]$ upon using (63):

$$T[0] = \begin{bmatrix} 1 & 0 & 0 & 0 \\ -2i\pi & 1 & 0 & 0 \\ -4\pi^2 & -2i\pi & 1 & 0 \\ 0 & 0 & -2i\pi & 1 \end{bmatrix} \quad . \quad (77)$$

Remarkably, this expression is independent of α_k , which underscores the universal behaviour of the Meijer periods in the large complex structure limit, as mentioned in the introduction. In particular, these periods are adapted to the large complex structure monodromy weight filtration, as can be seen from the form of $T[0]$ or directly from the expansions (53).

4.2.2 Meijer monodromies around $z = \infty$

The monodromy of the Meijer basis around $z = \infty$ is straightforward to extract. For this, first notice that:

$$((-1)^{j+1}z)^{-\alpha_k} = z^{-\alpha_k} \left(\delta_{j,odd} + \delta_{j,even} e^{-i\pi\alpha_k} \right) \quad (78)$$

where $\delta_{j,odd}$ equals 1 if j is odd, and 0 if j is even (and a similar definition holds for $\delta_{j,even}$). This allows us to write $U_j(z) = \sum_{k=0}^3 a_{jk} u_k(z)$, where $u_{k-1}(z) := z^{-\alpha_k} {}_4F_3 \left(\begin{matrix} \alpha_k, \alpha_k, \alpha_k, \alpha_k \\ 1 + \alpha_k - \alpha_1, \hat{1}, 1 + \alpha_k - \alpha_4 \end{matrix} \right) (1/z)$ and the transition matrix $A := (a_{jk})_{j,k=0 \dots 3}$ is given by:

$$A = \frac{1}{\prod_{i=1 \dots 4} \Gamma(\alpha_k)} CD \quad , \quad (79)$$

where:

$$\begin{aligned} C_{jk} &:= \left(\frac{\sin(\pi\alpha_{k+1})}{\pi} \right)^{3-j} \left(\delta_{j,odd} + \delta_{j,even} e^{-i\pi\alpha_{k+1}} \right) \\ D &:= \text{diag}(d_0, d_1, d_2, d_3) \\ d_k &:= \Gamma(\alpha_k + 1)^4 \prod_{l=1 \dots 4, l \neq k+1} \Gamma(\alpha_l - \alpha_{k+1}) \quad . \end{aligned}$$

The monodromy of the basis u has the simple form:

$$T_u[\infty] = \text{diag}(e^{-2\pi i \alpha_1} \dots e^{-2\pi i \alpha_4}) \quad , \quad (80)$$

which coincides with $T_J = e^{2\pi i R_J[\infty]^t}$, where $R_J[\infty]$ is the Jordan form of the matrix $R_{can}[\infty]$. This allows us to compute the monodromy of the Meijer basis via the relation $T[\infty] = AT_u[\infty]A^{-1}$. Since both D and $T_u[\infty]$ are diagonal, we have $DT_u[\infty]D^{-1} = T_u$, which allows us to reduce this relation to:

$$T[\infty] = CT_u[\infty]C^{-1} \quad . \quad (81)$$

The last equality is more convenient for computing $T[\infty]$ since it involves only the matrix C .

4.3 The mirror quintic revisited

Let us now show how the results of [42] can be recovered in our framework. Beyond acting as a check on our computations, this will also serve to illustrate the connection between vanishing cycles and arithmetic identities in a well-understood example.

The mirror quintic can be obtained as a particular case of the discussion above by choosing $\alpha_i = i/5$ for all $i = 1 \dots 4$. Let $\sigma := e^{\frac{2\pi i}{5}}$. In this case, one has:

$$\tilde{q}(0) = \begin{bmatrix} 1 & 0 & 5/3 \pi^2 & 40 \zeta(3) \\ 0 & -1 & i\pi & -7/3 \pi^2 \\ 0 & 0 & 1/2 & 0 \\ 0 & 0 & 0 & -1/6 \end{bmatrix} \quad , \quad T_u[\infty] = \begin{bmatrix} \sigma^{-1} & 0 & 0 & 0 \\ 0 & \sigma^{-2} & 0 & 0 \\ 0 & 0 & \sigma^{-3} & 0 \\ 0 & 0 & 0 & \sigma^{-4} \end{bmatrix} \quad ,$$

which immediately gives:

$$T[0] = \begin{bmatrix} 1 & 0 & 0 & 0 \\ -2i\pi & 1 & 0 & 0 \\ -4\pi^2 & -2i\pi & 1 & 0 \\ 0 & 0 & -2i\pi & 1 \end{bmatrix} \quad , \quad T[\infty] = \begin{bmatrix} -4 & -5/2 \frac{i}{\pi} & 5/4 \pi^{-2} & 5/8 \frac{i}{\pi^3} \\ -2i\pi & 1 & 0 & 0 \\ -4\pi^2 & -2i\pi & 1 & 0 \\ 0 & 0 & -2i\pi & 1 \end{bmatrix}$$

and $T[1] = T[0]^{-1}T[\infty]$. These matrices satisfy $(T[0]-I)^4 = 0$, $(T[1]-I)^2 = 0$, $T[\infty]^5 - I = 0$. To make contact with the results in [42], first note that our convention for monodromies differs from the one used there by a change of orientation – which implies an inversion of the matrices $T[0]$ and $T[\infty]$ ¹⁸. Then notice that the fundamental period U_0 is cyclic for the operator $T[\infty]^{-1}$. Thus one can generate a cyclic set by acting with $T[\infty]^{-1}$ on U_0 , which produces 5 periods ω_j related to the Meijer periods through:

$$\begin{bmatrix} \omega_0 \\ \omega_1 \\ \omega_2 \\ \omega_3 \\ \omega_4 \end{bmatrix} = \begin{bmatrix} 1 & 0 & 0 & 0 \\ 1 & 5/2 \frac{i}{\pi} & 0 & -5/8 \frac{i}{\pi^3} \\ -4 & -5 \frac{i}{\pi} & 5/4 \pi^{-2} & \frac{15}{8} \frac{i}{\pi^3} \\ 6 & 5 \frac{i}{\pi} & -5/2 \pi^{-2} & -\frac{15}{8} \frac{i}{\pi^3} \\ -4 & -5/2 \frac{i}{\pi} & 5/4 \pi^{-2} & 5/8 \frac{i}{\pi^3} \end{bmatrix} \begin{bmatrix} U_0 \\ U_1 \\ U_2 \\ U_3 \end{bmatrix} \quad . \quad (82)$$

¹⁸This is due to our use of different coordinates on the moduli space, as we explain below.

This corresponds to the procedure used in [42] (as well as in [40, 39, 36, 37]) in order to generate a basis of periods from the fundamental period. Indeed, the cyclic basis used in [42] corresponds to the periods $\omega_2, \omega_1, \omega_0$ and ω_4 denoted by the same letters in that paper. Up to a rescaling by $-(2\pi i/5)^3$, these form a period vector denoted there by ω . It follows that the Meijer period vector is related to the period vector ω of [42] through:

$$\omega = -\left(\frac{2\pi i}{5}\right)^3 \begin{bmatrix} \omega_2 \\ \omega_1 \\ \omega_0 \\ \omega_4 \end{bmatrix} = LU \quad \text{with} \quad L = \begin{bmatrix} -\frac{32}{125} i\pi^3 & \frac{8}{25} \pi^2 & \frac{2}{25} i\pi & -\frac{3}{25} \\ \frac{8}{125} i\pi^3 & -\frac{4}{25} \pi^2 & 0 & 1/25 \\ \frac{8}{125} i\pi^3 & 0 & 0 & 0 \\ -\frac{32}{125} i\pi^3 & \frac{4}{25} \pi^2 & \frac{2}{25} i\pi & -1/25 \end{bmatrix}.$$

In order to make contact with the results of [42], one must also take into account the fact that the monodromy matrices given there correspond to working on a 5-fold cover of the moduli space. This is parameterized in [42] by a variable ψ , related to our coordinate by $z = \psi^{-5}$. It follows that our monodromy matrices $LT[0]L^{-1}$, $LT[1]L^{-1}$, $LT[\infty]L^{-1}$ should be compared respectively with the matrices $t_\infty^{1/5}$, $t_\infty^{-1/5}a^{-1}$ and a^{-1} of [42], and it is easy to see that they agree. As a further check, one can easily show that the $|\psi| < 1$ expansions of ω_j given in Appendix B of [42] agree with the expansions of the cyclic basis following from (55).

A full sublattice of the integral lattice $\Lambda = H_3(Y, \mathbb{Z})$ can be identified as explained in Section 2. This gives a lattice Λ_0 characterized by the fact that the period vector associated with one of its bases (which we call E) is (up to a global factor):

$$U_E = EU = \begin{bmatrix} 1 & 0 & 0 & 0 \\ -4 & -5/2 \frac{i}{\pi} & 5/4 \pi^{-2} & 5/8 \frac{i}{\pi^3} \\ 6 & 5 \frac{i}{\pi} & -5/2 \pi^{-2} & -\frac{15}{8} \frac{i}{\pi^3} \\ -4 & -5 \frac{i}{\pi} & 5/4 \pi^{-2} & \frac{15}{8} \frac{i}{\pi^3} \end{bmatrix} U. \quad (83)$$

The integral basis P of Λ used in [42] is characterized by a period vector Π , which is related to the Meijer periods U by $\Pi = \Theta U$, with:

$$\Theta = \begin{bmatrix} 0 & \frac{12}{125} \pi^2 & \frac{2}{25} i\pi & 0 \\ -\frac{8}{125} i\pi^3 & 0 & 0 & 0 \\ 0 & \frac{4}{25} \pi^2 & \frac{4}{25} i\pi & 0 \\ 0 & -\frac{4}{25} \pi^2 & 0 & 1/25 \end{bmatrix}. \quad (84)$$

Hence the transition matrix from the basis P of $H_3(Y, \mathbb{Z})$ to the basis E of Λ_0 is:

$$K = (E\Theta^{-1})^t = \left(\frac{2\pi i}{5}\right)^{-3} \begin{bmatrix} 0 & 5 & -20 & 15 \\ 1 & -4 & 6 & -4 \\ 0 & -3 & 11 & -8 \\ 0 & 1 & -3 & 3 \end{bmatrix} = \left(\frac{2\pi i}{5}\right)^{-3} K_0. \quad (85)$$

Since $\det(K_0) = 5$, we see that $\Lambda'_0 = \left(\frac{2\pi i}{5}\right)^3 \Lambda_0$ is an index 5 sublattice of Λ , i.e. the finite group Λ/Λ'_0 has order 5.

The period ¹⁹ $-(2\pi i/5)^3(\omega_1 - \omega_0)$ which vanishes at the conifold point can be expressed in terms of the Meijer periods as $\frac{1}{25}(-4\pi^2 U_1 + U_3)$. Hence collapse of the

¹⁹This equals z^2 in the notations of [42].

associated 3-cycle at $z = 1$ is reflected by the relation:

$$U_3(1) = 4\pi^2 U_1(1) \quad , \quad (86)$$

which after a few simplifications can be seen to be equivalent to:

$$\begin{aligned} & 192\pi^5 \sqrt{2} \sqrt{5 + \sqrt{5}} (5 - 2\sqrt{5}) \Gamma(3/5)^5 {}_4F_3 \left(\begin{matrix} 1/5, 1/5, 1/5, 1/5 \\ 4/5, 2/5, 3/5 \end{matrix} \right) (1) + \\ & + 960\pi^5 \sqrt{2} \sqrt{5 + \sqrt{5}} (2\sqrt{5} - 5) \Gamma(4/5)^5 {}_4F_3 \left(\begin{matrix} 2/5, 2/5, 2/5, 2/5 \\ 4/5, 3/5, 6/5 \end{matrix} \right) (1) + \\ & + 3125 (11 - 5\sqrt{5}) \Gamma(3/5)^5 \Gamma(4/5)^{10} {}_4F_3 \left(\begin{matrix} 4/5, 4/5, 4/5, 4/5 \\ 8/5, 7/5, 6/5 \end{matrix} \right) (1) + \\ & + 3750 \Gamma(4/5)^5 \Gamma(3/5)^{10} {}_4F_3 \left(\begin{matrix} 3/5, 3/5, 3/5, 3/5 \\ 4/5, 7/5, 6/5 \end{matrix} \right) (1) = 0 \quad . \end{aligned} \quad (87)$$

One can of course write down a pair identity by using the expansions (53) around the large complex structure point, which can be thought of as following from the one above through analytic continuation. It is a challenging problem to find direct proofs of these identities.

Figures 6 and 7 compare the classical and quantum volumes of the even-dimensional cycles on the quintic. In Figure 6, we plot classical volumes as a function of the classical Kähler parameter s , defined by $J = se$ with e the generator of $H^2(X, \mathbb{Z})$. In figure 7, for ease of comparison, we plot the quantum volumes as a function of essentially the same parameter s — the so-called ‘algebraic measure’ on the quantum moduli space (see [33] for a discussion of this concept), which in this case is related to z via $s = \frac{1}{2\pi} \log(\frac{5^5}{z})$ (note that $\kappa = 5^{-5}$ in this example). In the language of [33], this coordinate is $s = \text{Im}(t_{alg})$, where $t_{alg} = \frac{1}{2\pi i} \log(\frac{z}{5^5})$.

For comparison with the classical situation, we consider only the region $s \geq 0$ in Figure 7, even though quantum mechanically we can continue s to negative values as well. The point P , where $s = \frac{5}{2\pi} \log 5 \approx 1.28$ and $z = 1$, corresponds to the conifold. Figure 7 also displays the values of the special coordinate $t = \frac{2(\omega_1 - \omega_0) + \omega_2 - \omega_4}{5\omega_0}$, which measures the volume of a D2-brane wrapped over the generator of $H_2(X, \mathbb{Z})$. We also plot the absolute value of the integral period $-\frac{2i}{25} U_2$, which can be interpreted as the mass of a wrapped D4-brane. Note that the scale used for the y -axis is different for the two graphs and different from the scale used on the x -axis (this is needed in order to fit the interesting portion of the graphs in the limited space available). Taking this rescaling into account, one can easily check that the curve $m = |t(s)|$ asymptotes to the line $m = s$ (the diagonal of the first quadrant) in the the large radius limit $s \rightarrow \infty$. In this limit, $|U_v|$ asymptotes to $1.923 - 4.134s + 1.653s^3$.

These figures capture the essential point, one that we will find repeated in various forms in subsequent examples. Namely, the classical relations between 2, 4, and 6 cycle volumes are significantly modified in the quantum setting. In particular, we see that a 6-cycle collapses to zero quantum volume at the conifold point, even though 2 and 4 cycle volumes stay positive.

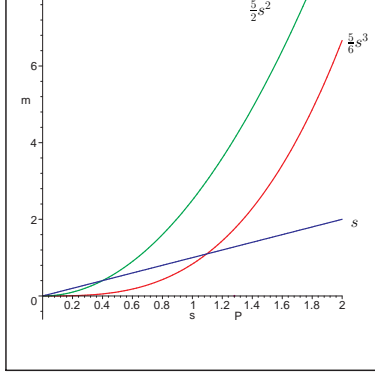


Figure 6. Graph of the classical volumes s , $\frac{5}{2}s^2$ and $\frac{5}{6}s^3$ of a set of two, four and six cycles vs. the classical Kahler parameter s .

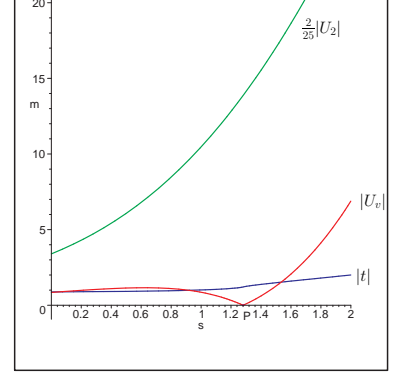


Figure 7. Graph of $|U_v|$ vs. the classical Kahler parameter s . For comparison, we also plot the absolute value of the special coordinate t , which measures the mass of a wrapped D2-brane, and the absolute value of the (integral) period $-\frac{2i}{25}U_2$.

5 Examples II: Some ‘degenerate’ models

Let us now consider the case when the parameters α_i satisfy conditions (2) and (3), but they violate condition (1). Namely, consider $0 < \alpha_i < 1$ chosen so that $\alpha_1, \alpha_2, \alpha_3$ are distinct but $\alpha_3 = \alpha_4$. This situation is encountered for some of the examples studied in [39] (see Table 3.1. on page 26 of that paper). In particular, it is satisfied for a complete intersection of a quadric and a quartic in \mathbb{P}^5 (the third entry of that table), a model which we will encounter as an interesting sub-locus of a two-parameter example in Section 4. Another case which satisfies this condition is the complete intersection $\mathbb{P}^6[2, 2, 3]$.

5.1 The Meijer periods

Clearly nothing qualitatively new happens in such a model when computing the expansions for $|z| < 1$, since closing the contour to the right only gives contributions from the poles in $\Gamma(-s)$ (the A-type poles) in (47), whose nature is independent of the relative values of α_i . Hence the expansions around the large complex structure point have the same form as above. On the other hand, closing the contour to the left gives two types of contributions from the (B) - type poles:

(B₁) Contributions from $s = -n - \alpha_3$ (n a nonnegative integer), which are double poles

(B₂) Contributions from $s = -n - \alpha_1$ and $s = -n - \alpha_2$ (n a nonnegative integer), which are simple poles.

Correspondingly, we can write the expansions of $U_j(z)$ for $|z| > 1$ as:

$$U_j(z) = u_j^{(1)}(z) + u_j^{(2)}(z) \quad , \quad (88)$$

separating the contributions from these two sub-types. The (B_2) -type contributions are of exactly the same form as above:

$$u_j^{(2)}(z) = \frac{1}{\Gamma(\alpha_1)\Gamma(\alpha_2)\Gamma(\alpha_3)^2} \sum_{k=1}^2 \left(\frac{\sin(\pi\alpha_k)}{\pi} \right)^{3-j} \Gamma(\alpha_k)^4 \prod_{l=1}^l \Gamma(\alpha_l - \alpha_k) ((-1)^{j+1}z)^{-\alpha_k} \times \\ \times {}_4F_3 \left(\begin{matrix} \alpha_k, \alpha_k, \alpha_k, \alpha_k \\ 1 + \alpha_k - \alpha_1, \dots, \hat{1}, \dots, 1 + \alpha_k - \alpha_4 \end{matrix} \right) (1/z) \quad , \quad (89)$$

but the B_1 -type poles induce logarithmic terms:

$$u_j^{(1)}(z) = \frac{1}{\Gamma(\alpha_1)\Gamma(\alpha_2)\Gamma(\alpha_3)^2} \left(\frac{\sin(\pi\alpha_3)}{\pi} \right)^{3-j} ((-1)^{j+1}z)^{-\alpha_3} \sum_{n=0}^{\infty} \frac{\Gamma(n+\alpha_3)^4 \Gamma(-n+\alpha_1-\alpha_3) \Gamma(-n+\alpha_2-\alpha_3)}{n!^2} z^{-n} \\ \left[\psi(-n+\alpha_1-\alpha_3) + \psi(-n+\alpha_2-\alpha_3) - (j+1) \psi(n+\alpha_3) - (3-j) \psi(1-n-\alpha_3) + 2\psi(1) + 2 \sum_{l=1}^n \frac{1}{l} + \log((-1)^{j+1}z) \right] \quad . \quad (90)$$

5.2 Monodromies of the Meijer basis

The monodromies about $z = 0$ follow by substituting $\alpha_4 = \alpha_3$ in the results of Section 3. In order to obtain the monodromies about $z = \infty$, one has to be a bit more careful, as we now explain.

By using the general results of Section 2, it is easy to compute the matrix $R_{can}[\infty]$:

$$R_{can}[\infty] = \begin{bmatrix} 0 & -1 & 0 & 0 \\ 0 & 0 & -1 & 0 \\ 0 & 0 & 0 & -1 \\ \alpha_1\alpha_2\alpha_3^2 & -2\alpha_1\alpha_2\alpha_3 - \alpha_1\alpha_3^2 - \alpha_2\alpha_3^2 & \alpha_1\alpha_2 + 2\alpha_1\alpha_3 + 2\alpha_2\alpha_3 + \alpha_3^2 & -\alpha_1 - \alpha_2 - 2\alpha_3 \end{bmatrix} \quad .$$

and its Jordan form:

$$R_J[\infty] = \begin{bmatrix} -\alpha_1 & 0 & 0 & 0 \\ 0 & -\alpha_2 & 0 & 0 \\ 0 & 0 & -\alpha_3 & 1 \\ 0 & 0 & 0 & -\alpha_3 \end{bmatrix} \quad . \quad (91)$$

These are related by a transition matrix $P \in GL(4, \mathbb{C})$ satisfying:

$$R_{can}[\infty] = PR_J[\infty]P^{-1} \quad . \quad (92)$$

While such a transition matrix is not unique, for what follows it suffices to pick any P with the property (92), for example the matrix:

$$P = \begin{bmatrix} -\frac{\alpha_2\alpha_3^2}{(\alpha_1-\alpha_3)^2(\alpha_1-\alpha_2)} & \frac{\alpha_1\alpha_3^2}{(\alpha_2-\alpha_3)^2(\alpha_1-\alpha_2)} & \frac{\alpha_1\alpha_2\alpha_3}{(\alpha_2-\alpha_3)(\alpha_1-\alpha_3)} & \frac{(-2\alpha_1\alpha_3+\alpha_1\alpha_2+3\alpha_3^2-2\alpha_2\alpha_3)\alpha_1\alpha_2}{(\alpha_2-\alpha_3)^2(\alpha_1-\alpha_3)^2} \\ -\frac{\alpha_1\alpha_2\alpha_3^2}{(\alpha_1-\alpha_3)^2(\alpha_1-\alpha_2)} & \frac{\alpha_1\alpha_2\alpha_3^2}{(\alpha_2-\alpha_3)^2(\alpha_1-\alpha_2)} & \frac{\alpha_1\alpha_2\alpha_3^2}{(\alpha_2-\alpha_3)(\alpha_1-\alpha_3)} & -\frac{\alpha_1\alpha_2\alpha_3^2(\alpha_1-2\alpha_3+\alpha_2)}{(\alpha_2-\alpha_3)^2(\alpha_1-\alpha_3)^2} \\ -\frac{\alpha_1^2\alpha_3^2\alpha_2}{(\alpha_1-\alpha_3)^2(\alpha_1-\alpha_2)} & \frac{\alpha_1\alpha_2^2\alpha_3^2}{(\alpha_2-\alpha_3)^2(\alpha_1-\alpha_2)} & \frac{\alpha_1\alpha_2\alpha_3^3}{(\alpha_2-\alpha_3)(\alpha_1-\alpha_3)} & -\frac{\alpha_1\alpha_2\alpha_3^2(\alpha_1\alpha_2-\alpha_3^2)}{(\alpha_2-\alpha_3)^2(\alpha_1-\alpha_3)^2} \\ -\frac{\alpha_1^3\alpha_2\alpha_3^2}{(\alpha_1-\alpha_3)^2(\alpha_1-\alpha_2)} & \frac{\alpha_1\alpha_2^3\alpha_3^2}{(\alpha_2-\alpha_3)^2(\alpha_1-\alpha_2)} & \frac{\alpha_1\alpha_2\alpha_3^4}{(\alpha_2-\alpha_3)(\alpha_1-\alpha_3)} & -\frac{\alpha_1\alpha_2\alpha_3^3(-\alpha_1\alpha_3+2\alpha_1\alpha_2-\alpha_2\alpha_3)}{(\alpha_2-\alpha_3)^2(\alpha_1-\alpha_3)^2} \end{bmatrix} \quad .$$

Assuming that we made such a choice, we can define a *Jordan basis* of periods (which depends on the choice of P) through $U_J(z) = P^{-t}U_{can}(z)$. In terms of fundamental matrices for the associated Picard-Fuchs system, this relation reads:

$$\Phi_{can}(z) = \Phi(z)P^{-1} \quad , \quad (93)$$

which implies that the monodromy of the basis U_J about $z = \infty$ is given by the matrix $R_J[\infty]$. The associated nilpotent orbits are related through $S_{can}(z) = S_J(z)P^{-1}$, which, together with the defining property $S_{can}[\infty] = I$, allows us to compute:

$$S_J[\infty] = P \quad . \quad (94)$$

The Jordan basis is a useful device for extracting the monodromy of the Meijer periods. To see this, note that equation (91) assures us that we can extract the nontrivial behaviour of periods about $z = \infty$ by writing:

$$U(z) = Z(z)q(z) \quad , \quad U_J(z) = Z(z)q_J(z) \quad , \quad (95)$$

where $q(z), q_J(z)$ are one-valued and regular at $z = \infty$ while the row vector $Z(z)$ is defined by²⁰:

$$Z(z) = \begin{bmatrix} z^{-\alpha_1} & z^{-\alpha_2} & z^{-\alpha_3} & z^{-\alpha_3} \log z \end{bmatrix} \quad . \quad (96)$$

Since the Jordan monodromy

$$T_J[\infty] = e^{2\pi i R_J[\infty]^t} = \begin{bmatrix} e^{-2\pi i \alpha_1} & 0 & 0 & 0 \\ 0 & e^{-2\pi i \alpha_2} & 0 & 0 \\ 0 & 0 & e^{-2\pi i \alpha_3} & 0 \\ 0 & 0 & 2\pi i e^{-2\pi i \alpha_3} & e^{-2\pi i \alpha_3} \end{bmatrix} \quad (97)$$

is trivially known, it follows that, in order to compute the monodromy of $U(z)$, it suffices to identify the transition matrix $M \in GL(4, \mathbb{C})$ such that $U(z) = MU_J(z)$. The latter can be determined from knowledge of $q(\infty)$ and $q_J(\infty)$ through the relation:

$$M = q(\infty)^t q_J(\infty)^{-t} \quad , \quad (98)$$

provided that we can compute the two matrices appearing in this equation. The matrix $q_J(\infty)$ is straightforward to extract by noting that $U_J(z)^t$ coincides with the first row of $\Phi_J(z) = S(z)z^{R_J}$ and by rewriting $U_j(z) = S_i(z)(z^{R_J})_{ij}$ in the form (95):

$$q_J(z) = \begin{bmatrix} S_{1,1}(z) & 0 & 0 & 0 \\ 0 & S_{1,2}(z) & 0 & 0 \\ 0 & 0 & S_{1,3}(z) & S_{1,4}(z) \\ 0 & 0 & 0 & S_{1,3}(z) \end{bmatrix} \quad , \quad (99)$$

which together with (94) gives:

$$q_J(\infty) = \begin{bmatrix} P_{1,1} & 0 & 0 & 0 \\ 0 & P_{1,2} & 0 & 0 \\ 0 & 0 & P_{1,3} & P_{1,4} \\ 0 & 0 & 0 & P_{1,3} \end{bmatrix} \quad . \quad (100)$$

²⁰Note that this differs from the vector $Z(z)$ used in Section 3.

On the other hand, the matrix $q(z)$ can be determined via its defining property (95) by using the expansions (89,90). This amounts to writing:

$$U_j(z) = \sum_{i=0}^4 q_{ij}(z) Z_i(z) \quad , \quad (101)$$

which immediately gives:

$$q(\infty) = \frac{1}{\Gamma(\alpha_1)\Gamma(\alpha_2)\Gamma(\alpha_3)^2} DC^t \quad , \quad (102)$$

with C and D given by:

$$\begin{aligned} C_{jk} &= \left(\frac{\sin \pi \alpha_k}{\pi} \right)^{3-j} (\delta_{j,odd} + \delta_{j,even} e^{-i\pi \alpha_k}) \quad \text{for } k = 0, 1, 3 \\ C_{j2} &= \left(\frac{\sin \pi \alpha_3}{\pi} \right)^{3-j} (\delta_{j,odd} + \delta_{j,even} e^{-i\pi \alpha_3}) (\psi(\alpha_1 - \alpha_3) + \psi(\alpha_2 - \alpha_3) - \\ &\quad - (j+1)\psi(\alpha_3) - (3-j)\psi(1 - \alpha_3) + 2\psi(1) + \delta_{j,even} i\pi) \quad . \end{aligned} \quad (103)$$

with $j = 0 \dots 3$ and:

$$\begin{aligned} D &= \text{diag}(d_1, d_2, d_3, d_4) \\ d_k &= \Gamma(\alpha_k)^4 \prod_{l=1}^4 \Gamma(\alpha_l - \alpha_k) \quad \text{for } k = 1, 2 \\ d_3 &= d_4 = \Gamma(\alpha_3)^4 \Gamma(\alpha_1 - \alpha_3) \Gamma(\alpha_2 - \alpha_3) \quad . \end{aligned}$$

These relations allow us to determine $M = \frac{1}{\Gamma(\alpha_1)\Gamma(\alpha_2)\Gamma(\alpha_3)^2} CD q_J(\infty)^{-t}$ and hence the Meijer monodromy $T[\infty] = MT_J[\infty]M^{-1}$. Moreover, it is possible to show that the matrices D and $q_J(\infty)^{-t} T_J[\infty] q_J(\infty)^t$ commute, so that we can use $N := C q_J(\infty)^{-t}$ instead of M . We conclude that the Meijer monodromy about the small radius point is given by:

$$T[\infty] = N T_J[\infty] N^{-1} \quad . \quad (104)$$

The reader will easily recognize that the procedure employed above is a natural generalization of the approach used in Section 3 for extracting the Meijer monodromy around $z = 0$. In that case, the canonical matrix $R_{can}[0]$ was already in Jordan form, so that the matrix P was simply the identity (while $q_J(0)$ was denoted there by $q'(0)$). The procedure presented above can be easily generalized for an arbitrary Jordan form, thus allowing for a uniform treatment of all possible types of boundary points of the moduli space.

5.3 The model $\mathbb{P}^5[2, 4]$

The mirror of this model can be described by an orbifold of the complete intersection $Y = \{p_1(u) = p_2(u) = 0\}$, where $u = [u_0 \dots u_5] \in \mathbb{P}^5$ and:

$$p_1(u) = u_0^2 + u_1^2 + u_2^2 + u_3^2 - 2\psi u_4 u_5 \quad (105)$$

$$p_2(u) = u_4^4 + u_5^4 - 4\psi u_0 u_1 u_2 u_3 \quad (106)$$

The fundamental period of this example was determined in [39] (see also [51] for other results on this model). By using our techniques, we can go beyond these results and determine a full basis of periods. We will also find a (weakly) integral period vanishing at $x = 1$, which can once again be interpreted as a massless 6-brane state.

The complex variable ψ gives a coordinate on a 6-fold cover of the moduli space, which is a copy of the Riemann sphere \mathbb{P}^1 . As before, we prefer to work with the ‘hypergeometric’ parameter $x = \frac{4}{\psi^6}$, which gives a coordinate on the moduli space itself²¹. The normalization of x is fixed by the requirement that $x = 0$ corresponds to the large complex structure point and $x = 1$ corresponds to the ‘conifold’ point. Then $x = \infty$ corresponds to the small radius limit of the model. As mentioned above, logarithmic behaviour of the periods for $|x| > 1$ prevents us from interpreting $x = \infty$ as Landau-Ginzburg point; rather, it is a more general type of non-geometric point (in the terminology of last paper in reference [32], it is a hybrid point).

The hypergeometric symbol of this model is easily computed by the techniques of [58, 59] with the result that it is given by $\left(\begin{smallmatrix} \alpha_1, \alpha_2, \alpha_3, \alpha_4 \\ 1, 1, 1 \end{smallmatrix} \right)$ with $\alpha_1 = 1/4, \alpha_2 = 3/4, \alpha_3 = \alpha_4 = 1/2$. Hence the model fits into the scheme of the previous subsection and we can directly apply the results derived above by simply substituting these particular values of α_i in relations (53) and (88), (89), (90)²².

Computation of the Meijer monodromies proceeds as explained above. The monodromy around $x = 0$ has the same form as in Section 3, while for the point $x = \infty$ we have:

$$R_{can}[\infty] = \begin{bmatrix} 0 & -1 & 0 & 0 \\ 0 & 0 & -1 & 0 \\ 0 & 0 & 0 & -1 \\ \frac{3}{64} & -\frac{7}{16} & \frac{23}{16} & -2 \end{bmatrix}, \quad R_J[\infty] = \begin{bmatrix} -1/4 & 0 & 0 & 0 \\ 0 & -3/4 & 0 & 0 \\ 0 & 0 & -1/2 & 1 \\ 0 & 0 & 0 & -1/2 \end{bmatrix}. \quad (107)$$

A choice for the matrix P is:

$$P = \begin{bmatrix} 6 & -2 & -3/2 & -3 \\ 3/2 & -3/2 & -3/4 & 0 \\ 3/8 & -\frac{9}{8} & -3/8 & 3/4 \\ \frac{3}{32} & -\frac{27}{32} & -3/16 & 3/4 \end{bmatrix}. \quad (108)$$

²¹In this subsection we denote the hypergeometric coordinate by x instead of z , for agreement with Section 7 below.

²²The reader can easily verify that the fundamental period $U_0 = {}_4F_3 \left(\begin{smallmatrix} 1/2, 1/2, 1/4, 3/4 \\ 1, 1, 1 \end{smallmatrix} \right) (x)$ coincides with the period $\omega_0 = \sum_{n=0}^{\infty} \frac{(2n)!(4n)!}{(n!)^6 (2^5 \psi^6)^n}$ given in Table 3.1 of [39]. This follows from the identity $\frac{(2n)!(4n)!}{(n!)^6} = 2^{10n} \frac{(1/2)_n^2 (1/4)_n (3/4)_n}{(n!)^4}$.

We can now compute:

$$N = \begin{bmatrix} \frac{1/24-1/24i}{\pi^3} & \frac{1/8+1/8i}{\pi^3} & 2/3 \frac{2i+2i\log(2)-\pi}{\pi^3} & 2/3 \frac{i}{\pi^3} \\ 1/12\pi^{-2} & -1/4\pi^{-2} & -4/3 \frac{1+\log(2)}{\pi^2} & -2/3\pi^{-2} \\ \frac{1/12-1/12i}{\pi} & \frac{1/4+1/4i}{\pi} & 2/3 \frac{2i+2i\log(2)-\pi}{\pi} & 2/3 \frac{i}{\pi} \\ 1/6 & -1/2 & -4/3 - 4/3\log(2) & -2/3 \end{bmatrix}, \quad (109)$$

thus obtaining the Meijer monodromies:

$$T[0] = \begin{bmatrix} 1 & 0 & 0 & 0 \\ -2i\pi & 1 & 0 & 0 \\ -4\pi^2 & -2i\pi & 1 & 0 \\ 0 & 0 & -2i\pi & 1 \end{bmatrix}, \quad T[\infty] = \begin{bmatrix} -5 & -3\frac{i}{\pi} & 2\pi^{-2} & \frac{i}{\pi^3} \\ -2i\pi & 1 & 0 & 0 \\ -4\pi^2 & -2i\pi & 1 & 0 \\ 0 & 0 & -2i\pi & 1 \end{bmatrix},$$

and $T[1] = T[0]^{-1}T[\infty]$. The monodromy matrices satisfy:

$$(T[0] - I)^4 = 0, \quad (T[1] - I)^2 = 0, \quad (T[\infty]^4 - I)^2 = 0.$$

Hence the monodromy about $x = \infty$ is neither unipotent, nor of finite order. This confirms our expectation that the small radius limit of the model has a ‘hybrid’ character (i.e. is not a Landau-Ginzburg orbifold).

A set of periods associated with a basis of a full sublattice of $H_3(Y, \mathbb{Z})$ (up to a *common* factor) can be obtained by the procedure discussed above:

$$U_E(x) = EU(x) \quad , \quad \text{with} \quad E = \begin{bmatrix} 1 & 0 & 0 & 0 \\ -5 & -3\frac{i}{\pi} & 2\frac{1}{\pi^2} & \frac{i}{\pi^3} \\ 11 & 8\frac{i}{\pi} & -\frac{6}{\pi^2} & -4\frac{i}{\pi^3} \\ -15 & -13\frac{i}{\pi} & \frac{8}{\pi^2} & 7\frac{i}{\pi^3} \end{bmatrix}. \quad (110)$$

Moreover, it is not hard to check that the period $U_v = \frac{1}{\pi^3}[U_3 - 3\pi^2 U_1]$ vanishes at $x = 1$; it is also easy to see that U_v is weakly integral:

$$U_v(x) = -i[3, 2, 2, 1] U_E(x). \quad (111)$$

We will see evidence of a different kind for the integrality of this period in Section 6. Collapse of the associated cycle once again rests on two arithmetic identities, of which we mention only the one induced by using the expansion of the periods for $|x| > 1$:

$$\begin{aligned} & \sum_{n=0}^{\infty} 4^{n+1} \sqrt{2} \frac{\Gamma(n + \frac{1}{2})^4 \Gamma(-2n - \frac{1}{2})}{n!^2} \left(\psi(-n - \frac{1}{4}) + \psi(-n + \frac{1}{4}) - \psi(n + \frac{1}{2}) - 3\psi(1/2 - n) + 2\psi(n + 1) \right) + \\ & \frac{1}{2} \Gamma(1/4)^6 {}_4F_3 \left(\begin{matrix} 1/4, 1/4, 1/4, 1/4 \\ 1/2, 3/4, 3/4 \end{matrix} \right) (1) - 16\Gamma(3/4)^6 {}_4F_3 \left(\begin{matrix} 3/4, 3/4, 3/4, 3/4 \\ 5/4, 5/4, 3/2 \end{matrix} \right) (1) = 0 \end{aligned} \quad (112)$$

Figure 8 plots the values of the vanishing period versus the coordinate $s = -\frac{1}{2\pi} \log(\kappa x)$ which defines the algebraic measure on the (uncomplexified) Kahler moduli space. In this case $\kappa = e^{\sum_{k=1}^4 \psi(\alpha_k) - 4\psi(1)} = 2^{-10}$. For comparison, we also display the values of the weakly integral periods $\frac{2}{\pi^2} U_2$ and $-\frac{4i}{\pi} U_1$. Up to a common factor, these periods correspond to the the integral of Ω over cycles mirror to a 6, 4 and 2-cycle respectively.

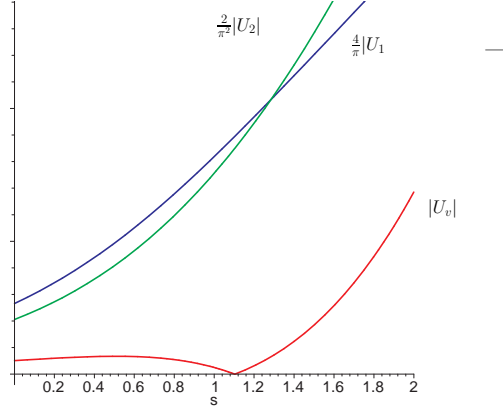


Figure 8. Graph of $|U_v|$ versus the imaginary part s of the algebraic coordinate $t_{alg} = \frac{1}{2\pi i} \log(\kappa x)$ for $s \in [0, 2]$. The point $x = 1$ corresponds to $s = \frac{5 \log 2}{\pi} \approx 1.103$. We also display the weakly integral periods $-\frac{4i}{\pi} U_1$ and $\frac{2}{\pi^2} U_2$.

5.4 The model $\mathbb{P}^6[2, 2, 3]$

This mirror of this model is realized as an orbifold of the complete intersection $Y = \{p_1 = p_2 = p_3 = 0\}$ of two quartics and a cubic in \mathbb{P}^6 :

$$\begin{aligned} p_1 &= x_1^2 + x_2^2 + x_3^2 - 2\psi x_6 x_7 \\ p_2 &= x_4^2 + x_5^2 - 2\psi x_1 x_2 \\ p_3 &= x_6^3 + x_7^3 - 3\psi x_3 x_4 x_5 \end{aligned} \quad (113)$$

The hypergeometric coordinate on the moduli space is given by $z = \frac{3}{2\psi^7}$, while the hypergeometric symbol is $\left(\begin{smallmatrix} 1/2, 1/2, 1/3, 2/3 \\ 1, 1, 1 \end{smallmatrix} \right)$. The large and small radius expansions are obtained from (53) and (88), (89), (90) by substituting $\alpha_1 = 1/3, \alpha_2 = 2/3$ and $\alpha_3 = \alpha_4 = 1/2$.

Computation of the Meijer monodromies proceeds as above, so we only list the results:

$$\begin{aligned} R_{can}[\infty] &= \begin{bmatrix} 0 & -1 & 0 & 0 \\ 0 & 0 & -1 & 0 \\ 0 & 0 & 0 & -1 \\ 1/18 & -17/36 & 53/36 & -2 \end{bmatrix}, \quad R_J[\infty] = \begin{bmatrix} -2/3 & 0 & 0 & 0 \\ 0 & -1/3 & 0 & 0 \\ 0 & 0 & -1/2 & 1 \\ 0 & 0 & 0 & -1/2 \end{bmatrix} \\ P &= \begin{bmatrix} -9 & 18 & -4 & -8 \\ -6 & 6 & -2 & 0 \\ -4 & 2 & -1 & 2 \\ -8/3 & 2/3 & -1/2 & 2 \end{bmatrix}, \quad N = \begin{bmatrix} 1/48 \frac{\sqrt{3}+3i}{\pi^3} & -\frac{1}{96} \frac{-\sqrt{3}+3i}{\pi^3} & -1/4 \frac{\pi-4i-4i\log(2)+3i\log(3)}{\pi^3} & 1/4 \frac{i}{\pi^3} \\ -1/12 \pi^{-2} & 1/24 \pi^{-2} & 1/4 \frac{-4-4\log(2)+3i\log(3)}{\pi^2} & -1/4 \pi^{-2} \\ 1/36 \frac{\sqrt{3}+3i}{\pi} & -\frac{1}{72} \frac{-\sqrt{3}+3i}{\pi} & -1/4 \frac{\pi-4i-4i\log(2)+3i\log(3)}{\pi} & 1/4 \frac{i}{\pi} \\ -1/9 & 1/18 & -1 - \log(2) + 3/4 \log(3) & -1/4 \end{bmatrix} \end{aligned}$$

$$T[0] = \begin{bmatrix} 1 & 0 & 0 & 0 \\ -2i\pi & 1 & 0 & 0 \\ -4\pi^2 & -2i\pi & 1 & 0 \\ 0 & 0 & -2i\pi & 1 \end{bmatrix}, \quad T[\infty] = \begin{bmatrix} -6 & -7/2 \frac{i}{\pi} & 3\pi^{-2} & 3/2 \frac{i}{\pi^3} \\ -2i\pi & 1 & 0 & 0 \\ -4\pi^2 & -2i\pi & 1 & 0 \\ 0 & 0 & -2i\pi & 1 \end{bmatrix},$$

and $T[1] = T[0]^{-1}T[\infty]$. The monodromy matrices satisfy:

$$(T[0] - I)^4 = 0, \quad (T[1] - I)^2 = 0, \quad (T[\infty]^6 - I)^2 = 0.$$

A set of periods associated with a basis of a full sublattice of $H_3(Y, \mathbb{Z})$ is (up to a common factor):

$$U_E(z) = EU(z), \quad \text{with } E = \begin{bmatrix} 1 & 0 & 0 & 0 \\ -6 & -7/2 \frac{i}{\pi} & \frac{3}{\pi^2} & 3/2 \frac{i}{\pi^3} \\ 17 & 23/2 \frac{i}{\pi} & -\frac{12}{\pi^2} & -15/2 \frac{i}{\pi^3} \\ -31 & -24 \frac{i}{\pi} & \frac{24}{\pi^2} & 18 \frac{i}{\pi^3} \end{bmatrix}. \quad (114)$$

One can check that the period $U_v = \frac{1}{\pi^3}(3U_3 - 7\pi^2 U_1)$, vanishes at $z = 1$. This can be expressed as:

$$U_v = -2i [4, 4, 3, 1] U_E, \quad (115)$$

which shows that U_v is weakly integral. The behaviour of this model is qualitatively very similar to that of the previous example, as we illustrate by drawing the graph of U_v versus $s = -\frac{1}{2\pi} \log(\kappa z)$ with $\kappa = e^{\sum_{k=1}^4 \psi(\alpha_k) - 4\psi(1)} = \frac{1}{432} = 2^{-4}3^{-3}$.

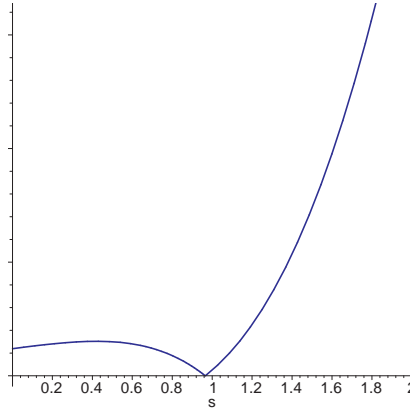


Figure 9. Graph of $|U_v|$ versus s for $s \in [0, 2]$. The point $z = 1$ corresponds to $s = \frac{1}{2\pi}(4\log 2 + 3\log 3) \approx 0.9658$.

5.5 A hypergeometric hierarchy

Before leaving the subject of compact one-parameter models, let us make a few methodological remarks. As illustrated above, starting with the ‘generic’ family of Section 3 and taking the limit where some of the parameters coincide produces new families of qualitatively different models. In this section, we studied only the first layer of such ‘degenerate’ models, namely the case where two of the parameters α coincide. The procedure clearly generalizes, leading to a hierarchy of models on five levels, which are characterized (up to permutations of the parameters) by the conditions:

- (0) all α_i are distinct
- (1) three of the parameters α_i are distinct
- (2) $\alpha_1 = \alpha_2$ and $\alpha_3 = \alpha_4$ but $\alpha_1 \neq \alpha_3$
- (3) $\alpha_1 = \alpha_2 = \alpha_3 = \alpha_4$.
- (4) $\alpha_1 = \alpha_2 = \alpha_3 \neq \alpha_4$

For example, it is easy to see that all of the complete intersection models in projective spaces investigated in [39] fit into one of these classes²³. In this section, we considered the two models of [39] which are of type (1), but it should be clear that a very similar approach can be followed for the other classes. In fact, one of the major advantages of using Meijer functions is that it allows for a very systematic treatment of entire families of models, as we have illustrated in some detail above. In the next section, we study a *non-compact* one-parameter model, which displays some new features. As we will show, our techniques are well adapted for this type of model as well.

6 Examples III: An orbifold example

In this section we consider a *non-compact* one-parameter example, namely the $\mathbb{C}^3/\mathbb{Z}_3$ orbifold. While non-compact and hence slightly unphysical, global orbifolds can be realized as local singularities of Calabi-Yau spaces, or as decompactification limits of singular Calabi-Yau varieties. In particular, the orbifold we consider can be realized as a limit of the 5-parameter model studied in [33]. For an overview of toric and mirror-symmetry techniques in the study of the moduli space of conformal field theories associated with partial resolutions of orbifolds we refer the reader to [31].

6.1 Classical geometry of the orbifold

We begin by reviewing the classical geometry of the model. Our orbifold X_0 can be realized as the quotient of \mathbb{C}^3 by the action:

$$(z_1, z_2, z_3) \rightarrow (\zeta z_1, \zeta z_2, \zeta z_3) \tag{116}$$

²³Class (4) is not realized through compact one-parameter complete intersections in toric varieties, though it could be realized through different constructions.

where $\zeta = e^{\frac{2\pi i}{3}}$. This has a straightforward toric description as the quotient:

$$X_0 = \mathbb{C}^4 / \mathbb{C}^* \quad (117)$$

of \mathbb{C}^4 by the torus action:

$$(x_0, x_1, x_2, x_3) \rightarrow (\lambda^{-3}x_0, \lambda x_1, \lambda x_2, \lambda x_3) \quad , \quad (118)$$

where $\lambda \in \mathbb{C}^*$, which corresponds to the fan in \mathbb{R}^3 consisting of a single simplicial cone with generators:

$$\nu_1 = (3, -1, -1) \quad (119)$$

$$\nu_2 = (0, 1, 0) \quad (120)$$

$$\nu_3 = (0, 0, 1) \quad . \quad (121)$$

Note that the interior of this cone contains the integral vector:

$$\nu_0 = (1, 0, 0) \quad . \quad (122)$$

The resolution X of X_0 can be achieved by a toric blow-up, which amounts to replacing X_0 by:

$$X = (\mathbb{C}^4 - Z) / \mathbb{C}^* \quad , \quad (123)$$

with the exceptional set $Z = \{x \in \mathbb{C}^4 | x_1, x_2, x_3 = 0\}$. This corresponds to adding ν_0 to our list of toric generators and taking the fan to consist of the 3 cones spanned by (ν_0, ν_i, ν_j) ($1 \leq i \leq j \leq 3$), thereby performing a star subdivision of the original cone (see Figure 10). Geometrically, this amounts to blowing-up the origin in the space $\mathbb{C}^3 / \mathbb{Z}_3$, thus producing an exceptional divisor D_0 associated with the generator ν_0 . The resolved space contains 4 toric divisors D_ρ , associated with the four toric generators ν_ρ ($\rho = 0 \dots 3$).

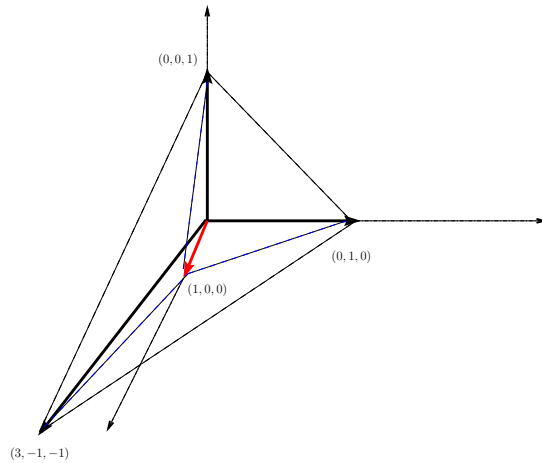


Figure 10. Fan for the $\mathbb{C}^3 / \mathbb{Z}_3$ orbifold.

The group $\text{Div}(X) \approx \text{Pic}(X)$ of divisor classes on X modulo linear equivalence is easy to compute by the general technology of [30] or by simple manipulations with the associated linear systems $\mathcal{O}(D_\rho)$, with the result that it is a free group generated by either of D_1 , D_2 or D_3 . In particular, we have the relation:

$$D_0 = -3D_1 = -3D_2 = -3D_3 \quad , \quad (124)$$

where we denote the linear equivalence class of a divisor D by the same letter. This corresponds to the fact that $\mathcal{O}(-D_0) \approx \mathcal{O}(D_1)^3 \approx \mathcal{O}(D_2)^3 \approx \mathcal{O}(D_3)^3$, as can be seen by considering the charges of x_ρ .

It follows that our model has a 1-dimensional Kähler moduli space, which can be parameterized by writing:

$$k = (B_0 + iJ_0)e_0 \quad , \quad (125)$$

where k is the complexified Kähler class, and e_0 is the Poincare dual of D_0 . In particular, the classical volume of D_0 is proportional to $-\int_{D_0} J^2 = 27J_0^2$, where we used the fact that $D_1^3 = 1$. Hence the orbifold point corresponds classically to $J_0 \rightarrow 0$, in which limit the volume of D_0 becomes zero.

6.2 The quantum moduli space and massless D -branes

As discussed for example in [31], the moduli space can be obtained without the need of an explicit construction of a mirror family. For this, it suffices to view the star-subdivision considered above as a perestroika associated with changing the phase in a mirror secondary fan, which in this case consist of two opposing semi-axes on the real line. It follows that the model has two phases, associated with two limits which correspond to blowing up the singularity until the exceptional divisor acquires very large area (the large radius point), respectively to blowing down the divisor to zero area (the deep interior of the orbifold phase). Hence the compactified moduli space can be identified with a copy of the Riemann sphere. Analyzing the associated Picard-Fuchs equation (see next subsection), which we write in terms of a convenient coordinate z gives two regular singular points at $z = 0, \infty$, which with our parameterization correspond to the large radius and deep orbifold points, respectively, as well as a regular singular point at $z = 1$, which can be thought of as defining the ‘boundary’ between the two regions (in sense which is explained precisely in [33, 32]). The special coordinate $t = B_0 + iJ_0$ on the quantum-corrected Kähler moduli space is then given by the mirror map as a function $t = t(z)$ which can be determined from the solutions of the Picard-Fuchs equation.

In the limit $z \rightarrow \infty$, the conformal field theory is an orbifold theory and hence exactly solvable. Based on the classical picture, one may expect that the D2-brane wrapping a cycle in the class e_1 , as well as the D4-brane wrapping the exceptional divisor would become massless at the orbifold point. As we discuss below, this picture

is drastically modified by quantum effects. First, based on the computations of \log^0 and \log^1 -monodromy periods already performed in [33] (and which will be subsumed by our more detailed results below), one can immediately see that the value of J_0 at the orbifold point is zero, but the value of B_0 equals $-1/2$ (in units where $2\pi\alpha' = 1$), so that a $D2$ -brane wrapping a rational curve in X has nonzero mass at $z = \infty$. This matches the fact that the conformal field theory is perfectly well-behaved there; an analogous observation was subsequently made in [41] in the context of K3 compactifications to explain the physical smoothness of orbifold points. On the other hand, we will argue that there exists a $D4$ -brane which becomes massless at the point $z = 1$, though no $D2$ -brane acquires vanishing mass there. Following our earlier discussion, we are unable to uniquely fix the lower brane charge on this $D4$ -brane, so it might well be interpretable as a $(D0,D4)$ -bound state.

6.3 Quantum volumes

6.3.1 The hypergeometric equation and the Meijer periods

The periods of this model satisfy the hypergeometric equation:

$$\left[\delta^3 - z\delta(\delta + 1/3)(\delta + 2/3) \right] u = 0 , \quad (126)$$

which corresponds to the hypergeometric symbol $\left(\begin{smallmatrix} 0, 1/3, 2/3 \\ 1, 1 \end{smallmatrix} \right)$. The Meijer periods can be obtained by the procedure discussed in Section 2 ²⁴:

$$U_0(z) = \Gamma\left(\begin{smallmatrix} 1, 1 \\ 0, 1/3, 2/3 \end{smallmatrix}\right) \mathbf{I}\left(\begin{smallmatrix} 0 & 0, 1/3, 2/3 \\ & 1, 1 \end{smallmatrix}\right) (-z) = 1, \quad (127)$$

$$U_1(z) = -\Gamma\left(\begin{smallmatrix} 1, 1 \\ 1/3, 2/3 \end{smallmatrix}\right) \mathbf{I}\left(\begin{smallmatrix} 0, 0 & 1/3, 2/3 \\ 1 & 1 \end{smallmatrix}\right) (-z), \quad (128)$$

$$U_2(z) = -\Gamma\left(\begin{smallmatrix} 1, 1 \\ 1/3, 2/3 \end{smallmatrix}\right) \mathbf{I}\left(\begin{smallmatrix} 0, 0, 0 & 1/3, 2/3 \\ 1 & \end{smallmatrix}\right) (+z). \quad (129)$$

For clarity, let us write down the integral representations for the nontrivial Meijer periods:

$$U_1(z) = \frac{1}{2\pi i \Gamma(1/3) \Gamma(2/3)} \int_{\gamma} ds \frac{\Gamma(s+1/3) \Gamma(s+2/3) \Gamma(-s)}{s \Gamma(s+1)} (-z)^s \quad (130)$$

$$U_2(z) = \frac{1}{2\pi i \Gamma(1/3) \Gamma(2/3)} \int_{\gamma} ds \frac{\Gamma(s+1/3) \Gamma(s+2/3) \Gamma(-s)^2}{s} z^s. \quad (131)$$

The reader can verify directly that U_j satisfy equation (126).

The expansions of the periods can be obtained as before. Instead of presenting details of the calculation, let us point out that closing the contour to the right (which

²⁴ The reader may worry that our expression for $U_0(z)$ is identically zero due to presence of the singular quantity $\Gamma(0)$ in the prefactor. However, this is a removable singularity. One can take $U_0(z)$ to be defined as a limit in which $\Gamma(0)$ in the denominator of $\Gamma\left(\begin{smallmatrix} 1, 1 \\ 0, 1/3, 2/3 \end{smallmatrix}\right)$ and $\Gamma(-s)$, $\Gamma(s)$ in the numerator of the integrand are replaced by $\Gamma(\epsilon)$ and $\Gamma(-s + \frac{\epsilon}{2})$, $\Gamma(s + \frac{\epsilon}{2})$ respectively, with a small positive ϵ which is taken to zero after performing the integral. When closing the contour to right or left, the factor $\Gamma(\epsilon)$ in the denominator will force us to keep only the residue corresponding to the pole at $s = 0$. Indeed, we have $\Gamma(\epsilon) \approx \frac{1}{\epsilon}$ and the quantity $\epsilon \operatorname{Res}_{s_0} [\Gamma(-s + \frac{\epsilon}{2}) \Gamma(s + \frac{\epsilon}{2})]$ (with s_0 a pole of type (A) or (B) of the regularized integrand) has a nonzero limit as ϵ tends to zero only if $s_0 = \frac{\epsilon}{2}$ or $s_0 = -\frac{\epsilon}{2}$; this limit is ± 1 , which forces the limiting value of the regularized integral to be identically 1 (remembering that the contours about $\pm\infty$ have opposite orientations). One can of course see directly that $U_0 = 1$ is a solution of the hypergeometric equation, but the argument just presented shows how this example fits into the general theory of Section 2. The solution U_1 is obtained from U_0 by performing *two* diagonal operations on the Meijer symbol. Lifting the parameter 1 along the second diagonal is the usual procedure for trying to make the (A)-type poles of the integrand become double, which assures that the solution thus produced has $\log^2(z)$ monodormy about $z = 0$. A further operation is performed along the first diagonal, by lowering the parameter 0. This replaces the factor $\Gamma(s)$ in the numerator by a factor $\Gamma(1-s) = -s\Gamma(-s)$ in the denominator, which cancels a $\Gamma(-s)$ introduced in the numerator by the first operation and leaves a factor of $-\frac{\Gamma(-s)}{s}$; hence all (A)-type poles remain simple except for the pole at $s = 0$. We also replace the prefactor $\Gamma\left(\begin{smallmatrix} 1, 1 \\ 0, 1/3, 2/3 \end{smallmatrix}\right)$ by $-\Gamma\left(\begin{smallmatrix} 1, 1 \\ 1/3, 2/3 \end{smallmatrix}\right)$ in order to avoid problems from $\Gamma(0)$. Such a rescaling is always allowed since the choice of normalization for our solutions is arbitrary. This slightly nonstandard behaviour is due to non-compactness of the model.

is possible for $|z| < 1$) leads to j -th order poles at $s = n$ (n a strictly positive integer) from the factors of $\Gamma(-s)^j$ in the integrand and to a $j + 1$ -th order pole at $s = 0$ from $\frac{\Gamma(-s)^j}{s}$. Computing the associated residues leads to the expansions for $|z| < 1$:

$$U_1(z) = \log(-z) + [\psi(1/3) + \psi(2/3) - 2\psi(1)] + \sum_{n=1}^{\infty} \frac{(1/3)_n(2/3)_n}{n!^2 n} z^n$$

$$U_2(z) = -\frac{1}{2} \left[(\psi'(1/3) + \psi'(2/3) + 2\psi'(1)) + (\psi(1/3) + \psi(2/3) - 2\psi(1) + \log z)^2 \right] -$$

$$\sum_{n=1}^{\infty} \left(\log(z) + \psi(n+1/3) + \psi(n+2/3) - 2\psi(1) \right) - \frac{3}{n} - 2 \sum_{k=1}^{n-1} \frac{1}{k} \cdot \frac{(1/3)_n(2/3)_n}{n!^2 n} z^n .$$

The expression for $U_1(z)$ can be simplified by noticing that:

$$\sum_{n=1}^{\infty} \frac{(1/3)_n(2/3)_n}{n!^2 n} z^n = \frac{2}{9} z {}_4F_3 \left(\begin{matrix} 4/3, 5/3, 1, 1 \\ 2, 2, 2 \end{matrix} \right) (z) \quad (132)$$

(to see this, one must first shift the summation variable according to $n \rightarrow n-1$ and then perform some basic manipulations on the Pochhammer symbols). Moreover, applying the identities (221) of Appendix B for $n = 3$ gives the relations:

$$\psi(1/3) + \psi(2/3) - 2\psi(1) = -3\log(3) \quad (133)$$

$$\psi'(1/3) + \psi'(2/3) + 2\psi'(1) = 10\psi'(1) = \frac{5\pi^2}{3} . \quad (134)$$

which allow one to further simplify $U_1(z)$ and $U_2(z)$.

The expansions of the Meijer periods for $|z| > 1$ can be obtained similarly. In this case, one can close the contour to the left, obtaining a Cauchy expansion over the simple poles $s = -n - 1/3$ and $s = -n - 2/3$, with n a nonnegative integer. The resulting residues can be simplified by making use of the completion formula and the identity:

$$(x+1)_n = (x)_n \frac{x+n}{x} \quad (135)$$

which allows for the replacement of $\frac{1}{n+x}$ with $\frac{1}{x} \frac{(x)_n}{(x+1)_n}$. In this way, one obtains:

$$U_1(z) = -3 \frac{\Gamma(1/3)}{\Gamma(2/3)^2} (-z)^{-1/3} {}_3F_2 \left(\begin{matrix} 1/3, 1/3, 1/3 \\ 2/3, 4/3 \end{matrix} \right) (1/z) + \frac{3}{2} \frac{\Gamma(2/3)}{\Gamma(1/3)\Gamma(4/3)} (-z)^{-2/3} {}_3F_2 \left(\begin{matrix} 2/3, 2/3, 2/3 \\ 4/3, 5/3 \end{matrix} \right) (1/z)$$

$$U_2(z) = -3 \frac{\Gamma(1/3)^2}{\Gamma(2/3)} z^{-1/3} {}_3F_2 \left(\begin{matrix} 1/3, 1/3, 1/3 \\ 2/3, 4/3 \end{matrix} \right) (1/z) + \frac{3}{2} \frac{\Gamma(2/3)^2}{\Gamma(4/3)} z^{-2/3} {}_3F_2 \left(\begin{matrix} 2/3, 2/3, 2/3 \\ 4/3, 5/3 \end{matrix} \right) (1/z) \quad (136)$$

6.3.2 Monodromies of the Meijer basis

The monodromies of the Meijer basis follow from arguments similar to those presented in Section 3. In our case, the matrix $\tilde{q}(0)$ is:

$$\tilde{q}(0) := \begin{bmatrix} 1 & i\pi & -\frac{5\pi^2}{6} \\ 0 & 1 & 0 \\ 0 & 0 & -\frac{1}{2} \end{bmatrix} , \quad (137)$$

where we used $\psi'(1/3) + \psi'(2/3) + 2\psi'(1) = \frac{5\pi^2}{3}$ and the expansions derived above for $|z| < 1$. The monomial-divisor mirror map gives the coordinate $w = \frac{z}{27}$ (in this example $\kappa = \psi(1/3) + \psi(2/3) - 2\psi(1) = 3^{-3}$), while the matrix $q'(0)$ has the form $q'(0) := \text{diag}(1, 1, 1/2)$. This information allows us to compute $\tilde{M} = \tilde{q}(0)^t q'(0)^{-1}$. The matrix $R_{can}[0]$ is again in Jordan form:

$$R_{can}[0] = \begin{bmatrix} 0 & 1 & 0 \\ 0 & 0 & 1 \\ 0 & 0 & 0 \end{bmatrix}, \quad (138)$$

leading to the following expression for the Meijer monodromy around $z = 0$:

$$T[0] := \tilde{M} T_u[0] \tilde{M}^{-1} = \begin{bmatrix} 1 & 0 & 0 \\ 2i\pi & 1 & 0 \\ 0 & -2i\pi & 1 \end{bmatrix} \quad (139)$$

(here $T_u[0] = e^{2\pi i R_{can}[0]^t}$). The monodromy around $z = \infty$ follows easily from the expansions (136):

$$T[\infty] = \begin{bmatrix} 1 & 0 & 0 \\ 0 & -2 & -\frac{3}{2}i \\ 0 & -2i\pi & 1 \end{bmatrix}. \quad (140)$$

Finally, the monodromy around $z = 1$ is given by:

$$T[1] = T[0]^{-1} T[\infty] = \begin{bmatrix} 1 & 0 & 0 \\ -2i\pi & -2 & -\frac{3i}{2\pi} \\ 4\pi^2 & -6i\pi & 4 \end{bmatrix}. \quad (141)$$

These monodromy matrices satisfy:

$$(T[0] - I)^3 = 0, \quad (T[1] - I)^2 = 0, \quad T[\infty]^3 - I = 0. \quad (142)$$

6.3.3 Integral structure

Following the general method described in Section 2, we now look for a cyclic period for this model. In this example we cannot use U_0 as a cyclic period, which is yet another effect of non-compactness. Indeed, U_0 is a constant function over the moduli space, which means that all monodromy operators $T[0]$, $T[1]$, $T[\infty]$ leave it invariant. In order to be able to carry out our program, it is thus necessary to identify another cyclic and weakly integral period. Here we present a possible approach to this problem, which makes use of the integrality conjecture of Aspinwall and Lutken [48]. It was argued in [48] that the cohomology class $\Omega \in H^3(Y, \mathbb{C})$ should align with a vector of the lattice $H^3(Y, \mathbb{Z})$ in the large complex structure limit. Taking this conjecture at face value²⁵, it is possible to obtain a candidate period with the desired properties, as we now explain.

²⁵In fact, the status of the arguments of [48] is not completely clear to us, for the following reason. In [48], it is argued that the Hodge subspaces $H^{3-p,p}(Y)$ ($p = 0..3$) should become rational subspaces of $H^3(Y)$ (with respect to $H^3(Y, \mathbb{Z})$) in the large complex structure limit. On the other hand, the standard approach to

Consider the asymptotic form of the period vector in the large complex structure limit $t_{alg} \rightarrow i\infty$, where $t_{alg} = \frac{1}{2\pi i} \log(\frac{z}{27})$ is the algebraic coordinate on the moduli space:

$$U(s) \approx \begin{bmatrix} 0 \\ 0 \\ 2\pi^2 \end{bmatrix} t_{alg}^2 + O(t_{alg}, e^{it_{alg}}) . \quad (143)$$

According to [48], the leading term in this equation should be proportional to a vector of the lattice $\Lambda = H_3(Y, \mathbb{Z})$. It follows that the Meijer period U_2 should coincide with the period of Ω over an integral cycle, up a *constant* complex factor. Assuming this is the case, we can use that cycle in order to generate a sublattice of Λ . In fact, it is easy to check that U_2 is cyclic for the action of all monodromies. Hence repeatedly acting on it with $T[0]$, $T[1]$ and $T[\infty]$ produces a basis of periods which are associated (up to a *common* factor) with a basis of a full sublattice Λ_0 of Λ . One can take $U_E(z) = EU(z)$ as the period vector associated to such a basis, with the matrix E given by:

$$E := \begin{bmatrix} 0 & 0 & 1 \\ 0 & -2i\pi & 1 \\ 4\pi^2 & -4i\pi & 1 \end{bmatrix} . \quad (144)$$

The monodromies of the basis E are given by integral matrices, as they should:

$$T_E[0] = \begin{bmatrix} 0 & 1 & 0 \\ 0 & 0 & 1 \\ 1 & -3 & 3 \end{bmatrix} , \quad T_E[1] = \begin{bmatrix} 2 & 1 & 1 \\ 0 & 1 & 0 \\ -1 & -1 & 0 \end{bmatrix} , \quad T_E[\infty] = \begin{bmatrix} 0 & 1 & 0 \\ -1 & -1 & 0 \\ -1 & -5 & 1 \end{bmatrix} .$$

As a further check, let us consider the period $U_\beta(z) = \frac{1}{2\pi i} U_1(z) - \frac{1}{2}$, which is associated with the vector:

$$\beta := \begin{bmatrix} -\frac{1}{2} & \frac{1}{2\pi i} & 0 \end{bmatrix} , \quad (145)$$

Since this period asymptotes to $U_\beta \approx s$ in the large complex structure limit, it is guaranteed to correspond to an integral cycle up to an unknown complex factor (see, for example, [29]). It is easy to express this period in the basis U_E , with the result that $U_\beta = \beta_{int} U_E$, where:

$$\beta_{int} = \frac{1}{8\pi^2} \begin{bmatrix} -3 & 4 & -1 \end{bmatrix} , \quad (146)$$

mirror symmetry computations does not actually use the Hodge subspaces as such but, rather, the subspaces $\mathcal{H}^{3-p,p}(Y) = \mathcal{F}_Y^p \cap W^{3-p}$ where \mathcal{F} is the Hodge filtration and W the monodromy weight filtration (see [61] for a clear explanation of this point). Doing so is desirable because $\mathcal{H}^{3-p,p}(Y)$ vary holomorphically over the moduli space, while the true Hodge subspaces do not. This makes the associated periods amenable for direct computation. Working with $\mathcal{H}^{3-p,p}(Y)$ is permitted at the level of the *closed* nonlinear sigma model due to arguments of [23] and [21] which show that working with elements of $\mathcal{H}^{3-p,p}$ instead of $H^{3-p,p}$ does not affect the closed conformal field theory correlators. However, the status of this claim needs to be reexamined when one includes boundary states thereby working at the level of open conformal field theory. While we have some preliminary calculations that are relevant to this issue, we will not consider it further here. We emphasize, though, that whereas the reasoning of subsection 6.3.3 involves the conjecture of [48], we will provide independent evidence for integrality of the vanishing period U_v below (see equation (149) for an independent argument to that effect), so that our conclusion that U_v is weakly integral is independent of the considerations of this subsection.

which is indeed an element of Λ_0 after rescaling by the factor $8\pi^2$.

6.3.4 A vanishing period and some arithmetic identities

Now consider the period $U_v := \frac{1}{8\pi^2}(4\pi^2 U_0 + 3U_2)$, which corresponds to the vector:

$$\gamma := \begin{bmatrix} \frac{1}{2} & 0 & \frac{3}{8\pi^2} \end{bmatrix} . \quad (147)$$

Then we have $U_v = \gamma_{int} U_E$, with:

$$\gamma_{int} = \frac{1}{8\pi^2} \begin{bmatrix} 4 & -2 & 1 \end{bmatrix} . \quad (148)$$

Hence U_v is again a weakly integral period. This can be checked independently by acting with $T[\infty]$ and $T[\infty]^2$ on U_β , thus producing a weakly integral basis in which U_v has rational coefficients:

$$U_v = -\frac{5}{6}U_\beta - \frac{1}{3}T_U[\infty]U_\beta + \frac{1}{6}T_U[\infty]^2U_\beta . \quad (149)$$

We claim that the period U_v vanishes for $z = 1$:

$$U_v(1) = 0 \iff U_2(1) = -\frac{4\pi^2}{3} . \quad (150)$$

Using the expansions of $U_2(z)$ for $|z| > 1$ and $|z| < 1$, this is equivalent to the following slightly nontrivial arithmetic identities:

$$-3 {}_3F_2 \left(\begin{matrix} 1/3, 1/3, 1/3 \\ 2/3, 4/3 \end{matrix} \right) (1) + \frac{27}{16\pi^3} \sqrt{3} {}_3F_2 \left(\begin{matrix} 2/3, 2/3, 2/3 \\ 5/3, 4/3 \end{matrix} \right) (1) \Gamma(2/3)^6 + \Gamma(2/3)^3 = 0 \quad (151)$$

and:

$$-\frac{1}{2} \left(\psi'(1/3) + \psi'(2/3) + \frac{1}{3}\pi^2 + 9\log(3)^2 \right) - \sum_{n=1}^{\infty} \frac{(\psi(n + \frac{1}{3}) + \psi(n + \frac{2}{3}) - \frac{3}{n} - 2\psi(n)) (1/3)_n (2/3)_n}{n!^2 n} = -\frac{4\pi^2}{3} \quad (152)$$

We checked both identities numerically, but we lack an analytic proof. Note that, given one of the two identities above, analytic continuation automatically produces the other. Figure 11 displays the values of $|U_v|$ as a function of the algebraic coordinate $s = -\frac{1}{2\pi}\log(\frac{z}{27})$. We also display the values of the special coordinate $t = U_\beta = \frac{1}{2\pi i}U_1(z) - 1$, which measures the mass of a $D2$ -brane.

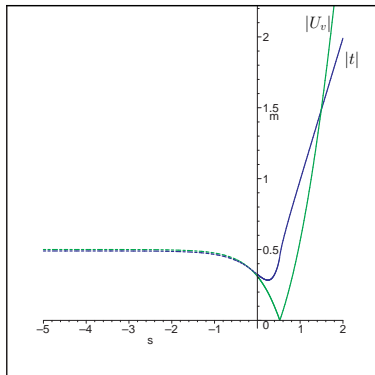


Figure 11. Graph of the vanishing period and special coordinate (in absolute value) versus the real Kahler parameter $s = -\frac{1}{2\pi}\log\left(\frac{z}{27}\right)$, for z belonging to the real axis. The point $z = 1$ corresponds to $s = \frac{3}{2\pi}\log 3$. We also plot the values of $|U_v(s)|$ and $|t|$ for negative s . The region $s \rightarrow -\infty$ corresponds to the small radius limit, which has no classical analogue. In this limit, both $|t|$ and $|U_v|$ asymptote to the value $1/2$.

6.4 Interpretation

Our results confirm the picture announced above. In particular, we obtained a vanishing period which has \log^2 monodromy around $z = 0$ and thus can be interpreted as a D4-brane state in a *IIA* compactification on X . This object becomes massless at $z = 1$, and not at $z = 0$ as one would have expected based on classical arguments. Moreover, when it becomes massless, the D2-brane states remain massive, something quite at odds with classical expectations.

Admittedly, our discussion of integral structure has been less than complete, essentially because we avoided working with an explicit construction of the mirror, which would necessitate a more careful discussion of the effects of non-compactness on the interpretation of standard mirror symmetry constructions. In the next section, we consider a compact model in which the integral structure is fully understood. In order to make the discussion more realistic, we focus on a two-parameter example, some features of which were discussed in [36].

7 Examples IV: A two-parameter example

In this section, we consider a special locus in the moduli space of a two-parameter example. We will show that there is a D4-brane state (possibly bound with a D0-brane) which becomes massless at every point on this locus. Comparison with classical geometry leads to some surprising conclusions. Two-parameter examples were studied in the papers [36, 37, 38]. We will focus on a model discussed in [36], to which we refer the reader for background.

7.1 The model and its mirror

One of the two models studied in [36] corresponds to the Kähler moduli space of a degree 8 hypersurface in the weighted projective space $WP^{1,1,2,2,2}$. This can be described as the space of partial resolutions of the Fermat hypersurface:

$$X_0 : x_1^8 + x_2^8 + x_3^4 + x_4^4 + x_5^4 = 0 \quad , \quad (153)$$

which has a curve Σ of singularities of arithmetic genus 3, given by:

$$\Sigma : x_1 = x_2 = 0, \quad x_3^4 + x_4^4 + x_5^4 = 0 \quad . \quad (154)$$

Partial resolutions X are obtained by blowing up X_0 along Σ , which produces an exceptional divisor E (a ruled surface over Σ). The Picard group of the resolved variety is generated by two linear systems L (a pencil of $K3$ surfaces) and H , in terms of which the (linear equivalence class of the) exceptional divisor can be expressed as:

$$E = H - 2L \quad . \quad (155)$$

In order to describe the full cohomology ring, consider the two classes l and h in $H_2(X, \mathbb{Z})$ defined by the fiber of the ruling of E , respectively by the intersection of H with L , respectively. Then the relations defining the intersection ring, whose derivation can be found in [36], are:

$$\begin{aligned} L^2 &= 0 & , & & H^2 &= 4l + 8h \\ H \cdot L &= 4h & , & & H^3 &= 8 \\ H^2 \cdot L &= 4 \end{aligned} \quad . \quad (156)$$

In particular, we have:

$$L \cdot l = H \cdot h = 1 \quad (157)$$

$$H \cdot l = L \cdot h = 0 \quad , \quad (158)$$

hence the bases (h, l) of $H_2(X, \mathbb{Z})$ and (H, L) of $H_4(X, \mathbb{Z})$ are dual with respect to the intersection form. The Kähler cone is then easily seen to be given by $J = \tau_1 \check{H} + \tau_2 \check{L}$ with $\alpha, \beta \geq 0$, where \check{A} denotes the Poincare dual of a homology class A .

The mirror manifold Y can be easily constructed via the methods of [56] or [57]. In the second approach Y can be described as the finite quotient \tilde{Y}/G where \tilde{Y} is the following hypersurface in $WP^{1,1,2,2,2}$:

$$\tilde{Y} : x_1^8 + x_2^8 + x_4^4 + x_5^4 - 8\psi x_1 x_2 x_3 x_4 x_5 - 2\phi x_1^4 x_2^4 = 0 \quad , \quad (159)$$

and the group G is a copy of \mathbb{Z}_4^3 acting in a way described in detail in [36]. The moduli space is the quotient $\mathbb{C}^2(\psi, \phi)/\mathbb{Z}_8$, with the generator of \mathbb{Z}_8 acting by:

$$(\psi, \phi) \rightarrow (\alpha\psi, -\phi) \quad , \quad (160)$$

where $\alpha := e^{\frac{2\pi i}{8}}$. Hence the parameters (ψ, ϕ) used in [36] give an eight-fold cover of the complex structure moduli space of Y . The discriminant locus has three components at finite-distance in the variables (ψ, ϕ) , which following [36] we denote as follows:

- (1) $C_{con} : (\phi + 8\psi^4)^2 = 1$, where Y acquires a conifold singularity
- (2) $C_1 : \phi^2 = 1$, where Y acquires an isolated singularity not of the conifold type
- (3) $C_0 : \psi = 0$, where the moduli space acquires orbifold singularities.

Beyond these, one must add at least the divisor:

- (4) $C_\infty : \psi, \phi \rightarrow \infty$

in order to form a reasonable compactification of the moduli space. The detailed description of this divisor depends on the precise compactification under consideration.

The natural compactification for the purpose of mirror symmetry is a toric compactification defined by the secondary fan [27, 28]. In the case under consideration, this turns out to be a certain partial resolution of the weighted projective space $WP^{1,1,2}$, whose toric diagram we draw in Figure 12. The model has four phases, the deep interior points of which are denoted in the figure by A , B , C and D . Point A corresponds to the smooth Calabi-Yau phase, point D is a compact singular phase in which the exceptional divisor E has been blown down, while points B and C correspond to non-geometric phases. The correct singularity structure of the moduli space is obtained upon replacing the generator $(0, 1)$ with $(0, 4)$, which leads to orbifold singularities at the points B, C and D . Point C is a Landau-Ginzburg point; at that point, the moduli space has a \mathbb{Z}_8 quotient singularity. In Figure 12, we indicate the divisors associated with the generators in square brackets. The divisors E , H and L are as before, while the generator $(0, 1)$ does not correspond to a divisor on X but must be added in order to build the moduli space of its mirror (this is sometimes called the ‘non-compact generator’). Figure 12 provides a parameterization of the moduli space by means of algebraic coordinates [33]. The dotted lines in the figure represent the compactification divisors, which connect the four deep interior points; these are the ‘rational curves at infinity’ of [33]. There exists a common point of intersection among C_0, C_1 and C_{con} , denoted by S in the figure. This point corresponds to $\psi = 0, \phi = 1$. The curve C_1 also intersects the divisor $D_{(0,-1)}$ in a point T , which corresponds to $\phi = 1, \psi = \infty$. We also indicate the point U of tangency between C_{con} and C_∞ , which corresponds to $\phi \rightarrow \infty, 8\phi^{-1}\psi^4 \rightarrow -1$. Note that the Kähler cone can be identified with the cone spanned by the generators $(1, 0)$ and $(0, -1)$; in particular, point A corresponds to the large radius limit of our two-parameter model²⁶.

²⁶Further resolutions—some of them non-toric—are needed in order to produce a compactification which is smooth and such that the various boundary divisors intersect with normal crossings [36]. This is useful for an exhaustive study of monodromies, but will not be important for us.

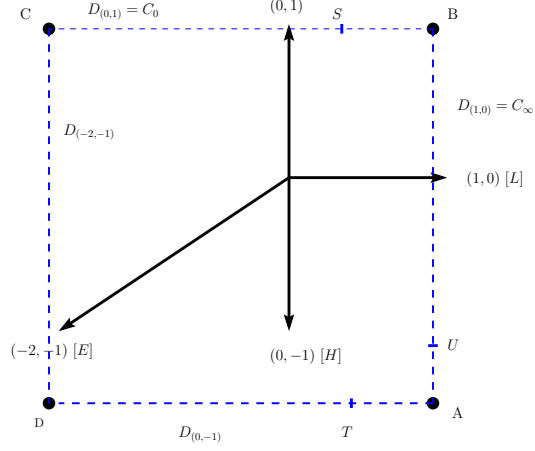


Figure 12. The secondary fan

Figure 13 is a diagram of the curves C_1 and C_{con} , as well as of the compactification divisors $D_{(0,1)} = C_0$, $D_{(1,0)} = C_\infty$ and $D_{(0,-1)}$ (we do not draw $D_{(-2,-1)}$, since it will not be important below). The curves C_1 and C_{con} intersect in two points, one of which is the point S already discussed above. The other is the point R , which corresponds to $8\psi^2 = -2, \phi = 1$. These points will play an important role below.

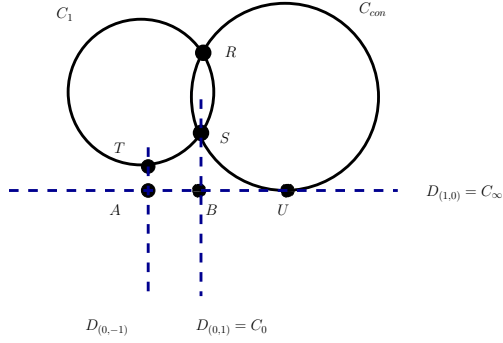


Figure 13. Components of the discriminant locus

In order to understand the role of C_{con} and C_1 in defining the phase structure of the model, it is useful to determine the image of these components of the discriminant

locus in the (uncomplexified) Kähler moduli space, with respect with the algebraic coordinates defined in [33]. This can be easily achieved by using the asymptotic form of the mirror map given on pages 40 – 41 of [36] (or by direct consideration of the monomial-divisor mirror map of [28]). The result is plotted in Figure 14. We see that the asymptotic branches of C_{con} separate phases A and B , B and C as well as phase C from A and D , but they do not separate phase A from D . This last phase boundary is induced by the curve C_1 , which also contributes to the separation between phases B and C .

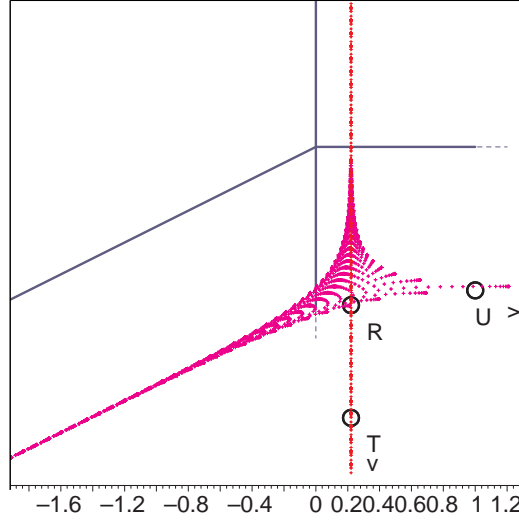


Figure 14. The image of the discriminant components C_1 and C_{con} with respect to the algebraic measure. The image of C_{con} is the three-pronged structure at the center of the diagram, extending towards infinity in directions parallel with the generators $(0, 1)$, $(1, 0)$ and $(-2, -1)$. The image of C_1 is the vertical line parallel with the generator $(0, 1)$, located at a distance given by $\frac{1}{2\pi}\log 4 \approx 0.2206$ in the positive direction along this generator. We also display the image of the points R, S, T and U . The image of R has coordinates $(\frac{1}{2\pi}\log 4, -\frac{9}{2\pi}\log 2) \approx (.2206, -.9928)$, while the images of S, T lie at infinity along the image of C_1 . The image of U lies at infinity on the horizontal branch of the image of C_{con} . This branch asymptotes to a line parallel with the generator $(1, 0)$ and placed at a distance $\frac{8}{2\pi}\log 2 \approx 0.882$ below it.

In what follows, we will only be interested in the locus C_1 , leaving a discussion of other interesting loci to future work. As observed in [36], this locus has the interesting property that for $(\psi, \phi) \in C_1$, the family Y is birationally equivalent to the mirror of a complete intersection of a quadric and a quartic in \mathbb{P}^5 , one of the models we studied in Section 5. Naively, one expects C_1 to be mirror to the locus \check{C}_1 where the fiber of the ruling of the exceptional divisor E of X is blown-down to zero size, since, as mentioned in [36], X becomes birational to a $(2, 4)$ complete intersection on this locus. Therefore, one naively expects that a D2-brane wrapping a rational curve in the class l becomes massless everywhere on the locus \check{C}_1 . Note that it is possible to keep the area of the \mathbb{P}^1 fiber l of the ruling equal to zero while varying the area of the base Σ , which is why we obtain a one-parameter locus; the classical volume of E is of course identically zero on \check{C}_1 . The entire locus \check{C}_1 corresponds to the wall in the Kähler moduli space where $\int_l J = 0$, i.e. $\tau_2 = 0$, $\tau_1 \geq 0$.

As we show below by direct computation, this picture receives important modifications due to quantum corrections. Indeed, we will see that the D2-brane wrapping l does *not* acquire vanishing mass on the mirror locus to C_1 due to the familiar fact that there is a nonzero B -field flux through cycles in l at generic points on this locus. Nevertheless, the classical conclusion that $\int_l J = 0$ is still valid after quantum corrections are taken into account. The D-brane which becomes massless everywhere on (the mirror to the locus) C_1 , is a $D4$ -brane, as we will see explicitly. In the last subsection, we also consider the restricted theory on the locus C_1 and show explicitly that it is equivalent to the model $\mathbb{P}^5[2, 4]$. In particular, this allows us to identify the collapsing 6-brane found in Section 5 with a certain 6-brane state of the ‘ambient’ two-parameter model.

7.2 Restriction of periods to the locus C_1

A basis of periods for our model was obtained in [36]. Such a basis consists of the 6 periods denoted there by $\omega_0 \dots \omega_5$, whose expansions were computed in [36] in some regions of the moduli space. The precise form of ω_i depends on whether i is even or odd, so we think of our collection of periods as being divided into two subsets, $\{\omega_{2j}\}_{j=0..2}$ and $\{\omega_{2j+1}\}_{j=1..2}$.

We start with the ψ -expansions of ω_i obtained in [36]:

$$\begin{aligned}\omega_{2j}(\psi, \phi) &= -\frac{1}{4\pi^3} \sum_{r=1}^3 (-1)^r \sin^3\left(\frac{\pi r}{4}\right) \alpha^{2jr} \xi_r(\psi, \phi) \\ \omega_{2j+1}(\psi, \phi) &= -\frac{1}{4\pi^3} \sum_{r=1}^3 (-1)^r \sin^3\left(\frac{\pi r}{4}\right) \alpha^{(2j+1)r} \eta_r(\psi, \phi)\end{aligned}\tag{161}$$

where:

$$\xi_r(\psi, \phi) = \frac{1}{2\pi i} \int_{\gamma} d\nu f_r(\nu, \psi, \phi) \quad , \quad \eta_r(\psi, \phi) = -\frac{1}{2\pi i} \int_{\gamma} d\nu e_r(\nu, \psi, \phi) \quad ,$$

with the integrands:

$$\begin{aligned}
f_r(\nu, \psi, \phi) &= \frac{\pi}{\sin \pi(\nu + r/4)} \frac{\Gamma^4(-\nu)}{\Gamma(-4\nu)} (2^{12}\psi^4)^{-\nu} u_\nu(\phi) \\
e_r(\nu, \psi, \phi) &= \frac{\pi}{\sin \pi(\nu + \frac{r}{4})} \frac{\Gamma^4(-\nu)}{\Gamma(-4\nu)} (2^{12}\psi^4)^{-\nu} \frac{u_\nu(\phi) \sin \pi(\nu + \frac{r}{4}) - u_\nu(-\phi) \sin(\frac{\pi r}{4})}{\sin(\pi\nu)} .
\end{aligned}$$

The contour γ is shown in Figure 15.

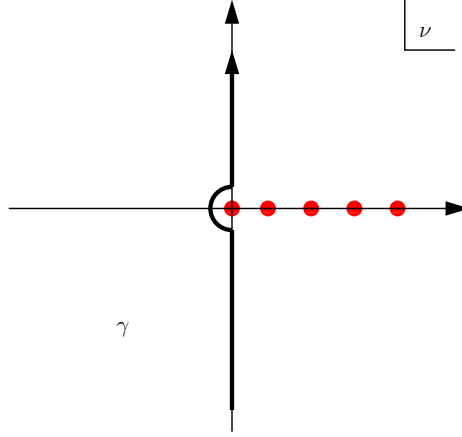


Figure 15. Contour of integration for ξ_r and η_r . We also display the poles of the integrands at $\nu = n$ (n a nonnegative integer) on the positive real axis. The integrands also have poles on the negative real axis, which are irrelevant for us.

The function $u_\nu(\phi)$ in the expressions above is defined by:

$$u_\nu(\phi) := (2\phi)^\nu {}_2F_1 \left(\begin{matrix} -\frac{\nu}{2} \\ 1 \end{matrix}, \frac{1-\nu}{2} \right) \left(\frac{1}{\phi^2} \right) . \quad (162)$$

We refer the reader to [36] for a discussion of the basic properties of the functions $u_\nu(\phi)$, some of which we will use below.

The identity (219) of Appendix B, together with the completion formula allows us to write:

$$\begin{aligned}
f_r(\nu, \psi, \phi) &= 8\pi^2 \frac{\Gamma(\nu + \frac{r}{4})\Gamma(-\nu)^3}{\prod'_{k=1 \dots 3} \Gamma(-\nu + \frac{k}{4})} z^{-\nu} u_\nu(\phi) \\
e_r(\nu, \psi, \phi) &= -8\pi \frac{\Gamma(\nu + \frac{r}{4})\Gamma(\nu + 1)\Gamma(-\nu)^4}{\prod'_{k=1 \dots 3} \Gamma(-\nu + \frac{k}{4})} z^{-\nu} \left[u_\nu(\phi) \sin \pi(\nu + \frac{r}{4}) + u_\nu(-\phi) \sin \frac{\pi r}{4} \right] ,
\end{aligned}$$

where $\prod'_{k=1 \dots 3} \{ \dots \} := \prod_{k=1 \dots 3, k \neq 4-r} \{ \dots \}$ and we defined $z := (2\psi)^4$.

We are interested in the behaviour of the periods near the curve C_1 , i.e. in the limit of (161) for $\phi \rightarrow 1$. The expansions of these periods in the region $|\frac{8\psi^4}{\phi \pm 1}| < 1$ are given in [36], but this is not what we need, since C_1 lies in the complement of that region. In order to extract the information we desire, we must obtain the expansions of (161) for large ψ , i.e. for $|z| \gg 1$. This can be achieved once again by a computation of residues.

Let us first discuss the expansion of ξ_r in this region. Since $|z| \gg 1$, we can close the defining contour to the right, towards $+\infty$. The resulting Cauchy expansion receives contributions only from the poles of f_r located at $\nu = n$, with n a nonnegative integer; these poles are all of order 3. Computation of the associated residues proceeds as before, giving:

$$\xi_r(\psi, \phi) = 4\pi^2 \sum_{n=0}^{\infty} \frac{\Gamma(n + \frac{r}{4})}{n!^3 \prod'_{k=1 \dots 3} \Gamma(-n + \frac{k}{4})} (-z)^{-n} H_r(n, \psi, \phi) u_n(\phi) \quad . \quad (163)$$

A similar computation for η_r (which receives contributions from poles of order 4) gives:

$$\eta_r(\psi, \phi) = -\frac{8\pi}{3} \sum_{n=0}^{\infty} \frac{\Gamma(n + \frac{r}{4})}{n!^3 \prod'_{k=1 \dots 3} \Gamma(-n + \frac{k}{4})} \sin(\frac{\pi r}{4}) (-z)^{-n} K_r(n, \psi, \phi) u_n(\phi) \quad . \quad (164)$$

To arrive at the last formula, we made use of the property:

$$u_n(-\phi) = (-1)^n u_n(\phi) \quad , \quad (165)$$

which can be easily deduced from the Euler representation of u_n (see [36]). In these expansions, the quantities H_r, K_r are defined by:

$$\begin{aligned} H_r(n, \psi, \phi) &:= (p_1(n, r) + \alpha_1(n, \phi) - \log(z))^2 + p_2(n, r) + \alpha_2(n, \phi) \\ K_r(n, \psi, \phi) &:= (q_1(n, r) + \beta_1(n, r, \phi) - \log(z))^3 + 3(q_1(n, r) + \beta_1(n, r, \phi) - \log(z))(q_2(n, r) + \beta_2(n, r, \phi)) + \\ &\quad + q_3(n, r) + \beta_3(n, r, \phi) \quad , \end{aligned}$$

where:

$$\begin{aligned} p_i(n, r) &:= \psi^{(i-1)}(n + \frac{r}{4}) - (-1)^i \left[\sum'_{k=1 \dots 3} \psi(-n + \frac{k}{4}) - 3(i-1)! \sum_{k=1}^n \frac{1}{k^i} - 3\psi^{(i-1)}(1) \right] \\ q_i(n, r) &:= \psi^{(i-1)}(n + \frac{r}{4}) + \psi^{(i-1)}(n+1) + (-1)^{i-1} \left[\sum'_{k=1 \dots 3} \psi^{(i-1)}(-n + \frac{k}{4}) - 4\psi^{(i-1)}(1) - 4(i-1)! \sum_{k=1}^n \frac{1}{k^i} \right] \end{aligned} \quad (166)$$

and:

$$\begin{aligned} \alpha_i(n, \phi) &:= \left[\frac{d^i}{d\nu^i} \log(u_\nu(\phi)) \right]_{\nu=n} \\ \beta_i(n, r, \phi) &:= \left[\frac{d^i}{d\nu^i} \log \left(u_\nu(\phi) \sin \pi(\nu + \frac{r}{4}) + u_\nu(-\phi) \sin(\frac{\pi r}{4}) \right) \right]_{\nu=n} \quad . \end{aligned}$$

One can rearrange the result in a form which displays ω_i as expansions in the basis of functions given by $z^{-n} (\log z)^s$. Write:

$$\begin{aligned} H_r(n, \psi, \phi) &:= \sum_{s=0}^2 \rho_s(r, n, \phi) (\log z)^s \\ K_r(n, \psi, \phi) &:= \sum_{s=0}^3 \lambda_s(r, n, \phi) (\log z)^s . \end{aligned}$$

with the coefficients:

$$\rho_0 := p_2 + \alpha_2 + (p_1 + \alpha_1)^2 \quad , \quad \rho_1 := -2(p_1 + \alpha_1) \quad , \quad \rho_2 := 1$$

and:

$$\begin{aligned} \lambda_0 &:= (q_1 + \beta_1)^3 + 3(q_1 + \beta_1)(q_2 + \beta_2) + (q_3 + \beta_3) & \lambda_2 &:= 3(q_1 + \beta_1) \\ \lambda_1 &:= -3[(q_1 + \beta_1)^2 + (q_2 + \beta_2)] & \lambda_3 &:= -1 \end{aligned} .$$

We also define $\rho_3 := 0$ in order to give a concise form to subsequent formulae. Then we have:

$$\omega_i(\psi, \phi) := \sum_{s=0}^3 \sum_{n=0}^{\infty} z^{-n} (\log z)^s M_i(s, n, \phi) \quad , \quad (167)$$

with the expansion coefficients:

$$M_i(s, n, \phi) = \frac{u_n(\phi)}{n!^3 \prod_{k=1}^3 \Gamma(-n + \frac{k}{4})} L_i(s, n, \phi) \quad , \quad (168)$$

where:

$$L_{2j}(s, n, \phi) := - \sum_{r=1}^3 (-1)^r \alpha^{2jr} \sin^2(\frac{\pi r}{4}) \rho_s(n, r, \phi) \quad (169)$$

$$L_{2j+1}(s, n, \phi) := \frac{2}{3\pi} \sum_{r=1}^3 (-1)^r \alpha^{(2j+1)r} \sin^3(\frac{\pi r}{4}) \lambda_s(n, r, \phi) \quad . \quad (170)$$

$$(171)$$

In order to arrive at these expressions, we made use of the identity:

$$\sin(\frac{\pi r}{4}) \frac{\Gamma(n + \frac{r}{4})}{\prod_{k=1}^3 \Gamma(-n + \frac{k}{4})} = \pi (-1)^n \frac{1}{\prod_{i=1}^3 \Gamma(-n + \frac{k}{4})} \quad , \quad (172)$$

which follows by applying the completion formula.

It is now straightforward to extract the behaviour of the periods in the limit $\phi \rightarrow 1$. Since $u_n(\phi)$ is a polynomial for integer n , it has a finite limit at the point $\phi = 1$, which is easily computed ([36]):

$$u_n(1) = \frac{(2n)!}{n!^2} \quad . \quad (173)$$

Moreover, we have:

$$u_\nu(1) = \frac{4^\nu \Gamma(1/2 + \nu)}{\sqrt{\pi} \Gamma(1 + \nu)} , \quad (174)$$

which allows us to compute the quantities $\alpha_i(n, 1)$ and $\beta_i(n, r, 1)$:

$$\begin{aligned} \alpha_1(n, 1) &= 2\log(2) - \psi(n) - \frac{1}{n} + \psi(n + 1/2) \\ \alpha_2(n, 1) &= -\psi'(n) + \frac{1}{n^2} + \psi'(n + 1/2) , \end{aligned} \quad (175)$$

and:

$$\begin{aligned} \beta_1(n, 1, 1) &= 2\log(2) - \psi(n) - \frac{1}{n} + \psi(n + 1/2) + \frac{1}{2}\pi + \frac{1}{2}i\pi = \alpha_1(n, 1) + \frac{1}{2}\pi + \frac{1}{2}i\pi \\ \beta_1(n, 2, 1) &= 2\log(2) + i\pi - \psi(n) - \frac{1}{n} + \psi(n + 1/2) = \alpha_1(n, 1) + i\pi \\ \beta_1(n, 3, 1) &= 2\log(2) - \psi(n) - \frac{1}{n} + \psi(n + 1/2) - \frac{1}{2}\pi + \frac{1}{2}i\pi = \alpha_1(n, 1) - \frac{1}{2}\pi + \frac{1}{2}i\pi \\ \beta_2(n, 1, 1) &= \frac{1}{n^2} + \psi'(n + 1/2) - \pi^2 - \psi'(n) - \frac{1}{2}i\pi^2 = \alpha_2(n, 1) - \pi^2 - \frac{1}{2}i\pi^2 \\ \beta_2(n, 2, 1) &= -\psi'(n) + \frac{1}{n^2} + \psi'(n + 1/2) = \alpha_2(n, 1) \\ \beta_2(n, 3, 1) &= -\psi'(n) + \frac{1}{n^2} + \psi'(n + 1/2) - \pi^2 + \frac{1}{2}i\pi^2 = \alpha_2(n, 1) - \pi^2 + \frac{1}{2}i\pi^2 \\ \beta_3(n, 1, 1) &= \frac{3}{2}i\pi^3 + \psi''(n + 1/2) + \frac{1}{2}\pi^3 - \psi''(n) - 2\frac{1}{n^3} \\ \beta_3(n, 2, 1) &= \psi''(n + 1/2) - \psi''(n) - 2\frac{1}{n^3} \\ \beta_3(n, 3, 1) &= \frac{3}{2}i\pi^3 - \psi''(n) + \psi''(n + 1/2) - 2\frac{1}{n^3} - \frac{1}{2}\pi^3 . \end{aligned} \quad (176)$$

The relations given above are valid for $n \neq 0$. While α, β are apparently singular at $n = 0$, the associated analytic extensions $\alpha_i(\nu, 1), \beta_i(\nu, r, 1)$ have finite limits for $\nu \rightarrow 0$, which we list in Appendix B. It follows that each of the periods ω_i has a finite limit for $\phi \rightarrow 1$, *as long as* $|z| > 4$ ²⁷. These limits are obtained by substituting $u_n(1), \alpha_i(n, 1)$ and $\beta_i(n, r, 1)$ in the expansions given above.

²⁷For $\phi = 1$, our expansions converge if $|z| > 4$.

7.3 Integral structure and a vanishing period

A symplectic basis of the lattice $H_3(Y, \mathbb{Z})$ was computed in [36]. If $\Pi = \begin{bmatrix} \Pi_0 \\ \Pi_1 \\ \Pi_2 \\ \Pi_3 \\ \Pi_4 \\ \Pi_5 \end{bmatrix} =$

$\begin{bmatrix} \mathcal{G}_0 \\ \mathcal{G}_1 \\ \mathcal{G}_2 \\ z^0 \\ z^1 \\ z^2 \end{bmatrix}$ is the period vector of Ω in this basis, then Π and $\omega := \begin{bmatrix} \omega_0 \\ \omega_1 \\ \omega_2 \\ \omega_3 \\ \omega_4 \\ \omega_5 \end{bmatrix}$ are related by $\Pi = m\omega$, with:

$$m = \begin{bmatrix} -1 & 1 & 0 & 0 & 0 & 0 \\ 1 & 0 & 1 & -1 & 0 & -1 \\ 3/2 & 0 & 0 & 0 & -1/2 & 0 \\ 1 & 0 & 0 & 0 & 0 & 0 \\ -1/4 & 0 & 1/2 & 0 & 1/4 & 0 \\ 1/4 & 3/4 & -1/2 & 1/2 & -1/4 & 1/4 \end{bmatrix} . \quad (177)$$

In particular, the periods $\Pi_4 = z^1, \Pi_5 = z^2$, which correspond to the integral of Ω along 3-cycles which are mirror to members of the classes h and l respectively, are given by the following linear combinations of the the periods ω :

$$c_1 = \begin{bmatrix} -1/4 & 0 & 1/2 & 0 & 1/4 & 0 \end{bmatrix} \quad (178)$$

$$c_2 = \begin{bmatrix} 1/4 & 3/4 & -1/2 & 1/2 & -1/4 & 1/4 \end{bmatrix} . \quad (179)$$

Moreover, the period $\Pi_3 = z^0$ coincides with the fundamental period ω_0 , which corresponds to the integral of Ω over a 3-cycle mirror to the homology class of a point.

Now let us look for an integral cycle with the property that the associated period of Ω vanishes identically on the locus C_1 . Such a period is of the form:

$$\omega_v = \beta\omega = \sum_{i=0 \dots 5} \beta_i \omega_i , \quad (180)$$

where the row vector β is such that $\beta_{int} = \beta m^{-1}$ has integral entries. By virtue of (167), the condition that $\Omega_v|_{C_1}$ is identically zero implies that the following linear combination of the coefficients L must vanish for all nonnegative integers n and all $s = 0, 1, 2, 3$:

$$\sum_{i=0 \dots 5} \beta_i L_i(s, n, 1) = 0 . \quad (181)$$

View $L_i = L_i(s, n, 1)$ ($i = 0 \dots 5$) as sequences defined over the countable set $\{0, 1, 2, 3\} \times \{0, 1, 2, \dots\}$. Then we are looking for a nontrivial linear relation among these five sequences. The existence of such a relation requires that all truncated determinants associated with the infinite linear system (181) vanish, a condition which is easily seen

to hold numerically. Then a solution of (181) can be found by doing a numerical search for small integer values of β_i , with the result that the vector:

$$\beta_v := \begin{bmatrix} 0 & 0 & 1 & -1 & 1 & -1 \end{bmatrix} \quad (182)$$

satisfies (181). We conclude that the period:

$$\omega_v(\psi, \phi) = \omega_2(\psi, \phi) - \omega_3(\psi, \phi) + \omega_4(\psi, \phi) - \omega_5(\psi, \phi) \quad (183)$$

vanishes when restricted to C_1 . To check integrality of the associated 3-cycle γ_v , it suffices to compute the row vector:

$$\beta_{int} = \beta m^{-1} = \begin{bmatrix} 0 & 1 & -2 & 2 & 0 & 0 \end{bmatrix} , \quad (184)$$

which is integral indeed.

The nature of the cycle $\tilde{\gamma}_v$ mirror to γ_v can be determined by finding the position of the periods ω_v in the monodromy weight filtration of $H_3(Y)$ associated with the large complex structure point. By using the monodromy matrices computed in [36], one can easily see that this filtration can be represented in the basis ω by ²⁸:

$$\mathcal{W} = [\mathcal{W}_0, \mathcal{W}_1, \mathcal{W}_2, \mathcal{W}_3] = \left[\begin{bmatrix} 1 \\ 0 \\ 0 \\ 0 \\ 0 \\ 0 \end{bmatrix}, \begin{bmatrix} 1 & 0 & 0 \\ 0 & 3 & 0 \\ 0 & 0 & 2 \\ 0 & 2 & 0 \\ 0 & 0 & 1 \\ 0 & 1 & 0 \end{bmatrix}, \begin{bmatrix} 1 & 0 & 0 & 0 & 0 \\ 0 & 0 & -3 & 3 & 0 \\ 0 & 1 & 0 & 0 & 0 \\ 0 & 0 & 0 & 1 & 0 \\ 0 & 0 & 0 & 0 & 1 \\ 0 & 0 & 1 & 0 & 0 \end{bmatrix}, \begin{bmatrix} 0 & 0 & 0 & 0 & 0 & 1 \\ 0 & 0 & 0 & 0 & 1 & 0 \\ 0 & 0 & 0 & 1 & 0 & 0 \\ 0 & 0 & 1 & 0 & 0 & 0 \\ 0 & 1 & 0 & 0 & 0 & 0 \\ 1 & 0 & 0 & 0 & 0 & 0 \end{bmatrix} \right]$$

where the periods associated with the linear combination of $\omega_0 \dots \omega_5$ given by the columns of each matrix span the corresponding weight subspace. It is easy to see that β_v is a linear combination of the columns of \mathcal{W}_2 , so that the mirror cycle $\tilde{\gamma}_v$ is a 4-cycle.

Numerical analysis also shows that the periods $\Pi_1 = \mathcal{G}_1, \Pi_2 = \mathcal{G}_2, \Pi_3 = z^0, \Pi_5 = z^2$ have vanishing imaginary part along the locus C_1 , though none of them vanishes identically on this locus. In particular, none of the special coordinates on the moduli space, which are given by:

$$t_1 = \frac{\Pi_4}{\Pi_3} = \frac{z^1}{z^0} , \quad t_2 = \frac{\Pi_5}{\Pi_3} = \frac{z^2}{z^0} \quad (185)$$

vanishes identically on C_1 . The coordinate t_2 is *real* along the locus C_1 , while the coordinate t_1 is neither purely real, nor purely imaginary. Since the mirror Kähler class is given by:

$$k = B + iJ = t_1 \check{H} + t_2 \check{L} , \quad (186)$$

it follows that:

$$\int_l k = t_2 , \quad \int_h k = t_1 , \quad (187)$$

and since $J = \text{Im}(k) = \text{Im}(t_1) \check{H}$, this implies:

$$\int_l J = 0 , \quad \int_h J = \text{Im}(t_1) . \quad (188)$$

²⁸This is the reduced form of the filtration – see Appendix A.

As reviewed above, the mirror of C_1 is classically a locus in the moduli space of X where the exceptional divisor E has been blown down to an curve of genus 3. The result $\int_l J = 0$ on this locus confirms that part of this classical geometric intuition is preserved in the quantum setting: the geometric volume of the fiber of the ruling remains zero. However, the result $|\int_l k| = |t_2| \neq 0$ shows that the B-field modifies this conclusion for the quantum volume of l , ensuring that the mass of the $D2$ -brane wrapping l does not vanish identically on C_1 . In fact, we have some numerical evidence that no $D2$ -brane becomes identically massless on this locus. Rather, as shown above, the vanishing period we found:

$$\omega_v = \Pi_1 - 2\Pi_2 + 2\Pi_3 = \mathcal{G}_1 - 2\mathcal{G}_2 + 2z^0 \quad (189)$$

corresponds to a 4 - cycle. Hence it is the exceptional divisor E — possibly mixed together with lower dimensional cycles — which has zero quantum volume on the locus C_1 .

In this example it proves instructive to compare these exact results with semiclassical calculations. To do so, consider the quantities:

$$\begin{aligned} \int_H k^2 &= 8t_1(t_1 + t_2) \quad , \quad \int_L k^2 = 4(t_1)^2 \\ \int_E k^2 &= \int_H k^2 - 2 \int_L k^2 = 8t_1 t_2 \quad , \end{aligned} \quad (190)$$

and:

$$\begin{aligned} \int_H J^2 &= 8(\text{Im}(t_1))^2 \quad , \quad \int_L J^2 = 4(\text{Im}(t_1))^2 \\ \int_E J^2 &= 0 \quad . \end{aligned} \quad (191)$$

This amounts to using the *classical* relations for the volume, but applied to the quantum-mechanically correct values of J and k on the locus mirror to C_1 . The result $\int_E J^2 = 0$ agrees with classical reasoning, showing that the mirror of C_1 is indeed the locus where E collapses to zero classical volume. Thus, whereas in all previous examples the location in the Kähler moduli space where we expect to find collapsed cycles based on classical reasoning is shifted by quantum effects, in this model the classical and quantum loci agree. (This is somewhat akin to what happens in flop transitions where the flopping curve has zero quantum volume on the classical flop wall.) However, the $D4$ -brane state which becomes massless at least naively seems to carry some $D0$ -brane charge (though this statement is, of course, affected by the ambiguities discussed above). Moreover, the $D2$ -branes wrapping holomorphic subcycles of E remain massive on C_1 , a result in stark contrast with classical geometric reasoning.

7.4 Postscript: Quantum geometry of the restricted theory

As mentioned above, it is believed that the restriction of our two-parameter model to the locus C_1 is equivalent to the one-parameter model $\mathbb{P}^5[2, 4]$ discussed in Section 4.

The argument given in [36] for this equivalence is based on classical geometry, namely on the fact that the restrictions of both Y and X to the locus C_1 and its naive mirror locus are birationally equivalent to the one-parameter mirror families Y' , respectively X' describing the model of subsection 4.1.

Having computed the required analytic continuations of all periods, we are in a position to perform a detailed check of this statement, which will also serve to complete the picture given above of what happens quantum-mechanically when one restricts to C_1 . For this purpose, we must understand precisely how the one-parameter model $\mathbb{P}^5[2, 4]$ is ‘embedded’ in the two-parameter model at the quantum level. We start with the following natural geometric proposal for the embedding of Y' into Y . Consider a period U of the two-parameter model Y as one approaches the locus C_1 . If U has nontrivial monodromy around C_1 , then the process of restricting U to C_1 is in general ill-defined. Therefore, it is natural to postulate that only those periods U which have trivial monodromy around C_1 have a counterpart in the restricted model Y' .²⁹

We thus identify $H_3(Y')$ with the subspace of $H_3(Y)$ consisting of those classes which have trivial monodromy around C_1 . The latter can be easily determined as the subspace of period vectors fixed by the associated monodromy operator (denoted by B in [36]), with the result that it is spanned by the linear combinations of $\omega_0 \dots \omega_5$ defined by the rows of the following matrix:

$$A := \begin{bmatrix} 0 & 0 & 0 & 0 & 1 & 1 \\ 0 & 1 & 0 & -3 & -3 & 0 \\ 1 & 0 & 0 & 3 & 3 & 0 \\ 0 & 0 & 1 & 1 & 0 & 0 \end{bmatrix} . \quad (192)$$

Denote the associated periods (restricted to C_1) by:

$$\omega'_j(z) := \sum_{i=0 \dots 5} A_{ji} \omega_i(z, 1) \quad \text{for all } j = 0 \dots 3 . \quad (193)$$

In order to understand the precise relation between the two models, we must compute the transition matrix P from the Meijer basis U_j of $\mathbb{P}^5[2, 4]$ to the basis ω'_j . The existence of a *constant* such matrix on the locus C_1 amounts to a proof of the quantum equivalence between the restriction of Y to C_1 and this model.

²⁹The alert reader may have noticed that this intuitive argument is not as clear-cut as it may seem. Indeed, it is perfectly possible to have periods with nontrivial monodromy around some component of the discriminant locus, which however do have a well-defined limit along that component. A familiar example in lower dimension is provided by a generic period on the mirror quintic in the vicinity of the conifold point. As shown in [42], such a period has the form:

$$U = \text{constant } (z - 1) \log(z - 1) + g(z) ,$$

with g a function regular at $z = 1$; in that case, U has a well-defined limit at $z = 1$ even though it has nontrivial monodromy around the conifold. Hence the argument above is based on something more than the existence of a well-defined limit on C_1 ; essentially, it is an argument about the monodromy weight filtration defined by the degeneration associated with C_1 . In any case, correctness of this ansatz is justified by the consistency of the results we will obtain.

In order to check this statement and obtain the matrix P , it is convenient to use a matrix formalism. Considering the column vectors $\omega' := \begin{bmatrix} \omega'_0 \\ \omega'_1 \\ \omega'_2 \\ \omega'_3 \end{bmatrix}$ and $U := \begin{bmatrix} U_0 \\ U_1 \\ U_2 \\ U_3 \end{bmatrix}$, the row vector $Z(z) = [1 \quad \log z \quad (\log z)^2 \quad (\log z)^3]$ as well as the matrix $M(n) = (M_{si}(n))_{s=0 \dots 3, i=0 \dots 5}$ with entries $M_{si}(n) := M_i(s, n)$ (where $M_i(s, n)$ are given in (167)), we can write :

$$\omega'(z)^t = \sum_{n=0}^{\infty} z^{-n} Z(z) M'(n) \quad , \quad (194)$$

with $M'(n) = M(n)A^t$. Using the results of Section 4, one can similarly write:

$$U(x)^t = \sum_{n=0}^{\infty} x^n Z(x) l(n) \quad , \quad (195)$$

where x is the coordinate on C_1 defined by the property that $U_0(x) = {}_4F_3 \left(\begin{smallmatrix} 1/2, 1/2, 1/4, 3/4 \\ 1, 1, 1 \end{smallmatrix} \right) (x)$ and $l(n) = (l_{sj}(n))_{s,j=0 \dots 3}$ is a matrix with entries:

$$l_{sj}(n) = \frac{(-1)^j}{j!} \frac{(1/2)_n (1/2)_n (1/4)_n (3/4)_n}{n!^4} v_{sj}(n) \quad . \quad (196)$$

Here $v_{sj}(n) := v_j(s, n)$ with $v_j(s, n)$ given in (64) and (65).

It is important to notice that the ‘hypergeometric’ coordinate x on C_1 does not coincide with z . In fact, these two coordinates are expected to differ by the rescaling:

$$z = -\frac{4}{x} \quad , \quad (197)$$

as can be seen by comparing the expression for ω_0 given on page 27 of [36] and the expression of the $\mathbb{P}^5[2, 4]$ fundamental period given in Table 3.1. of [39]. In other words, we expect the relation:

$$\omega'(z) = PU(x) \quad . \quad (198)$$

Instead of testing this relation directly, it proves more convenient to proceed as follows. Define a new coordinate y on C_1 by $y = \frac{1}{w} = \frac{1}{\kappa x}$, where $w = \kappa x$ is the natural variable on the moduli space of $\mathbb{P}^5[2, 4]$ required by the monomial-divisor mirror map; thus $\kappa > 0$ is given by:

$$\log \kappa = 2\psi(1/2) + \psi(1/4) + \psi(3/4) - 4\psi(1) = -5\log(4) \quad . \quad (199)$$

Hence $\kappa = 4^{-5}$ and $y = \frac{4^5}{x}$. Then we expect $z = -\frac{4}{x} = \frac{1}{\mu} y$ with $\mu = -4^4$ and we must test the existence of a matrix P such that $\omega'(\frac{y}{\mu}) = PU(\frac{1}{\kappa y})$. It is now easy to see that the associated rescalings have the following effect on the matrix function Z :

$$Z\left(\frac{y}{\mu}\right) = Z(y)C(\mu) \quad , \quad Z\left(\frac{1}{\kappa y}\right) = Z(y)c(\kappa) \quad . \quad (200)$$

Here $C(\mu), c(\kappa)$ are two upper triangular matrices whose nonzero entries are given by:

$$C_{sp}(\mu) = (-1)^{p-s} \binom{p}{s} (\log \mu)^{p-s} \quad , \quad c_{sp}(\kappa) = (-1)^p \binom{p}{s} (\log \kappa)^{p-s} \quad (201)$$

for all $0 \leq s \leq p \leq 3$. It follows that there should exist an invertible matrix $P \in \mathbf{GL}(4, \mathbb{C})$ such that:

$$\mu^n C(\mu) M(n) A^t = \kappa^{-n} c(\kappa) l(n) P^t \quad \text{for all integers } n \geq 0. \quad (202)$$

To determine a candidate for P , it suffices to consider this equation for $n = 0$, which gives:

$$P^t = l(0)^{-1} c(\kappa)^{-1} C(\mu) M(0) A^t. \quad (203)$$

The reason why we prefer to work with the variable y can now be made clear. Substituting the formulae for the expansion coefficients of $\omega_i(z)$ and $U_j(x)$ gives very complicated expressions for $M(0)$ and $l(0)$, which are difficult to simplify directly. However, by virtue of our experience in Section 3, it can be expected that rescaling to the variable y has the effect of dramatically simplifying the expressions involved. This is because it is much easier in practice to simplify the linear combinations of the elements of $l(0)$ which form the matrix $c(\kappa)l(0)$ than the elements of $l(0)$ themselves; the same turns out to be the case for $C(\mu)M(0)$. Going through this exercise leads to the following remarkably simple expressions:

$$\begin{aligned} C(\mu)M(0)A^t &= \sqrt{2\pi} \begin{bmatrix} -2/3 \frac{-7\pi^3+99i\zeta(3)}{2\pi} & \frac{61\pi^3-1320i\zeta(3)}{29i} & \frac{-13\pi^3+396i\zeta(3)}{15i} & 3 \frac{-\pi^3+22i\zeta(3)}{9i} \\ -\frac{4}{\pi^2} & -\frac{11}{2\pi^2} & -\frac{9}{2\pi^2} & -\frac{3}{\pi^2} \\ -\frac{i}{2\pi^3} & -\frac{5i}{3\pi^3} & \frac{2i}{2\pi^3} & \frac{i}{2\pi^3} \end{bmatrix} \\ c(\kappa)l(0) &= \begin{bmatrix} 1 & 0 & 7/6\pi^2 & 22\zeta(3) \\ 0 & 1 & -i\pi & \frac{11}{6}\pi^2 \\ 0 & 0 & 1/2 & 0 \\ 0 & 0 & 0 & 1/6 \end{bmatrix}, \end{aligned} \quad (204)$$

which immediately give:

$$P = \sqrt{2\pi} \begin{bmatrix} 14 & 6\frac{i}{\pi} & -8\pi^{-2} & -3\frac{i}{\pi^3} \\ 23 & 17\frac{i}{\pi} & -11\pi^{-2} & -10\frac{i}{\pi^3} \\ -17 & -15\frac{i}{\pi} & 9\pi^{-2} & 9\frac{i}{\pi^3} \\ -10 & -4\frac{i}{\pi} & 6\pi^{-2} & 3\frac{i}{\pi^3} \end{bmatrix}. \quad (205)$$

In order to arrive at these results, we used relations (223) of Appendix B. Using this value of P , one can now check numerically that (202) is indeed satisfied. We did this up to $n = 40$ and with 60 significant digits, but we were not able to simplify the resulting expressions in order to give an analytic proof to this claim.

The matrices (192) and (205), give a complete characterization of the *quantum* relation between the restricted model $\mathbb{P}^5[2,4]$ and the ambient two-parameter model. It should be noted that we obtained considerably more detailed information about this relation than could have been extracted by less direct methods such as those of

[33]. For example, following [33], one can consider the restriction of the Picard-Fuchs equations of the two-parameter model to the locus C_1 and check that the resulting ordinary equation is equivalent to the hypergeometric equation of the model $\mathbb{P}^5[2, 4]$ after performing an appropriate change of variable. While this procedure suffices to show that the restricted model is equivalent to $\mathbb{P}^5[2, 4]$ at the quantum level, it does not fix the precise isomorphism between the two. Doing so requires knowledge of the relation between two bases of periods of these models, which is precisely the information encoded by the matrices P and A computed above.

Now let us consider the vanishing period $U_v = U_3 - 3\pi^2 U_1$ which we found for the restricted model in Section 5. Since we know the integral structure of the 2-parameter model, we can obtain the integral structure of $\mathbb{P}^5[2, 4]$ by restriction. In particular, since $\Pi = m\omega$ is the period vector in an integral basis, and since $\omega' = A\omega = Am^{-1}\Pi$, while $U_v = \beta U$, with $\beta := \left(\frac{1}{\pi^3}\right) \begin{bmatrix} 0 & -3\pi^2 & 0 & 1 \end{bmatrix}$ and $U = P^{-1}\omega'$, it follows that the vanishing period U_v which we found in Section 5 can be expressed as:

$$U_v = \beta P^{-1} A m^{-1} \Pi = \beta_{int} \Pi \quad , \quad (206)$$

with:

$$\beta_{int} = -86i\sqrt{2\pi} \begin{bmatrix} 86 & -79 & 252 & -190 & 172 & -156 \end{bmatrix} \quad , \quad (207)$$

i.e. we have:

$$U_v = -86i\sqrt{2\pi}(86\mathcal{G}^0 - 79\mathcal{G}^1 + 252\mathcal{G}^2 - 190z^0 + 172z^1 - 156z^2) \quad (208)$$

In particular, we see that U_v is an integral linear combination of integral periods up to a global factor; hence it is indeed associated with an integral 3-cycle which collapses at $x = 1$. The reader can easily check that the large integers appearing in (208) are coprime. This underscores the rather nontrivial character of this vanishing period, when viewed from the perspective of the ambient two-parameter model. It would be a difficult task to identify U_v directly from the data of the two-parameter model, without making use of independent knowledge of the vanishing period for the model $\mathbb{P}^5[2, 4]$.

It is instructive to re-interpret the result from this ‘ambient’ perspective. The point $x = 1$ corresponds to $z = -4$; this is the point R , one of the two points where C_1 intersects C_{con} (the other point S corresponds to $z = 0 \iff x = \infty$, which is the small radius limit of the model $\mathbb{P}^5[2, 4]$). As shown in [36], there exists an integral cycle vanishing identically on the locus C_{con} , namely the cycle corresponding to the period $\omega_1 - \omega_0 = \mathcal{G}^0$; however, it is easy to see that this period has nontrivial monodromy around C_1 and hence it does not restrict to a period of the model $\mathbb{P}^5[2, 4]$. Clearly both of our cycles belong to the highest component \mathcal{W}_3 of the (reduced) large radius monodromy weight filtration of the two-parameter model; hence both can be interpreted as 6-brane states in the mirror theory (the *IIA* theory compactified on X). It follows that a partial picture of massless D-branes in the type IIA compactification on X is as follows. First, there is a 6-brane state which becomes massless everywhere on the conifold locus C_{con} ; second, there is another 6-brane state which becomes massless

at one of the intersection points (the point R) between C_1 and C_{con} ; when restricting to the locus C_1 , this state induces the vanishing 6-brane of the resulting one-parameter model. Finally, there is a 4-brane state which becomes massless everywhere on the locus C_1 .

8 Summary and Conclusions

One of the essential lessons of recent years is that much interesting physics can be learned from studying systems at points in their moduli space which naively appear to be singular. In a wide range of examples, these singularities signal the appearance of new massless degrees of freedom that are responsible for yielding non-singular physics. In the context of compactified string theory, these singularities are often associated with geometrical degenerations of one form or another, and the new massless degrees of freedom often arise from D-branes wrapped around collapsing cycles.

In this paper, we have studied in some detail the D-branes that become massless along various loci in the moduli space of Calabi-Yau examples — compact and non-compact — and used this to extract properties of quantum volume in string theory. The features we find confirm and extend previous results, and highlight significant qualitative and quantitative departures from classical expectations. Figures 6, 7, 8, 9 and 11 illustrate some of the new features of quantum volume and can be thought of as a visual summary of our results. Although we have not overly stressed this point, we also showed that the physical arguments which ensure that some D-brane mass vanishes within a phase boundary can be used to generate interesting and seemingly novel arithmetic identities. Equations (87), (112), (151) and (152) give some representative examples. In fact, one can reverse the argument and use degenerations of Calabi-Yau manifolds in order to produce such identities in a systematic manner. It would be interesting to gain a better understanding of the mathematics behind this process, as well as of the connection between these results and the considerations of [20].

From the physical point of view, there are, perhaps, two main issues that remain unresolved. The first is to determine the precise action of mirror symmetry on the integral structures of a mirror pair (X, Y) . As we have seen, our inability to resolve this issue prevents the precise identification of the even dimensional D-branes on X mirror to specified odd dimensional D-branes on Y . Nevertheless, it is only the lower brane charges that remain ambiguous as we can use the leading logarithmic behaviour of periods on Y to identify the maximal dimensional component of mirror D-branes on X . Certainly, though, filling this gap in our understanding is an important subject for the future. The second issue is that of marginal stability. While we have studied D-branes at geometrical degenerations, there are other loci in moduli space where a given D-brane state might be massive, but unstable to decay. Perhaps the techniques of this paper, as well as the important contributions of [45, 20], will allow us to understand the marginal stability loci in detail for Calabi-Yau compactifications. We hope to return to this issue in future work.

A The monodromy weight filtration

In this appendix, we give a very brief account of role played by monodromies in the study of moduli spaces of Calabi-Yau threefolds. This topic is intimately connected with the theory of variations of Hodge structure. Basic references for this subject (which we will not attempt to present in detail) are [46] for the general theory of local systems and the geometric formulation of Fuchsian equations, [22] for the abstract theory of Hodge structures, [24] as general references and [25] for the monodromy theorem. An excellent introduction to the mathematical structures underlying mirror symmetry (up to date at the level of 1997) can be found in [61].

For our purpose, the set-up is that of a family of Calabi-Yau threefolds (understood as complex manifolds of vanishing first Chern class), i.e. a (proper) holomorphic map $\pi : \mathcal{X} \rightarrow S$ over a connected base S whose fibers $X_s = \pi^{-1}(s)$ are all diffeomorphic with a given Calabi-Yau manifold X . The complex manifold S plays the role of a parameter space for the complex structure on X_s . For simplicity, we assume that $\dim S := r$ is equal to $h^{2,1}(X)$, so that our family captures the full space of deformations of complex structure of X . In general, one must allow for bases S which are non-contractible; this appears because one is usually interested not only in the family \mathcal{X} , but in a compactification $\bar{\pi} : \bar{\mathcal{X}} \rightarrow \bar{S}$ given by a (proper) map $\bar{\pi}$ which has singularities above the locus $\bar{S} - S$; in other words, we wish to allow the complex structure of X to degenerate as we vary the parameters $s \in S$. In order to describe the middle cohomology of the various fibers X_s , one considers the derived sheaf $R^3\pi_*\mathbb{C}_{\mathcal{X}}$, which is intuitively the sheaf having $H^3(X_s, \mathbb{C})$ as its stalk above each point s . The sections of this sheaf are simply the topologically constant families of cohomology classes. The important subtlety is that, for a general basis S , such sections will have nontrivial monodromies around the components of $\bar{S} - S$; these are described by actions $\rho_s : \pi_1(S, s) \rightarrow \text{Aut}(H^3(X_s))$ of the fundamental group of S on the spaces $H^3(X_s)$. In other words, if $g(s) \in H^3(X)$ is such a section, then upon following a closed path $l : [0, 1] \rightarrow S$ starting and ending at a given point s_0 , the cohomology class $g(s)$ does not necessarily return to its original value $g(s_0)$ but rather to the value $\rho_{s_0}([l])g(s_0)$, where $[l]$ is the homotopy class of l in $\pi_1(S, s_0)$. An important device for studying this situation, discussed at length in [46] is to represent the local system $R^3\pi_*\mathbb{C}_{\mathcal{X}}$ as the sheaf of flat holomorphic sections of a pair (\mathcal{H}, ∇) , where $\mathcal{H} = \mathcal{O}_S \otimes R^3\pi_*\mathbb{C}_{\mathcal{X}}$ is a holomorphic vector bundle and ∇ is a connection on \mathcal{H} which, in our context, is called the *Gauss-Manin* connection. In other words, each topologically-constant cohomology class in $H^3(X, \mathbb{C})$ can be viewed as a holomorphic section of \mathcal{H} which is covariantly-constant with respect to ∇ . The existence of nontrivial monodromies around the components of $\bar{S} - S$ is then reflected by the fact that the connection coefficients of ∇ in a basis of sections which extend to smooth sections over a component of $\bar{S} - S$ will have poles along that locus (this is made more precise by the nilpotent orbit theorem, as we explain below).

In order to understand the nature of the monodromies around a compactification point $P \in \bar{S} - S$, we consider the case when P is the intersection of r compactification divisors having normal crossings at P . This situation can be represented by taking S

to be locally a Cartesian product Δ of r punctured disks:

$$\Delta = (D^*)^r = \{z = (z_1 \dots z_r) \in \mathbb{C}^r \mid 0 < |z_i| < 1, \forall i = 1..r\} \quad , \quad (209)$$

where $D^* = \{z \in \mathbb{C} \mid 0 < |z| < 1\}$. This has a natural compactification $\overline{\Delta} = (D)^r$, with D a copy of the unit disc. The compactification divisors intersecting at $P = (0, 0 \dots 0)$ are then locally given by the equations $z_i = 0$. The fundamental group $\pi_1(\Delta)$ is generated by the r circles $\gamma_i : \{z_i = \frac{1}{2}e^{2\pi it} \ (t \in [0, 1]), z_j = 0 \text{ for } j \neq i\}$. The *monodromy theorem* [25] assures us that the automorphisms T_i of $H^3(X)$ defined by transporting the cohomology classes around γ_i are *quasi-unipotent*, i.e. each of them satisfies:

$$(T_i^{a_i} - I)^{r_i} = 0 \quad (210)$$

for some pair of positive integers (a_i, r_i) .

To avoid lengthening this discussion, let us focus on the case when all T_i are unipotent, i.e. one can take $a_i = 1$ in (210). Then one can define operators $N_i = \log T_i := \sum_{k=1..r_i-1} \frac{(-1)^{k-1}}{k} (T_i - I)^k$ (the series defining the logarithm terminates due to the fact that T_i is unipotent) as well as an operator-valued function:

$$\mathcal{N}(z) := e^{-\frac{1}{2\pi i} \sum_{i=1..r} (\log z_i) N_i} \quad (211)$$

(this series again reduces to a finite sum, since the operators N_i are obviously nilpotent).

We can now state another basic fact of relevance for us, namely the *nilpotent orbit theorem*. This states that one can use the monodromy operators T_i in order to generate an extension of \mathcal{H} to a holomorphic vector bundle $\overline{\mathcal{H}}$ over $\overline{\Delta}$. More precisely, given a flat local frame ³⁰ $(e_j(z))_{j=1..2r+2}$ of \mathcal{H} , the sections $e_j(z)$ will generally have non-trivial monodromies around the curves γ_i (which can be identified with the holonomy transformations of ∇ along these curves). It follows that e_i do not directly extend to $\overline{\Delta}$. However, the nilpotent orbit theorem states that the sections:

$$\sigma_j(z) := \mathcal{N}(z)e_j(z) \quad (212)$$

are single-valued (i.e. have trivial monodromy) around each of the curves γ_i . It follows that one can extend the bundle \mathcal{H} to $\overline{\Delta}$ trivially, i.e. by declaring that $\overline{\mathcal{H}}$ is trivializable on a vicinity of each of γ_i and extending σ_i to a frame over that vicinity by continuity of their local representations in that trivialization. Then a simple computation in the frame σ_i shows that ∇ extends to a connection with regular singular points on $\overline{\mathcal{H}}$ ³¹.

We can now describe the associated *monodromy weight filtration*. This is simply a filtration:

$$0 \subset W_0 \subset W_1 \subset \dots \subset W_6 = H^3(X) \quad (213)$$

³⁰Flat with respect to the Gauss-Manin connection.

³¹Concretely, the connection matrix in a local frame of $\overline{\mathcal{H}}$ above the origin has poles along the curves γ_i . Abstractly, the extended connection gives a map $\overline{\nabla} : \overline{\mathcal{H}} \rightarrow \Omega^1(\log Z) \otimes \overline{\mathcal{H}}$, where $\Omega^1(\log Z)$ is the space of '1-forms in $d\log z_i = \frac{dz_i}{z_i}$ ' and $Z := \overline{\Delta} - \Delta$.

of $H^3(X)$ with the property:

$$N_i W_k \subset W_{k-2} \quad , \quad \text{for all } k \quad (214)$$

and such that for all positive $a_1 \dots a_r$, the powers of the operator $N = \sum_{i=1..r} a_i N_i$ induce isomorphisms:

$$N^p : W_{3+p}/W_{2+p} \rightarrow W_{3-p}/W_{2-p} \quad (215)$$

for all $p = 0 \dots 3$, where W_{-1} is defined to be the null vector space. These properties can be used in order to determine W .

Finally, let us recall some useful concepts introduced in [29, 54, 62]. The boundary point P is called *maximally unipotent* (or a *large complex structure limit point*) if:

- (1) All monodromy transformations T_j are unipotent
 - (2) $\dim W_0 = \dim W_1 = 1$ and $\dim W_2 = 1 + r$
 - (3) If $g_0 \dots g_r$ is a basis of W_2 such that $g_0 \in W_0$, then the matrix $M := (m_{ij})_{i,j=1..r}$ (defined by $N_i g_j = m_{ij} g_0$) is invertible.
- Then (215) gives $W_0 = W_1 \subset W_2 = W_3 \subset W_4 = W_5 \subset W_6 = H^3(X)$ so we can work with the *reduced filtration*:

$$0 \subset \mathcal{W}_0 \subset \mathcal{W}_1 \subset \mathcal{W}_2 \subset \mathcal{W}_3 = H^3(X) \quad , \quad (216)$$

where $\mathcal{W}_k := W_{2k}$ for all $k = 0 \dots 3$.

For a one-parameter model ($r = 1$), one has a single monodromy operator T around P and this definition is equivalent to the requirement that T is maximally unipotent, i.e. $(T - I)^4 = 0$ and $(T - I)^3 \neq 0$ ³². Then (216) can be viewed as the natural filtration defined by the nilpotent operator $N = \log(T - I)$. In other words, the fact that $T - I$ is nilpotent of maximal order means that the Jordan form of N is:

$$N_J = \begin{bmatrix} 0 & 1 & 0 & 0 \\ 0 & 0 & 1 & 0 \\ 0 & 0 & 0 & 1 \\ 0 & 0 & 0 & 0 \end{bmatrix} \quad , \quad (217)$$

and $\mathcal{W}_k = \langle e_0 \dots e_k \rangle$, where $e_0 \dots e_3$ is any basis of $H^4(X)$ in which the matrix of N has this form. In terms of the associated Picard-Fuchs system, such a monodromy matrix corresponds to a basis of solutions $u_0 \dots u_3$ with the property that³³:

$$u_j(z) = \sum_{0 \leq i \leq j} a_i(z) \log(z)^i \quad , \quad (218)$$

where a_i are single-valued around $z = 0$. In other words, the spaces \mathcal{W}_j consist of the ‘ \log^j -monodromy periods’, where the terminology indicates the *leading* logarithmic behaviour.

³²We assume a *compact* one-parameter model; the correct generalization for a non-compact case such as the $\mathbb{C}^3/\mathbb{Z}_3$ orbifold considered in Section 5 is to require $(T - I)^3 = 0$ and $(T - I)^2 \neq 0$.

³³If N has the form (217), then $T = e^N$ has the form $\begin{bmatrix} 1 & 1 & 1/2 & 1/6 \\ 0 & 1 & 1 & 1/2 \\ 0 & 0 & 1 & 1 \\ 0 & 0 & 0 & 1 \end{bmatrix}$.

B Some useful identities

For the convenience of the reader, we list a few identities which are important for simplifying some of the expressions encountered in this paper. A first group of identities can be obtained by starting with the basic equality:

$$\prod_{k=0}^{n-1} \Gamma(x + k/n) = (2\pi)^{\frac{n-1}{2}} n^{1/2-nx} \Gamma(nx) \quad , \quad (219)$$

which immediately leads to:

$$\begin{aligned} \sum_{k=0}^{n-1} \psi(x + k/n) - n\psi(nx) &= -n\log(n) \\ \sum_{k=0}^{n-1} \psi^{(j)}(x + k/n) - n^{j+1} \psi^{(j)}(nx) &= 0 \quad . \end{aligned} \quad (220)$$

These relations can be used for $x = 1/n$ to give:

$$\begin{aligned} \sum_{k=1}^{n-1} \psi(k/n) - (n-1)\psi(1) &= -n\log(n) \\ \sum_{k=1}^{n-1} \psi^{(j)}(x + k/n) &= (n^{j+1} - 1)\psi^{(j)}(1) \quad . \end{aligned} \quad (221)$$

We also recall that $\psi(1) = -\gamma$, where γ is Euler's constant and that:

$$\psi^{(j)}(1) = (-1)^{j-1} j! \zeta(j+1) \quad , \quad \zeta(2k) = (-1)^{k-1} \frac{(2\pi)^{2k}}{2(2k)!} B_{2k} \quad (222)$$

with B_j the Bernoulli numbers. In particular, we have $\zeta(2) = \frac{\pi^2}{6}$.

Another set of identities, useful for simplifying some of the expressions encountered in Section 6, is:

$$\begin{aligned} \psi(1/4) &= -\gamma - 3 \log 2 - \frac{\pi}{2} \quad , \quad \psi(3/4) = -\gamma - 3 \log 2 + \frac{\pi}{2} \\ \psi(3/4) &= -56 \zeta(3) + 2\pi^3 \quad , \quad \psi(1/4) = -56 \zeta(3) - 2\pi^3 \\ \psi'(1/4) + \psi'(3/4) &= 2\pi^2 \quad , \quad \psi''(3/4) = -56 \zeta(3) + 2\pi^3 \quad . \\ \psi''(1/4) &= -56 \zeta(3) - 2\pi^3 \quad , \quad \psi(1/2) = -\gamma - 2 \log 2 \\ \psi'(1/2) &= \frac{1}{2} \pi^2 \quad , \quad \psi''(1/2) = -14 \zeta(3) \end{aligned} \quad (223)$$

These follow by applying (221) for $n = 4$ and $n = 2$, together with the relation:

$$\psi(x) - \psi(1-x) = -\pi \operatorname{ctg}(\pi x) \quad (224)$$

and the identities following from it by differentiation.

Finally, we list the limiting values of the quantities $\alpha_i(\nu, 1)$ and $\beta_i(\nu, r, 1)$ of Section 7 for $\nu \rightarrow 0$:

$$\alpha_1(0, 1) = 0 \quad , \quad \alpha_2(0, 1) = 1/3\pi^2 \quad (225)$$

and:

$$\begin{aligned}
\beta_1(0, 1, 1) &= 1/2i\pi + 1/2\pi & , & \beta_1(0, 2, 1) = i\pi \\
\beta_1(0, 3, 1) &= 1/2i\pi - 1/2\pi & , & \beta_2(0, 1, 1) = -1/2i\pi^2 - 2/3\pi^2 \\
\beta_2(0, 2, 1) &= 1/3\pi^2 & , & \beta_2(0, 3, 1) = -2/3\pi^2 + 1/2i\pi^2 \\
\beta_3(0, 1, 1) &= 3/2i\pi^3 - 12\zeta(3) + 1/2\pi^3 & , & \beta_3(0, 2, 1) = -12\zeta(3) \\
\beta_3(0, 3, 1) &= -1/2\pi^3 - 12\zeta(3) + 3/2i\pi^3 & . &
\end{aligned} \tag{226}$$

References

- [1] A. Klemm, E. Zaslow, *Local Mirror Symmetry at Higher Genus*, hep-th/9906046.
- [2] R. P. Horja, *Hypergeometric functions and mirror symmetry in toric varieties*, math.AG/9912109.
- [3] M. Gromov, *Pseudo-holomorphic curves on almost complex manifolds*, Invent. Math. **82** (1985), 307–347.
- [4] E. Witten, *Topological sigma models*, Commun. Math. Phys **118** (1988), 411–449.
- [5] P. Candelas, X. de la Ossa, *Moduli space of Calabi-Yau manifolds*, Nucl.Phys. **B355**(1991) 455-481.
- [6] A. Ashtekar, C. Rovelli, L. Smolin, *Weaving a classical geometry with quantum threads*, Phys.Rev.Lett. **69** (1992) 237-240, hep-th/9203079.
- [7] N. Hitchin, *Lectures on special Lagrangian submanifolds*, math.DG/9907034.
- [8] M. Gross, *Topological Mirror Symmetry*, math.AG/9909015; *Special Lagrangian Fibrations I: Topology*, alg-geom/9710006, *Special Lagrangian Fibrations II: Geometry*, math.AG/9809072 .
- [9] D. Joyce, *On counting special Lagrangian homology 3-spheres*, hep-th/9907013.
- [10] S. Kachru, J. McGreevy, *Supersymmetric Three-cycles and (Super)symmetry Breaking*, Phys. Rev. D **61** (2000) 026001, hep-th/9908135.
- [11] R. Minasian, G. Moore, *K-theory and Ramond-Ramond charge*, JHEP **9711** (1997) 002, hep-th/9710230; Y-K. E. Cheung, Z. Yin *Anomalies, Branes, and Currents*, Nucl. Phys. **B517** (1998) 69-91, hep-th/9710206, E. Witten, *D-Branes And K-Theory*, JHEP **9812** (1998) 019, hep-th/9810188; G. Moore, E. Witten, *Self-Duality, Ramond-Ramond Fields, and K-Theory*, hep-th/9912279.
- [12] D. R. Morrison, *Mirror symmetry and the type II string*, Nucl. Phys. Proc. Suppl. **46** (1996) 146-155, hep-th/9512016.
- [13] A. Strominger, *Massless Black Holes and Conifolds in String Theory*, Nucl.Phys. **B451** (1995) 96-108, hep-th/9504090.
- [14] J. Polchinski, A. Strominger, *New Vacua for Type II String Theory*, Phys. Lett. **B388** (1996) 736-742, hep-th/9510227.

- [15] A. Strominger, S.-T. Yau, E. Zaslow, *Mirror Symmetry is T-Duality*, Nucl. Phys. **B479** (1996) 243-259, hep-th/9606040.
- [16] C. Vafa, *Extending Mirror Conjecture to Calabi-Yau with Bundles*, hep-th/9804131.
- [17] M. Kontsevich, *Homological Algebra of Mirror Symmetry*, Proceedings of the International Congress of Mathematicians, (Zurich, 1994), 120–139, Birkhauser, alg-geom/9411018.
- [18] A. Ceresole, R. D’Auria, S. Ferrara, A. Van Proeyen, *Duality transformations in supersymmetric Yang-Mills theories coupled to supergravity*, Nucl. Phys. **B444** (1995) 92, hep-th/9502072.
- [19] J. A. Harvey, G. Moore, *On the algebras of BPS states*, Commun.Math.Phys. 197 (1998) 489-519, hep-th/9609017.
- [20] G. Moore, *Attractors and Arithmetic*, hep-th/9807056, *Arithmetic and Attractors*, hep-th/9807087.
- [21] B. R. Greene, D. R. Morrison, M. R. Plesser, *Mirror Manifolds in Higher Dimension*, Commun. Math. Phys. 173 (1995) 559-598.
- [22] P. Deligne, *Theorie de Hodge, II, III*, Publ. IHES **40**(1972),**44**(1974).
- [23] M. Bershadsky, S. Cecotti, H. Ooguri, C. Vafa, *Kodaira-Spencer theory of gravity and exact results for quantum string amplitudes*, Commun. Math. Phys. **165** (1994) 311, hep-th/9309140.
- [24] P. Griffiths (ed.). *Topics in transcendental algebraic geometry*, Ann. of Math. Stud., vol **106**, Princeton Univ. Press, 1984; W. Schmidt, *Variation of Hodge structure: the singularities of the period mapping*, Invent. Math. **22** (1973), 211–319.
- [25] A. Landman, *On the Picard-Lefschetz transformations*, Trans. Amer. Math. Soc. **181** (1973), 89–126.
- [26] D. McDuff, D. Salamon, *J-Holomorphic curves and Quantum Cohomology*, University Lecture Series, vol. **6**, American Mathematical Society, Providence, 1994; W. Fulton, R. Pandharipande, *Notes on stable maps and quantum cohomology*, Algebraic geometry—Santa Cruz 1995, 45–96, Proc. Sympos. Pure Math. **62**, Part 2, Amer. Math. Soc., Providence, 1997.
- [27] T. Oda and H. S. Park, *Linear Gale transforms and Gelfand-Kapranov-Zelevinski decompositions*, Tohoku Math. J. (2) **43** (1991), 375–399.
- [28] P. S. Aspinwall, B. R. Greene, D. R. Morrison, *The Monomial-Divisor Mirror Map*, Internat. Math. Res. Notices (1993), 319-337, alg-geom/9309007.
- [29] D. R. Morrison, *Mirror symmetry and rational curves on quintic threefolds: a guide for mathematicians*, J. Amer. Math. Soc. **6** (1993) 223–247, alg-geom/9202004.

- [30] W. Fulton, *Introduction to toric varieties*, Annals of Mathematics Studies **131**, Princeton U.P., 1993; T. Oda, *Convex bodies and algebraic geometry: an introduction to the theory of toric varieties*, Ergebnisse der Mathematik und ihrer Grenzgebiete; 3.Folge, **15**, Springer, 1988; D. A. Cox, *Recent developments in toric geometry*, alg-geom/9606016.
- [31] P. Aspinwall, *Resolution of Orbifold Singularities in String Theory*, in Mirror symmetry II, eds. B. Greene and S.-T. Yau, hep-th/9403123.
- [32] P. S. Aspinwall, B. R. Greene, D. R. Morrison, *Calabi-Yau Moduli Space, Mirror Manifolds and Spacetime Topology Change in String Theory*, Nucl. Phys. **B416** (1994) 414–480; P. S. Aspinwall, B. R. Greene, D. R. Morrison, *Multiple Mirror Manifolds and Topology Change in String Theory*, Phys. Lett. **B303** (1993) 249–259; E. Witten, *Phases of $N = 2$ Theories In Two Dimensions*, Nucl. Phys. **B403** (1993) 159.
- [33] P. S. Aspinwall, B. R. Greene, D. R. Morrison, *Measuring small distances in $N=2$ sigma models*, Nucl. Phys. **B420** (1994) 184–242, hep-th/9311042.
- [34] P. Aspinwall, *Minimum Distances in Non-Trivial String Target Spaces*, Nucl.Phys. **B431** (1994) 78–96, hep-th/9404060.
- [35] B. R. Greene, Y. Kanter, *Small Volumes in Compactified String Theory*, Nucl. Phys. **B497** (1997) 127–145, hep-th/9612181.
- [36] P. Candelas, X. de la Ossa, A. Font, S. Katz, D. R. Morrison, *Mirror Symmetry for Two Parameter Models – I*, Nucl. Phys. **B416** (1994) 481–538, hep-th/9308083.
- [37] P. Candelas, X. de la Ossa, A. Font, S. Katz, D. R. Morrison, *Mirror Symmetry for Two Parameter Models – II*, Nucl. Phys. **B429** (1994) 626–674, hep-th/9403187.
- [38] S. Hosono, A. Klemm, S. Theisen, S.-T. Yau, *Mirror Symmetry, Mirror Map and Applications to Calabi-Yau Hypersurfaces*, Commun. Math. Phys. **167** (1995) 301–350, hep-th/9308122; S. Hosono, A. Klemm, S. Theisen, S.-T. Yau, *Mirror Symmetry, Mirror Map and Applications to Complete Intersection Calabi-Yau Spaces*, Nucl. Phys. **B433** (1995) 501–554, hep-th/9406055.
- [39] P. Berglund, P. Candelas, X. de la Ossa, A. Font, T. Hubsch, D. Jancic, F. Quevedo, *Periods for Calabi–Yau and Landau–Ginzburg Vacua*, Nucl.Phys. **B419** (1994) 352–403.
- [40] A. Font, *Periods and Duality Symmetries in Calabi-Yau Compactifications*, Nucl. Phys. **B391** (1993) 358, hep-th/9203084.
- [41] P. S. Aspinwall, *Enhanced Gauge Symmetries and K3 Surfaces*, Phys.Lett. **B357** (1995) 329–334, hep-th/9507012.
- [42] P. Candelas, X. C. De La Ossa, P. S. Green and P. Parkes, *A Pair of Calabi-Yau Manifolds as an Exactly Soluble Superconformal Theory*, Nucl. Phys. **B359** (1991) 21.

- [43] H. Ooguri, Y. Oz, Z. Yin, *D-Branes on Calabi-Yau Spaces and Their Mirrors*, Nucl.Phys. **B477** (1996) 407-430, hep-th/9606112.
- [44] K. Becker, M. Becker, A. Strominger, *Fivebranes, Membranes and Non-Perturbative String Theory*, Nucl.Phys. **B456** (1995) 130-152.
- [45] I. Brunner, M. R. Douglas, A. Lawrence, C. Romelsberger, *D-branes on the Quintic*, hep-th/9906200.
- [46] P. Deligne, *Equations différentielles a points singuliers réguliers*, Lecture Notes in Mathematics, vol. **163**, Springer, Berlin, Heidelberg, New York, 1970.
- [47] M. R. Douglas, *Topics in D-geometry*, hep-th/9910170.
- [48] P. S. Aspinwall, C. A. Lutken, Quantum algebraic geometry of superstring compactifications, Nucl. Phys. **B355** (1991) 482–510.
- [49] A. Recknagel, V. Schomerus, *Moduli Spaces of D-branes in CFT-backgrounds*, hep-th/9903139, *Boundary Deformation Theory and Moduli Spaces of D-Branes*, Nucl.Phys. B545 (1999) 233-282, hep-th/9811237, *D-branes in Gepner models*, Nucl.Phys. B531 (1998) 185-225, hep-th/9712186.
- [50] N. Ishibashi, *The boundary and crosscap states in conformal field theories*, Mod. Phys. Lett. **A4** (1989) 251; N. Ishibashi, T. Onogi, *Conformal field theories on surfaces with boundaries and crosscaps*, Mod. Phys. Lett. **A4** (1989) 161.
- [51] A. Libgober, J. Teitelbaum, *Lines on Calabi-Yau complete intersections, mirror symmetry, and Picard-Fuchs equations*, Internat. Math. Res. Notices 1993, **no. 1**, 29–39.
- [52] O. I. Marichev, *Handbook of integral transforms of higher transcendental functions: theory and algorithmic tables*, Ellis Horwood series in mathematics and its applications, Halsted Press, New York 1983; A. Erdelyi, W. Magnus, F. Oberhettinger, F. G. Tricomi, *Higher transcendental functions*; Y. Luke, *The special functions and their approximations*, Academic Press, 1969.
- [53] E. A. Coddington, N. Levinson, *Theory of ordinary differential equations*, New York, McGraw-Hill, 1955.
- [54] D. R. Morrison, *Picard-Fuchs equations and mirror maps for hypersurfaces*, in Essays on mirror manifolds, 241–264, Internat. Press, Hong Kong, 1992, hep-th/9111025.
- [55] N. E. Norlund, *Hypergeometric functions*, Acta Mathematica, **4** (1955), 289–349.
- [56] V. V. Batyrev, *Dual polyhedra and mirror symmetry for Calabi-Yau hypersurfaces in toric varieties*, J. Algebraic Geom. **3** (1994), no. 3, 493–535.
- [57] B. R. Greene, M. R. Plesser, *Duality In Calabi-Yau Moduli Space*, Nucl. Phys. **B338** (1990) 15.
- [58] V. V. Batyrev, D. van Straten, *Generalized hypergeometric functions and rational curves on Calabi-Yau complete intersections in toric varieties*, Comm. Math. Phys. **168** (1995), no. 3, 493–533.

- [59] I. Gelfand, M. Kapranov, A. Zelevinski, *Discriminants, resultants and multidimensional determinants*, Birkhauser, Boston, 1994.
- [60] I. M. Gelfand, A. V. Zelevinskii, and M. M. Kapranov, *Discriminants of polynomials in several variables and triangulations of Newton polyhedra*, Leningrad Math. J. **2** (1991), 449–505.
- [61] D. R. Morrison, *Mathematical aspects of Mirror Symmetry*, Complex Algebraic Geometry (J. Kollar, ed.), IAS/Park City Math. Series, vol. 3, 1997, pp. 265–340, alg-geom/9609021.
- [62] D. R. Morrison, *Compactifications of moduli spaces inspired by mirror symmetry*, Journées de Géométrie Algébrique d’Orsay (Juillet 1992), Astérisque, vol. **218**, 1993, pp. 243–271, alg-geom/9304007.